



# Modelling net sediment transport in the swash zone

---

October 2020

---

University of Twente  
Chris van der Stoop

UNIVERSITY  
OF TWENTE.



UNIVERSITY OF TWENTE.

# Modelling net sediment transport in the swash zone

The analysis of a net sediment transport formulation

MASTER THESIS

## Author

Name: ing. C.J.M. van der Stoop  
Programme: MSc. Civil Engineering and Management  
Water Engineering and Management  
Insitute: University of Twente  
Enschede, The Netherlands  
Student number s2026651  
E-mail: chris.van.der.stoop@hotmail.com

## Graduation Committee

|                             |                               |
|-----------------------------|-------------------------------|
| prof. dr. S.J.M.H. Hulscher | University of Twente          |
| dr. ir. J.J. van der Werf   | University of Twente/Deltares |
| S. Dionisio Antonio MSc     | University of Twente          |



## Acknowledgements

This research is my final piece of art as a student at the University of Twente to complete my master's degree in 'River and Coastal Engineering'. The research took me six months (excluding a summer break) to write, ten if you include the literature search and proposal. Looking back, it was an exciting journey during the COVID-19 period with a new challenge for every new phase. During my master's thesis I received a lot of help and support. Therefore, I would like to take a moment to express my sincere gratitude.

The first person I would like to thank is Sara Dionisio Antonio, my daily supervisor of the university of Twente. I would like to thank her for the time, support, enthusiasm, and guidance to keep me on the right track. In spite of the new situation with working from home and all the obstacles it presented, Sara was always available for questions, digital meetings, feedback and to check my English which helped me very much.

In the same manner I would like to thank my other supervisors, Suzanne Hulscher and Jebbe van der Werf, and also Erik Horstman during the initial six weeks. Even though the meetings were less regular, I would like to thank them for their time, feedback and suggestions that were very valuable to me.

Thirdly, my gratitude goes to my fellow students who helped me during my master Thesis at the university of Twente and during my master itself. They were good sparring partners to help me when I got stuck, but especially they made the days a lot more enjoyable. This definitely contributed to how much I enjoyed studying at the university.

Finally, I would like to thank all my friends and family. They have supported me along every phase of this research, with their patience during my master Thesis, but also with the necessary distraction and relaxation.

I hope that you will enjoy reading this thesis and that you will gain a valuable insight into the net sediment transport in the swash zone. Please do not hesitate to contact me if you have further questions or feedback on this research.

Thank you all again!

Chris van der Stoop

*Enschede, October 2020*

## Summary

The swash zone is the area where waves run-up the beach resulting in that the swash zone is alternately covered and exposed by waves. Although this zone not wide, it is an essential zone for the development of the beach, because when the net sediment transport is directed offshore, the beach will erode and when it is onshore, accretion will occur. The amount of sediment transported depends on different hydrodynamic processes. Due to all these processes, the swash zone is a complex area and still not fully understood. However, the swash zone is a crucial area for coastal management.

To better understand the swash zone, different net sediment transport formulations are developed for the swash zone. In this research, three formulations are analysed and tested. For the formulations three data sets are used; Shaping the Beach and BARDEX II which uses random waves and RESIST which uses bichromatic waves. For this research, one erosive and one accretive wave condition were selected for each data set. For these wave conditions, the wave height and period are determined to analyse changes in the whole wave flume. Furthermore, the velocities in the swash zone are determined as input for the formulations. In addition, the morphodynamic changes are determined and analysed. The net sediment transport rates of Shaping the Beach are the lowest (maximum  $5 \times 10^{-5} \text{ m}^2/\text{s}$ ) in comparison to RESIST (maximum  $6 \times 10^{-5} \text{ m}^2/\text{s}$ ) and BARDEX II (maximum  $15 \times 10^{-5} \text{ m}^2/\text{s}$ ). Furthermore, the erosive wave conditions for Shaping the Beach and RESIST are offshore directed and the accretive wave conditions onshore directed in the swash zone. For BARDEX II both wave conditions are onshore directed in the swash zone.

The first formulation for calculating the net transport rate is the SANTOSS formulation. This formulation has not been developed for the swash zone. The formulation is based on three essential processes for the swash zone: wave skewness and asymmetry, bed shear stress and sediment response time. The calculated net sediment transport rates with this formulation are generally overestimated and directed onshore, which for the accretive wave conditions is the same direction as measured, but for the erosive wave conditions in the opposite direction as measured. These results can be explained by the high velocity skewness and the absence of the bed slope effects in the formulation, which drives the sediment offshore.

Secondly, the bed shear stress formulation of Larson, Kubota, and Erikson (2004) is analysed. The formulation uses the wave skewness and asymmetry, bed shear stress and the bed slope effects to calculate the net sediment transport rate. The formulation has better results for the accretive wave conditions than for the erosive wave conditions. This can be explained by the velocity skewness for Shaping the Beach and RESIST. For BARDEX II, the net sediment transport rates are underestimated. This is due to the fact that the bed shear stresses are almost the same during the uprush and backwash period.

The last formulation is a simplified formulation from the bed shear stress formulation of Larson et al. (2004), resulting in a formulation based on the run-up limit and bed slope. Another essential point of this formulation is the calibration coefficient  $K_c$ . For the erosive wave conditions, the calculated transport rates are in the same direction as measured, and the amounts are within an acceptable range of the 1:1-line. The results for the accretive wave condition are less accurate. The results are vertically scattered, which means that the results are overestimated. Furthermore, it is noticeable that the formulation is better for a longer period (total wave conditions) than for shorter periods of time (individual runs).

For the final step of the research, the run-up limit formulation of Larson et al. (2004) was chosen to be improved. This choice was made because this formulation has the best correlation based on the coefficients of Spearman and Pearson. In addition, the formulation has a calibration coefficient, which has a high potential to be improved. The two parameters with the most significant influence on the Larson et al. (2004) run-up limit formulation are the run-up limit and  $K_c$ . To improve the run-up limit, two formulations are tested to estimate the run-up limit. These formulations are tested because, in the first comparison of model-data, measured run-up levels were used. This is not possible when the formulation is used to predict net sediment transport. The best formulation of these two formulations is the formulation based on the surf similarity parameter. The calculated transport rates are close to the rates calculated with the measured run-up limit. However, the results are still better with the use of the measured run-up limit. The  $K_c$ -value has been calibrated for Shaping the Beach and RESIST data set based on the Root-Mean-Square- Error. The founded  $K_c$ -values for the erosive wave conditions are ten times smaller. For the accretive wave conditions, they are 100-1000 times smaller. These results show that the  $K_c$ -value is probably too high for Shaping the Beach and RESIST data set. Further, the  $K_c$ -value shows a tendency with the wave period. However, these results ( $K_c$ -value and trend) have not been validated due to the limited data and time available.

## Samenvatting

De swash zone is een gebied op het strand waar de golven het strand op- en af rollen, waardoor het strand soms droog staat en soms niet. Ondanks het feit dat de swash zone niet breed is, is de zone wel erg belangrijk voor de ontwikkeling van het strand. Het strand groeit namelijk als het netto zandtransport in de swash zone richting de kust is, maar het strand erodeert als het richting zee gaat. Hoeveel zand transport er plaats vindt hangt af van de hydrodynamisch processen. Door al de verschillende processen die plaats vinden is de swash zone een complex gebied en is er nog veel onduidelijk. Desondanks is de swash zone zeer belangrijk voor kustbeheer.

Om de swash zone beter te begrijpen zijn er verschillende formules ontwikkeld. In dit onderzoek worden drie formules voor de swash zone geanalyseerd en getest. Voor het testen van de formules zijn drie data sets gebruikt. Twee daarvan, Shaping the Beach en BARDEX II, maken gebruik van random golven en de derde, RESIST, gebruikt bi-chromatische golven. Van elke van deze data sets is één erosieve golfconditie en één accretive golfconditie geselecteerd. Voor de hele golfgoot is van elke golfconditie de golfhoogte en periode bepaald. Daarnaast is de stroomsnelheid bepaald in de swash zone. Verder zijn de morfodynamische veranderingen bepaald en geanalyseerd. Het netto zandtransport was het laagste voor Shaping the Beach (maximaal  $5 \times 10^{-5} \text{ m}^2/\text{s}$ ) gevolgd door RESIST (maximaal  $6 \times 10^{-5} \text{ m}^2/\text{s}$ ) en (maximaal  $15 \times 10^{-5} \text{ m}^2/\text{s}$ ) BARDEX II. Het netto zandtransport gedurende de erosieve golfcondities van Shaping the Beach en RESIST zijn richting strand en voor de accretive golfconditie richting zee. Voor BARDEX II is het netto zandtransport voor beide golfcondities richting zee.

De SANTOSS-formule is de eerste geteste formule voor het netto zandtransport in de swash zone. Deze formule is van origine niet ontwikkeld voor de swash zone. Voor de berekening is de formule afhankelijk van de golf skewness en asymmetrie, bodemschuifspanning en reactietijd van het zand. De berekende zandtransporten zijn voor bijna alle data punten overschat en in de richting van het strand. Dit is de goede richting voor de accretive golfcondities maar niet voor de erosieve golfcondities. Dit kan verklaard worden door de skewness in de stroomsnelheid en de afwezigheid van de effecten als gevolg van de bodemhelling.

De tweede formule is de formule van Larson et al. (2004) gebaseerd op de bodemschuifspanning. Net als de SANTOSS-formule, zijn de golf skewness, asymmetrie en de bodemschuifspanning benodigd. Daarnaast is ook de bodemhelling benodigd. De resultaten voor de accretive golfconditie van Shaping the Beach en RESIST zijn over het algemeen beter dan die van de erosieve golfconditie. Dit komt vooral door de skewness in de snelheid. Voor BARDEX II zijn de netto zandtransporten onderschat. Wat het gevolg is van bijna gelijke tijdgemiddelde bodemschuifspanningen voor de uprush en backwash.

Als laatste is de formule van Larson et al. (2004) gebaseerd op de run-up limiet gebruikt. Deze formule is een simplificatie van de bodemschuifspanning formule van Larson et al. (2004). De belangrijkste input voor de formule is de run-up limiet en de bodemhelling. Daarnaast is de kalibratie coëfficiënt  $K_c$  erg belangrijk. Voor de erosieve golfconditie berekend de formule de richtingen hetzelfde als gemeten en is de hoeveelheid van het netto getransporteerde zand niet ver van de gemeten waarde. De resultaten voor de accretive golfconditie zijn minder goed. De data punten zijn verticaal verspreid, dit betekent dat de zandtransporten zijn overschat. Daarnaast valt wel op dat de formule het beter doet voor langere golfcondities (gehele golfconditie) dan kortere (individuele runs).

De laatste stap is het verbeteren van één van de formules. Hiervoor is de run-up limiet formule van Larson et al. (2004) gekozen. Deze keuze is gemaakt, omdat deze formule de hoogste correlatie had voor zowel de Spearman als de Pearson coëfficiënt. Daarnaast bevat deze formule en kalibratie parameter  $K_c$ , waar relatief gemakkelijk aan gesleuteld kan worden. Voor de verbetering zijn twee parameters geanalyseerd. De eerste is de run-up limiet. Hiervoor zijn twee formules die de run-up limiet kunnen berekenen getest. Het voordeel van deze formules is dat de run-up limiet niet achteraf pas kan worden bepaald maar vooraf, waardoor de LARSON formule kan worden gebruikt om te voorspellen. De beste formule van de twee is de formule gebaseerd op de surf similarity parameter. Met deze formule zijn de berekende zandtransporten het dichtste bij die met de gemeten run-up limiet. Echter zijn de resultaten met de gemeten run-up limiet wel beter. De tweede parameter is de kalibratie coëfficiënt  $K_c$ . De  $K_c$  coëfficiënt is gekalibreerd voor de golfcondities van Shaping the Beach en RESIST. Hieruit bleek dat de  $K_c$  waarde voor de erosieve golfcondities tien keer kleiner was dan de gevonden waarde door Larson et al. (2004). Voor de accretive golfconditie bleek de  $K_c$  waarde 100-1000 keer kleiner. Hieruit valt te concluderen dat de kalibratie coëfficiënt gevonden bij Larson et al. (2004) waarschijnlijk te hoog is voor Shaping the Beach en RESIST. Verder was er een trend zichtbaar tussen de  $K_c$  waarde en de golf periode. Echter zijn de resultaten, door gelimiteerde tijd en data, niet gevalideerd.

## Table of contents

|   |             |
|---|-------------|
| <b>Acknowledgements</b> .....                                   | <b>I</b>    |
| <b>Summary</b> .....  | <b>II</b>   |
| <b>Samenvatting</b> .....                                       | <b>III</b>  |
| <b>Table of contents</b> .....                                  | <b>V</b>    |
| <b>List of Figures</b> .....                                    | <b>VI</b>   |
| <b>List of Tables</b> .....                                     | <b>VIII</b> |
| <b>1 Introduction</b> .....                                     | <b>1</b>    |
| 1.1 Background .....  | 1           |
| 1.2 Problem statement .....                                     | 2           |
| 1.3 Goal of the research .....                                  | 2           |
| 1.4 Practical and scientific relevance .....                    | 2           |
| 1.5 Research questions .....                                    | 2           |
| 1.6 General approach .....                                      | 3           |
| 1.7 Outline of the report .....                                 | 3           |
| <b>2 Theoretical background</b> .....                           | <b>4</b>    |
| 2.1 The swash zone .....  | 4           |
| 2.2 Sediment transport in the swash zone .....                  | 4           |
| 2.2.1 General processes .....                                   | 5           |
| 2.2.2 Onshore directed processes .....                          | 6           |
| 2.2.3 Offshore directed processes .....                         | 7           |
| 2.3 Net sediment transport formulations .....                   | 7           |
| 2.3.1 Formulations of Larson: Bed shear stress .....            | 7           |
| 2.3.2 Formulations of Larson: Run-up limit .....                | 8           |
| 2.3.3 SANTOSS formulations .....                                | 9           |
| 2.4 Suitable data sets .....                                    | 10          |
| <b>3 Methodology</b> .....                                      | <b>11</b>   |
| 3.1 Data collection and analysing .....                         | 11          |
| 3.2 Data processing .....                                       | 14          |
| 3.2.1 Hydrodynamics .....                                       | 14          |
| 3.2.2 Morphodynamics .....                                      | 15          |
| 3.3 The net sediment transport formulations .....               | 17          |
| 3.3.1 Net sediment transport formulations .....                 | 17          |
| 3.3.2 Formulation for improvement .....                         | 18          |
| 3.4 Improvement of the net sediment transport formulation ..... | 19          |
| 3.4.1 Input data .....  | 19          |
| 3.4.2 Calibration coefficient .....                             | 19          |
| <b>4 Results of the wave conditions</b> .....                   | <b>20</b>   |
| 4.1 Wave hydrodynamics .....                                    | 20          |
| 4.1.1 Shaping the Beach .....                                   | 20          |
| 4.1.2 RESIST .....  | 22          |
| 4.1.3 BARDEX II .....   | 24          |
| 4.2 Morphodynamics .....  | 26          |
| 4.2.1 Shaping the Beach .....                                   | 26          |
| 4.2.2 RESIST .....  | 27          |
| 4.2.3 BARDEX II .....   | 29          |
| 4.3 Data sets comparison .....                                  | 31          |
| 4.3.1 Hydrodynamics .....                                       | 31          |
| 4.3.2 Morphodynamics .....                                      | 31          |

|          |   |           |
|----------|---|-----------|
| <b>5</b> | <b>Validation of the net sediment transport formulations</b>      | <b>32</b> |
| 5.1      | SANTOSS formulation   | 32        |
| 5.1.1    | Hypothesis  | 32        |
| 5.1.2    | Results   | 32        |
| 5.2      | Formulations of Larson: Bed shear stress                          | 37        |
| 5.2.1    | Hypothesis  | 37        |
| 5.2.2    | Results   | 37        |
| 5.3      | Formulations of Larson: Run-up limit                              | 42        |
| 5.3.1    | Hypothesis  | 42        |
| 5.3.2    | Results   | 42        |
| 5.4      | Formulation assessment  | 47        |
| 5.4.1    | Strong and weak points of the formulations.                       | 47        |
| 5.4.2    | Error statistics  | 48        |
| 5.4.3    | Formulation for improvement                                       | 48        |
| <b>6</b> | <b>Improve the net sediment transport formulation</b>             | <b>49</b> |
| 6.1      | Run-up limit  | 49        |
| 6.1.1    | Individual runs   | 49        |
| 6.1.2    | Total wave condition  | 50        |
| 6.1.3    | Conclusion Run-up limit   | 52        |
| 6.2      | Calibration coefficient   | 53        |
| 6.2.1    | Results   | 53        |
| 6.2.2    | Conclusion calibration coefficient                                | 54        |
| <b>7</b> | <b>Discussion</b>   | <b>55</b> |
| 7.1      | Phase 1: Processing the data of the wave conditions               | 55        |
| 7.2      | Phase 2: Working with the net sediment transport formulations     | 55        |
| 7.3      | Phase 3: Improvement of the formulation                           | 56        |
| <b>8</b> | <b>Conclusions</b>  | <b>58</b> |
| 8.1      | Research questions  | 58        |
| 8.2      | Goal of the research  | 59        |
| <b>9</b> | <b>Recommendations</b>  | <b>60</b> |
|          | <b>References</b>   | <b>61</b> |
|          | <b>Appendix A Representative velocity and acceleration signal</b> | <b>64</b> |
|          | <b>Appendix B Hydrodynamic and morphological processes</b>        | <b>65</b> |
|          | <b>Appendix C Hypotheses</b>                                      | <b>66</b> |
|          | C.1 Hypotheses SANTOSS  | 66        |
|          | C.2 Hypotheses formulation of Larson: Bed shear stress            | 68        |
|          | C.3 Hypotheses formulation of Larson: Run-up limit                | 69        |
|          | <b>Appendix D The run-up limits for the different methods</b>     | <b>71</b> |
|          | <b>Appendix E Figures: improvement run-up limit each run</b>      | <b>72</b> |

## List of Figures

|      |   |    |
|------|---|----|
| 1.1  | Definition sketch for the nearshore (swash zone height exaggerated), figure taken from Lanckriet (2016) .....                   | 1  |
| 2.1  | Definition sketch for the nearshore littoral zone (swash zone width exaggerated) Elfrink and Baldock (2002) .....               | 4  |
| 2.2  | One swash event (Jongedijk, 2017) .....   | 5  |
| 2.3  | Nonlinearities of waves propagating (Rocha, 2014) .....   | 6  |
| 2.4  | Swash-swash interaction (Chardón-Maldonado, Pintado-Patiño, & Puleo, 2015) .....  | 6  |
| 3.1  | The three phases of the research .....  | 11 |
| 3.2  | Swash zone instrumentation Shaping the Beach .....  | 12 |
| 3.3  | Swash zone instrumentation RESIST .....   | 13 |
| 3.4  | Deltares instrumentation BARDEX II .....  | 14 |
| 3.5  | Weighted mean of left and right-hand side net sediment transport rates .....  | 16 |
| 3.6  | Difference between no profile correction and long-shore correction for the erosive wave condition of Shaping the Beach .....    | 16 |
| 3.7  | Example good, reasonable and bad prediction .....   | 18 |
| 3.8  | Calibration diagram for a formulation (Milivojević, Simić, Orlić, Milivojević, & Stojanović, 2009) .....                        | 19 |
| 4.1  | Spectral analysis from the erosive wave in deep water at $x=-52.05$ m, Shaping the Beach .                                      | 20 |
| 4.2  | Spectral analysis from the accretive wave in deep water at $x=-52.05$ m, Shaping the Beach                                      | 20 |
| 4.3  | Average wave heights and profiles erosive wave, Shaping the Beach .....   | 20 |
| 4.4  | Average wave heights and profiles accretive wave, Shaping the Beach .....   | 21 |
| 4.5  | Mean, maximum and minimum velocities, Shaping the Beach .....   | 21 |
| 4.6  | Spectral analysis from the erosive wave in deep water at $x=-56.04$ m, RESIST .....   | 22 |
| 4.7  | Spectral analysis from the accretive wave in deep water at $x=-56.04$ m, RESIST .....   | 22 |
| 4.8  | Average wave heights and profiles erosive wave, RESIST .....  | 22 |
| 4.9  | Average wave heights and profiles accretive wave, RESIST .....  | 23 |
| 4.10 | Mean, maximum and minimum velocities, RESIST .....  | 23 |
| 4.11 | Spectral analysis from the erosive wave in deep water at $x=-50.3$ m, BARDEX II .....   | 24 |
| 4.12 | Spectral analysis from the accretive wave in deep water at $x=-50.3$ m, BARDEX II .....   | 24 |
| 4.13 | Average wave heights and profiles erosive wave, BARDEX II .....   | 24 |
| 4.14 | Average wave heights and profiles accretive wave, BARDEX II .....   | 25 |
| 4.15 | Mean, maximum and minimum velocities, BARDEX II .....   | 25 |
| 4.16 | Net sediment transport rates, Erosive wave Shaping the Beach .....  | 26 |
| 4.17 | Net sediment transport rates, Accretive wave Shaping the Beach .....  | 26 |
| 4.18 | Shoreline evolution Shaping the Beach .....   | 27 |
| 4.19 | Net sediment transport rates, Erosive wave RESIST .....   | 28 |
| 4.20 | Net sediment transport rates, Accretive wave RESIST .....   | 28 |
| 4.21 | Shoreline evolution RESIST .....  | 29 |
| 4.22 | Net sediment transport rates, Wave A1 BARDEX II .....   | 29 |
| 4.23 | Net sediment transport rates, Wave A6 BARDEX II .....   | 30 |
| 4.24 | Shoreline evolution BARDEX II .....   | 30 |
| 4.25 | Total transport rates for the six wave conditions .....   | 31 |
| 5.1  | Shaping the Beach erosive wave condition net sediment transport calculated using the SANTOSS formulation .....                  | 33 |
| 5.2  | RESIST erosive wave condition net sediment transport calculated using the SANTOSS formulation .....                             | 33 |
| 5.3  | BARDEX II erosive wave condition net sediment transport calculated using the SANTOSS formulation .....                          | 34 |
| 5.4  | Shaping the Beach accretive wave condition net sediment transport calculated using the SANTOSS formulation .....                | 34 |
| 5.5  | RESIST accretive wave condition net sediment transport calculated using the SANTOSS formulation .....                           | 35 |
| 5.6  | BARDEX II accretive wave condition net sediment transport calculated using the SANTOSS formulation .....                        | 35 |
| 5.7  | Total net sediment transport of the whole wave conditions of the three data sets calculated using the SANTOSS formulation ..... | 36 |

|      |  |    |
|------|--|----|
| 5.8  | Total mean net sediment transport of the runs per wave conditions of the three data sets calculated using the SANTOSS formulation . . . . .  | 36 |
| 5.9  | Shaping the Beach erosive wave condition net sediment transport calculated using the formulation of Larson et al. (2004) based on the bed shear stress . . . . .                             | 37 |
| 5.10 | RESIST erosive wave condition net sediment transport calculated using the formulation of Larson et al. (2004) based on the bed shear stress . . . . .  | 38 |
| 5.11 | BARDEX II erosive wave condition net sediment transport calculated using the formulation of Larson et al. (2004) based on the bed shear stress . . . . .                                     | 38 |
| 5.12 | Shaping the Beach accretive wave condition net sediment transport calculated using the formulation of Larson et al. (2004) based on the bed shear stress . . . . .                           | 39 |
| 5.13 | RESIST accretive wave condition net sediment transport calculated using the formulation of Larson et al. (2004) based on the bed shear stress . . . . .                                      | 40 |
| 5.14 | BARDEX II accretive wave condition net sediment transport calculated using the formulation of Larson et al. (2004) based on the bed shear stress . . . . .                                   | 40 |
| 5.15 | Total net sediment transport of the whole wave conditions of the three data sets calculated using the formulation of Larson et al. (2004) based on the bed shear stress . . . . .            | 41 |
| 5.16 | Total net sediment transport of the whole wave conditions of the three data sets calculated using the formulation of Larson et al. (2004) based on the bed shear stress . . . . .            | 41 |
| 5.17 | Shaping the Beach erosive wave condition net sediment transport calculated using the formulation of Larson et al. (2004) based on the run-up limit . . . . .                                 | 42 |
| 5.18 | RESIST erosive wave condition net sediment transport calculated using the formulation of Larson et al. (2004) based on the run-up limit . . . . .  | 43 |
| 5.19 | BARDEX II erosive wave condition net sediment transport calculated using the formulation of Larson et al. (2004) based on the run-up limit . . . . .   | 43 |
| 5.20 | Shaping the Beach accretive wave condition net sediment transport calculated using the formulation of Larson et al. (2004) based on the run-up limit . . . . .                               | 44 |
| 5.21 | RESIST accretive wave condition net sediment transport calculated using the formulation of Larson et al. (2004) based on the run-up limit . . . . .  | 44 |
| 5.22 | BARDEX II accretive wave condition net sediment transport calculated using the formulation of Larson et al. (2004) based on the run-up limit . . . . .                                       | 45 |
| 5.23 | Total net sediment transport of the whole wave conditions of the three data sets calculated using the formulation of Larson et al. (2004) based on the run-up limit . . . . .                | 45 |
| 5.24 | Total net sediment transport of the whole wave conditions of the three data sets calculated using the formulation of Larson et al. (2004) based on the run-up limit . . . . .                | 46 |
| 6.1  | The net sediment transport rates of the total wave condition calculated using the run-up limit based on the velocity . . . . .   | 50 |
| 6.2  | The mean net sediment transport rates of the individual runs calculated using the run-up limit based on the velocity . . . . .   | 51 |
| 6.3  | The net sediment transport rates of the total wave condition calculated using the run-up limit based on the deep water wave conditions . . . . .   | 51 |
| 6.4  | The mean net sediment transport rates of the individual runs calculated using the run-up limit based on the deep water wave conditions . . . . .   | 52 |
| 6.5  | The RMSE with different $K_c$ -value, started from the $K_c$ -value founded by Larson et al. (2004) of $1.6 \times 10^{-3}$ . The optimal $K_c$ -values are indicated with the dots. . . . . | 53 |
| B.1  | Schematic of hydrodynamic and sediment transport processes occurring within a single swash event (Chardón-Maldonado et al., 2015). . . . .   | 65 |
| E.1  | Shaping the Beach erosive wave condition net sediment transport calculated using the run-up limit based on the velocity (Hughes, 1992) . . . . .   | 72 |
| E.2  | Shaping the Beach erosive wave condition net sediment transport calculated using the run-up limit based on the deep water wave conditions (Mase & Iwagaki, 1985) . . . . .                   | 72 |
| E.3  | Shaping the Beach accretive wave condition net sediment transport calculated using the run-up limit based on the velocity (Hughes, 1992) . . . . .   | 72 |
| E.4  | Shaping the Beach accretive wave condition net sediment transport calculated using the run-up limit based on the deep water wave conditions (Mase & Iwagaki, 1985) . . . . .                 | 73 |
| E.5  | RESIST erosive wave condition net sediment transport calculated using the run-up limit based on the velocity (Hughes, 1992) . . . . .  | 73 |
| E.6  | RESIST erosive wave condition net sediment transport calculated using the run-up limit based on the deep water wave conditions (Mase & Iwagaki, 1985) . . . . .                              | 73 |

|      |  |    |
|------|--|----|
| E.7  | RESIST accretive wave condition net sediment transport calculated using the run-up limit based on the velocity (Hughes, 1992) . . . . .                              | 74 |
| E.8  | RESIST accretive wave condition net sediment transport calculated using the run-up limit based on the deep water wave conditions (Mase & Iwagaki, 1985) . . . . .    | 74 |
| E.9  | BARDEX II erosive wave condition net sediment transport calculated using the run-up limit based on the velocity (Hughes, 1992) . . . . .                             | 74 |
| E.10 | BARDEX II erosive wave condition net sediment transport calculated using the run-up limit based on the deep water wave conditions (Mase & Iwagaki, 1985) . . . . .   | 75 |
| E.11 | BARDEX II accretive wave condition net sediment transport calculated using the run-up limit based on the velocity (Hughes, 1992) . . . . .                           | 75 |
| E.12 | BARDEX II accretive wave condition net sediment transport calculated using the run-up limit based on the deep water wave conditions (Mase & Iwagaki, 1985) . . . . . | 75 |

## List of Tables

|     |  |    |
|-----|--|----|
| 2.1 | Sediment transport processes overview which are include in the formulations . . . . .  | 7  |
| 3.1 | Shaping the Beach irregular wave characteristics, b = benchmark, E = erosive wave condition and A = accretive wave condition . . . . .   | 11 |
| 3.2 | Shaping the beach locations of the AWG and ADV . . . . .   | 12 |
| 3.3 | RESIST bichromatic wave characteristics, b = benchmark, E = erosive wave condition and A = accretive wave condition . . . . .  | 12 |
| 3.4 | RESIST locations of the AWG and ADV . . . . .  | 12 |
| 3.5 | BARDEX II irregular wave characteristics . . . . .   | 13 |
| 3.6 | BARDEX II locations of the EMs, VECs and PTs . . . . .   | 13 |
| 3.7 | Used locations for the net sediment transport rates . . . . .  | 17 |
| 4.1 | Difference in sediment during each run (30 min) of the erosive wave of Shaping the beach   | 27 |
| 4.2 | Difference in sediment during each run (60 min) of the accretive wave of Shaping the beach   | 27 |
| 4.3 | Difference in sediment during each run (60 min) of the erosive wave of RESIST . . . . .  | 28 |
| 4.4 | Difference in sediment during each run (60 min) of the accretive wave of RESIST . . . . .  | 29 |
| 4.5 | Difference in sediment during each run (60 min) of wave condition A1 of BARDEX II . . . . .  | 30 |
| 4.6 | Difference in sediment during each run (60 min) of wave condition A6 of BARDEX II . . . . .  | 30 |
| 4.7 | Overview of the hydrodynamics of the three data sets . . . . .   | 31 |
| 5.1 | Hypotheses SANTOSS for the total wave conditions . . . . .   | 32 |
| 5.2 | Hypotheses Larson et al. (2004) based on bed shear stress for the total wave conditions . . . . .  | 37 |
| 5.3 | Hypotheses Larson et al. (2004) based on the run-up limit for the total wave conditions . . . . .  | 42 |
| 5.4 | Overview of the results of the formulations based on the direction and amount of the net sediment transport rate. with a - for disagree, -/+ for mid term and + for agree . . . . .  | 47 |
| 5.5 | Error statistics for the three formulations where one is the best possible correlation, in bold the best correlation. S = SANTOSS formulation, B = Bed shear stress formulation Larson et al. (2004) and R = Run-up limit formulation Larson et al. (2004) . . . . .                         | 48 |
| 6.1 | Error statistics for the different methods to determine the Run-up limit. R = based on the beach profiles, U = based on the velocity (Hughes, 1992) and W = based on the deep water wave conditions. A correlations of one is the best possible correlation (Mase & Iwagaki, 1985) . . . . . | 50 |
| 6.2 | Error coefficient of the total wave condition. R = based on the beach profiles, U = based on the velocity (Hughes, 1992) and W = based on the deep water wave conditions (Mase & Iwagaki, 1985) . . . . .  | 52 |
| 6.3 | Optimal $K_c$ -values for Shaping the Beach and RESIST . . . . .   | 53 |
| 6.4 | Optimal $K_c$ -values for Shaping the Beach and RESIST . . . . .   | 54 |
| C.1 | Hypotheses SANTOSS for each run off the different wave condition . . . . .   | 66 |
| C.2 | Hypotheses Larson et al. (2004) based on bed shear stress for each run off the different wave condition . . . . .  | 68 |
| C.3 | Hypotheses Larson et al. (2004) based on the run-up limit for each run off the different wave condition . . . . .  | 69 |
| D.1 | Run-up limits. R = based on the beach profiles, U = based on the velocity (Hughes, 1992) and W = based on the deep water wave conditions (Mase & Iwagaki, 1985) . . . . .  | 71 |

## List of symbols

### Roman symbols

|                 |   |
|-----------------|---|
| $A_u$           | wave asymmetry  |
| $B$             | total non-linearity   |
| $c_f$           | friction coefficient  |
| $d$             | difference between two rankings                                       |
| $D_{50}$        | sediment diameter   |
| $f$             | dimensionless factor  |
| $g$             | gravitational force   |
| $H_0$           | deep water wave height  |
| $H_s$           | significant wave height   |
| $K_c$           | dimensionless coefficient   |
| $m$             | dimensionless coefficient   |
| $m_0$           | 0th spectral moment   |
| $n$             | dimensionless coefficient   |
| $P$             | phase lag parameter   |
| $q_s$           | net sediment transport rate   |
| $r$             | non-linearity index   |
| $R$             | run-up limit  |
| $s$             | relative density of sediment  |
| $S_u$           | wave skewness   |
| $t$             | time  |
| $T$             | wave period   |
| $T_i$           | wave period for crest (i=c) and wave period for trough (i=t)          |
| $T_{iu}$        | time length of accelerating part of wave crest (i=c) and trough (i=t) |
| $u$             | cross-shore velocity  |
| $u_{rms}$       | root-mean-square velocity   |
| $u_s$           | velocity at the start of the swash zone                               |
| $u_w$           | wave orbital velocity   |
| $\hat{u}$       | peak orbital velocity   |
| $w_s$           | fall velocity   |
| $x$             | horizontal spatial coordinate   |
| $z$             | bed level elevation   |
| $\frac{dh}{dx}$ | local beach slope   |

### Greek symbols

|                    |  |
|--------------------|--|
| $\alpha$           | calibration coefficient  |
| $\tan(\beta_{eq})$ | equilibrium beach slope  |
| $\delta_{si}$      | sheet flow layer thickness   |
| $\varepsilon_0$    | porosity   |
| $\eta$             | ripple height  |
| $\theta$           | Shields parameter  |
| $\theta_{cr}$      | critical shields parameter   |
| $\theta_i$         | Shields parameter for the wave crest (i=c) and trough (i=t)                              |
| $\xi$              | coefficient accounting for the shape of the velocity and concentration profile (SANTOSS) |
| $\xi$              | surf similarity parameter  |
| $\rho$             | density of water   |
| $\sigma_{u_w}$     | the standard deviation of $U_w$  |
| $\tau$             | bed shear stress   |
| $\phi$             | waveform parameter   |
| $\phi$             | phase  |
| $\Phi$             | non-dimensional sand transport rate  |
| $\phi_m$           | friction angle of a moving grain   |
| $\omega$           | angular frequency  |
| $\Omega$           | Dean number  |
| $\Omega_{cc}$      | the sand load that enters during the wave crest and is transported during the crest      |
| $\Omega_{tc}$      | the sand load that enters during the wave crest and is transported during the trough     |
| $\Omega_{ct}$      | the sand load that enters during the wave trough and is transported during the trough    |
| $\Omega_{tt}$      | the sand load that enters during the wave trough and is transported during the crest     |

## 1 Introduction

This chapter outlines an overview of the background of the research (1.1) followed by the goal of the research (1.3) and the research question (1.5). At last, the general approach (1.6) and structure of the research (1.7) are explained.

### 1.1 Background

The swash zone is the transition zone between the land and sea or ocean (figure 1.1). The swash zone is alternatively covered and exposed by waves. An individual swash cycle consists of an uprush period (onshore directed velocities) and a backwash period (offshore directed velocities). Sediment transport in the swash zone is high in both landward and seaward direction and depends on the hydrodynamic processes and beach conditions (for example, sediment characteristics and slope). The essential hydrodynamic processes are: swash - swash interaction (Cáceres & Alsina, 2012), wave asymmetry and skewness (Grasso, Michallet, & Barthélemy, 2011), bed slope effects (Jongedijk, 2017), bed shear stress (Chardón-Maldonado et al., 2015), bore turbulence (Masselink & Puleo, 2006), the sediment response time (Jongedijk, 2017) and groundwater in- and exfiltration (Bakhtyar, Barry, Li, Jeng, & Yeganeh-Bakhtiary, 2009). The difference between the incoming sediment and outgoing sediment (the net sediment transport) determines the bed profile evolution. Because the swash zone is the transition zone between land and sea, the swash zone determines the shoreline development. Furthermore, the swash determines whether sand is stored on the upper beach or is transported offshore.

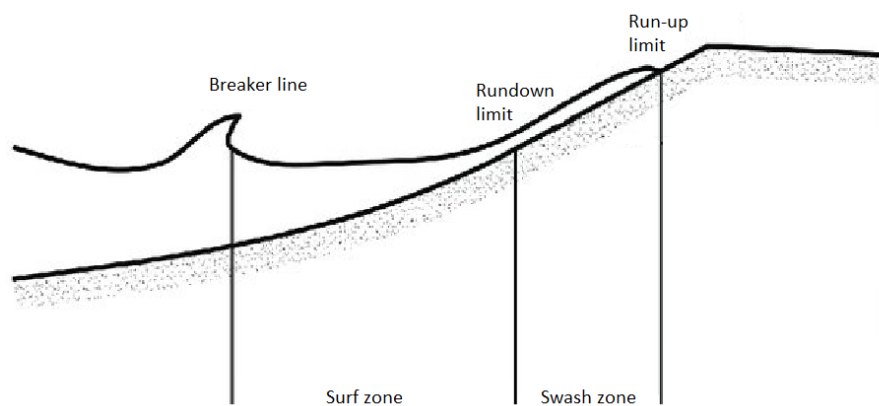


**Figure 1.1:** Definition sketch for the nearshore (swash zone height exaggerated), figure taken from Lanckriet (2016)

The net sediment transport rates are crucial for coastal management, because the net sediment transport in the swash zone determines the development of the shoreline (erosion or accretion). To obtain and estimate the net sediment transport rates in the swash zone, formulations are used. The formulation of Larson et al. (2004) is an often used formulation. This formulation is developed for the swash zone and includes a dimensionless coefficient  $K_c$ . It is needed to calibrate the  $K_c$  coefficient every time the formulation is used. The need for a calibration means that data is necessary to obtain the  $K_c$ -value before it can be used, which is a weak point of the formulation. The formulation is a simplification of a bed shear stress formulation (Madsen, 1993) integrated over a swash cycle. This second formulation is depended on other input parameters, so could result in a different outcome.

Another approach is using the SANTOSS formulation (Ribberink, 2011). The formulation is original not developed for the swash zone but further offshore. For these areas, the formulation shows promising net sediment transport rates. The benefit of this formulation is that there is no calibration needed; it can directly be used. However, the SANTOSS formulation is never applied to the swash zone, and therefore it is not known how the results will be.

There are two existing data sets available for the swash zone, the BARDEX II, and the RESIST data set. Furthermore, there is a new data set available from the Shaping the Beach project (Dionísio António et al., 2020). To obtain the Shaping the Beach and BARDEX II data set, multiple irregular waves are used. While for RESIST bichromatic waves are used. All the experiments are carried out with a 1:15 initial bed slope and different instruments to obtain the hydrodynamics and net sediment transport rate.

## 1.2 Problem statement

The erosion or accretion of the shoreline is crucial for coastal management. Because of the following reasons:

- Shoreline development (van der Zanden et al., 2019);
- Coastal engineering design and applications (Kobayashi, 1999);
- The beach groundwater may be influenced by the swash zone (Horn, 2006);

Therefore, a better understanding of sediment transport in the swash zone is essential (Jackson & Masselink, 2004; van der Zanden et al., 2019). A better understanding requires reliable formulations for the simulation of sediment transport in the swash zone. The problem is that the existing formulations do not sufficiently simulate the net sediment transport rate in the swash zone. The formulations are not sufficient because the net sediment transport rates are over- and underestimated, which results in a different bed profile than the measured bed profile. According to Bakhtyar, Barry, et al. (2009), formulations are not sufficient because the formulations are unable to "resolve all potentially important details of the flow and sediment transport in the swash zone". The main reason for this is that the swash zone is not fully understood (Masselink & Puleo, 2006). In other words, it is crucial to develop a formulation that provides a reliable simulation of the swash zone for most of the situations without needing a calibration first. Because if calibration is required, the formulation cannot be used to predict the transport rates but can only be used after a (field)experiment.

## 1.3 Goal of the research

This research aims to improve a formulation to calculate the net sediment transport rate in the swash zone. The improved formulation will help to understand the development of the shoreline and the correlated sediment transport for coastal management purposes. This research contributes to understanding of the net sediment transport formulation in the swash zone.

*"The goal of this research is to assess and improve practical formulations for net cross-shore sand transport in the swash zone."*

## 1.4 Practical and scientific relevance

The research is relevant in two ways:

- **Scientific relevance**

As mentioned in paragraph 1.1, the net sediment transport in the swash is not fully understood but is essential for coastal management. Therefore a better understanding of the net sediment transport in the swash zone is necessary (Jackson & Masselink, 2004). More research on the net sediment transport rates in the swash zone will contribute to a more clear understanding of the development of the swash zone.

- **Practical relevance**

According to van der Zanden et al. (2019) is the development of the coastline determined by the net sediment transport in the swash zone. To estimate the development of the shoreline (and thereby the erosion/accretion of the beach), a reliable formulation is required.

## 1.5 Research questions

The objective, as mentioned above, will be achieved by answering the following three research questions. Question one is posed to obtain an overview of the net sediment transport rates of the various data sets available. The second question is posed to research which formulation has the biggest potential to be improved, while the last question is posed to improve the formulation with the biggest potential.

1. What are the differences in net sediment transport between the different swash zone laboratory data sets (RESIST, BARDEX II, and Shaping the Beach)?
  - (a) What are the net sediment transport rates for various swash zone laboratory experiments?
  - (b) What are the differences in net sediment transport rate between the swash zone laboratory experiments?
  - (c) What causes the differences in net sediment transport between the swash zone laboratory experiments?

2. To what extent do the net sediment transport formulations (of Larson et al. (2004) and the SANTOSS project) simulate the net sediment transport rate in the swash zone?
  - (a) Which processes are represented in the net sediment formulation?
  - (b) What is the difference between the simulated and the measured net sediment transport in the swash zone?
  - (c) Which formulation has the highest mean correlation for multiple experiments between the simulated and the measured net sediment transport in the swash zone?
3. How can the formulation with the best correlation be improved to increase the agreement between the simulated and the measured net sediment transport in the swash zone?
  - (a) Which process(es) cause(s) the most significant differences between the flume experiments and simulations?
  - (b) How can the identified process(es) be improved in the net sediment transport formulation?

## 1.6 General approach

As shortly described above, the research is structured in three phases (three questions). In the first phase, the available data is structured, and the hydrodynamics (wave characteristics and velocities) are analysed. Furthermore, the net sediment transport rates are determined based on the profile evolution. In the second phase, the formulations are represented and used to calculate the net sediment transport rates based on the analysed hydrodynamics in the first phase. Subsequently, the results are interpreted, and the formulation with the best results in combination with the highest potential is chosen for improvement in the third phase. In this third phase, the formulation for improvement is analyzed to see where the most significant improvement can be achieved, followed by improving these parts and a recommendation about the improvement.

## 1.7 Outline of the report

The current research has been structured as follows. In chapter 2 the net sediment transport processes in the swash zone are explained and the formulations are presented. Furthermore, the available data sets are shortly introduced. The third chapter elaborates on the data sets used in this research and contains a description of the applied methods. In chapters 4, 5, and 6 the results of the research are presented. Each chapter corresponds to one phase of the research (one research question). The discussion follows these chapters in chapter 7. The final chapters, chapter 8 and 9 contains the conclusion, which includes the answer on the research questions, and recommendations for the next research.

## 2 Theoretical background

### 2.1 The swash zone

The swash zone is defined as the zone which is alternately covered and exposed by waves due to uprush and backwash. Where uprush is the flow in the direction of the beach and backwash is the flow in offshore direction. The swash zone is bounded by the surf zone on the seaside, as can be seen in figure 2.1. On the beachside, the swash zone is bounded by the backshore. The backshore is never covered by the uprush of waves (Elfrink & Baldock, 2002).

The swash zone is the transition zone between offshore and onshore. Therefore, the swash zone plays a critical role in the development of the shoreline (van der Zanden et al., 2019). This is enhanced due to the crucial role of the swash zone in sediment transport (Jackson & Masselink, 2004) and sedimentation and erosion of the beach. This is also one of the main reasons why the swash zone is analysed in several studies. Other reasons are:

- Coastal engineering design and applications (Kobayashi, 1999);
- The beach groundwater may be influenced by the swash zone (Horn, 2006);
- Key element for beach ecosystems (Moreno et al., 2006);
- Transport of pollutants due to the production of air-bubbles and seawater droplets.

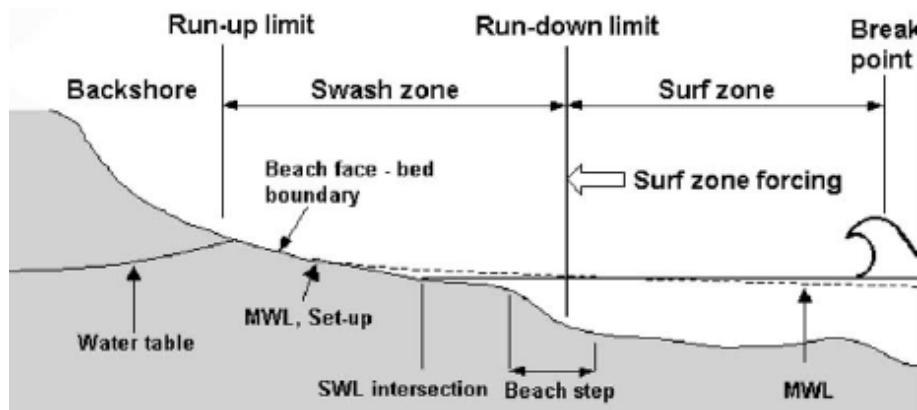


**Figure 2.1:** Definition sketch for the nearshore littoral zone (swash zone width exaggerated) Elfrink and Baldock (2002)

### 2.2 Sediment transport in the swash zone

According to Masselink and Puleo (2006), the sediment transport rates in the swash zone are much higher than in the surf zone. However, the net sediment transport (the difference between onshore and offshore transport) is small. To understand how sediment is transported in the swash zone, a comparison to one swash cycle is useful. One swash cycle can start with the braking of an incident wave, causing the wave to lose energy due to turbulence. The wave height will decrease, and wave refraction occurs. When the bore hits the shoreline, the bore collapses and the front will rapidly accelerate. According to Jongedijk (2017), can this happening be described in four phases, as shown in figure 2.2 and more elaborate in appendix B:

- Phase 1: The bore passes, which causes high onshore accelerating velocity. Close to the bed strong, offshore velocities and high vertical mixing
- Phase 2: The bore pushes, which causes slow onshore accelerating velocity and possible groundwater infiltration
- Phase 3: The run-up limit is reached and offshore acceleration occurs due to gravity. It is only a very thin layer of water
- Phase 4: Interaction with the next bore, which decreases the offshore velocity and can cause groundwater exfiltration

The grain size does not directly influence the swash zone processes but does influence sediment transport. Small grains are less difficult to transport, which causes that more sediment is transported than with larger grains.

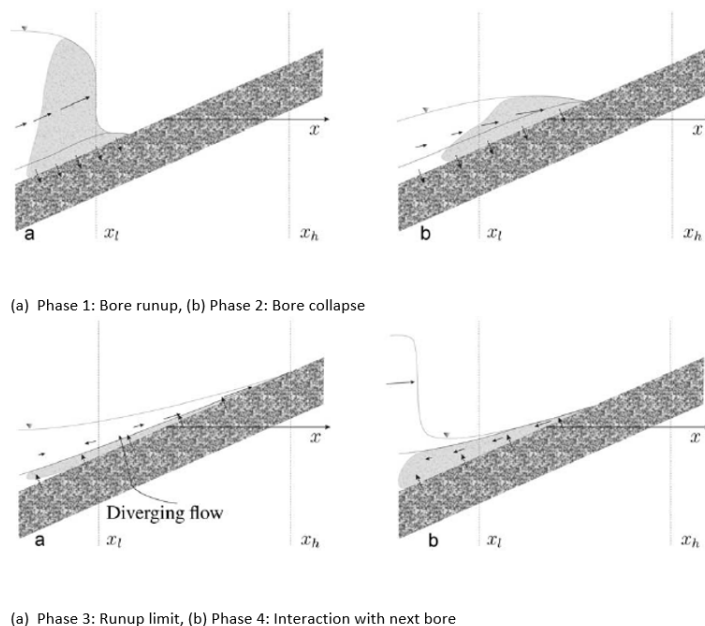


**Figure 2.2:** *One swash event (Jongedijk, 2017)*

The swash zone is a complex area due to all the processes that occur and due to that sediment is transport as bed load/sheet flow and suspended load (Bakhtyar, Barry, et al., 2009). The most relevant processes (on average) for cross-shore sediment transport are: swash - swash interaction (Cáceres & Alsina, 2012), wave asymmetry and skewness (Grasso et al., 2011), bed slope effects (Jongedijk, 2017), bed shear stress (Chardón-Maldonado et al., 2015), bore turbulence (Masselink & Puleo, 2006), sediment response time Jongedijk (2017) and groundwater (Bakhtyar, Barry, et al., 2009). These processes are divided into three groups general (can be both directions), onshore directed and offshore directed.

### 2.2.1 General processes

Water flowing over the bed induces a bed shear stress ( $\tau$ ). The bed shear stress is an important parameter related to the start of movement of sediment. If the bed shear stress is higher than the critical bed shear stress, sediment starts to move. Further, causes higher bed shear stress more sediment transport (Van Rijn, 2013). The bed shear stress can be calculated with equation 1 and depends on the bed friction and velocity.  $c_f$  represents the friction coefficient,  $\rho$  the density and  $u$  the velocity.

$$\tau = \frac{1}{2} \rho c_f u |u| \quad (1)$$

Because the bed shear stress depends on the velocity, the bed shear stress during the backwash is in the opposite direction compared to the uprush. The highest bed shear stress occurs at the beginning of the uprush and mid-backwash, see appendix B (Chardón-Maldonado et al., 2015).

Groundwater also does not specifically cause onshore or offshore transport. Water infiltrates during uprush and exfiltrates during the backwash. How much water in- or exfiltrates during a swash cycle depends on the grain size, slope, and groundwater level (Bakhtyar, Barry, et al., 2009).

Infiltration ensures extra pressure on the bed, which increases the sediment's effective weight, which causes less sediment in suspension. If there is exfiltration, the opposite occurs, and more sediment is brought in suspension. Another effect of in- and exfiltration is the change in the boundary layer. The boundary layer is reduced with infiltration, while exfiltration thickens the boundary layer (Bakhtyar, Barry, et al., 2009).

### 2.2.2 Onshore directed processes

The swash zone is characterized by high turbulence levels. The turbulence plays a relevant role in sediment transport (J. Puleo, Beach, Holman, & Allen, 2000). It causes that sediment is stirred up and bringing it into a well-mixed suspension. During uprush, turbulence is dominated by the wave bore, while during the backwash, it is dominated by the bed turbulence and the growing boundary layer. Masselink and Puleo (2006) found that the wave bore turbulence during the uprush is greater than the bed turbulence, and the crowing boundary layer during backwash.

The wave bore turbulence is the largest at the beginning of the swash zone, where the bore interacts with the offshore directed backwash. This results in large amounts of suspended sediment brought into the swash zone (Masselink & Puleo, 2006), which means a higher potential for onshore directed sediment transport.

Another important aspect of onshore directed sediment transport is wave asymmetry and skewness. Research shows that these nonlinearities are relevant to sediment transport in the swash zone (Austin, Masselink, O'Hare, & Russell, 2009). Although the water level fluctuations in the swash cannot strictly be seen as waves anymore, wave skewness and wave asymmetry can indirectly influence the sediment transport in the swash zone (Rooijen, 2011). The wave skewness and asymmetry influence the run-up limit, swash asymmetry and velocities of a single swash event.

Wave skewness is defined as waves with a sharp crest and flat trough (figure 2.3). Due to this, the velocities are higher under the crest compared to the trough. This causes an onshore directed sediment transport. Wave asymmetry means that a wave has a steep wavefront and a gentler wave back, as shown in figure 2.3. Grasso et al. (2011) found that a weak skewness or a strong wave skewness in combination with a large enough wave asymmetry results in onshore directed sediment transport. However, a small wave asymmetry combined with a strong wave skewness induces offshore sediment transport.

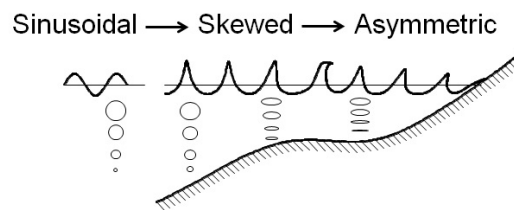


**Figure 2.3:** *Nonlinearities of waves propagating (Rocha, 2014)*

Swash-swash interaction is depending on the incoming wave period in relation to the time needed for the uprush and backwash of a wave. This interaction can be divided into three categories, as showed in figure 2.4 (Cáceres & Alsina, 2012):

1. Wave capture, the second wave has a higher velocity and captures the first one during the uprush. This interaction is not expected to change the sediment transport because the sediment transport from the original uprush will be combined with the overtaking bore.
2. Weak wave-backwash, the incoming wave faces the previous wave, which is in the offshore direction. The incoming wave contains more energy, which results in an onshore directed flow. This causes high suspended sediment concentrations and net onshore directed transport.
3. Strong wave-backwash, the same as weak wave-backwash. Though, the incoming wave contains less energy. This results in a stationary bore and finally to an offshore directed flow. These interactions lead to onshore sediment transport.

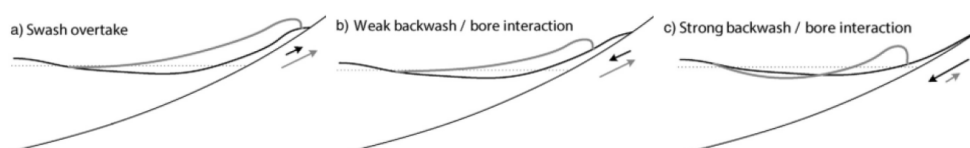


**Figure 2.4:** *Swash-swash interaction (Chardón-Maldonado et al., 2015)*

### 2.2.3 Offshore directed processes

Bed slope effects stimulate offshore directed sediment transport. Due to the gravitational force on the sediment particles. The gravitational force stimulates sediment transport during backwash and suppresses sediment transport during uprush, which enhances offshore sediment transport. According to Walstra, Van Rijn, Van Ormondt, Brière, and Talmon (2007) influences the bed slope effect the net sediment transport in three ways: change in direction when the sediment is in motion, change the threshold for sediment motion or/and influences in the near bed flow velocity. A steeper beach has a stronger influence on sediment transport (Jongedijk, 2017).

Another process that stimulates offshore sediment transport is sediment response time. Sediment response time is the time needed for sediment before it starts to move. A high sediment response time causes that less sediment is transported because the swash cycle can be finished before the grains start to move (Jongedijk, 2017). However, when the sediment response time is lower than the uprush period, it causes that the threshold for grains to move can be reached within the uprush while the sediment is transported during the backwash, which results in more offshore directed sediment transport.

## 2.3 Net sediment transport formulations

Nearshore sediment transport formulations are most of the times based on the relation between dimensionless bed shear stress (Shields parameter) and Meyer-Peter and Muller sediment transport formulation (Bakhtyar, Ghaheri, Yeganeh-Bakhtiary, & Barry, 2009). This relation is applicable to the seaward end of the swash zone. Bed shear stress formulations have previously been used to calculate the total sediment load, therefore it can be assumed that formulations based on the dimensionless bed shear stress can also be used to calculate the total sediment load (Larson et al., 2004).

The first formulation is the formulation of Larson et al. (2004) (section 2.3.1) based on the bed shear stress ( $\tau_b$ ) in combination with bed slope effects, as can be seen in table 2.1. The second formulation can be found in section 2.3.2, and is a simplification of the formulation of Larson et al. (2004) based on the bed shear stress. The third formulation is the SANTOSS formulation (Ribberink, 2011). This formulation is, like the bed shear stress formulation of Larson et al. (2004), based on the wave skewness and asymmetry, bed shear stress and sediment response time (section 2.3.3).

**Table 2.1:** *Sediment transport processes overview which are included in the formulations*

| Direction | Process                        | SANTOSS | Larson et al. (2004),<br>Bed shear stress | Larson et al. (2004),<br>Run-up |
|-----------|--------------------------------|---------|---|---------------------------------|
| General   | Bed shear stress               | X       | X   |                                 |
|           | Groundwater                    |         |   |                                 |
| Onshore   | Bore turbulence                |         |   |                                 |
|           | Wave skewness and<br>asymmetry | X       | X   | X                               |
|           | Swash-swash<br>interaction     |         |   |                                 |
| Offshore  | Bed slope                      |         | X   | X                               |
|           | Response time                  | X       |   |                                 |

### 2.3.1 Formulations of Larson: Bed shear stress

Madsen (1991) derived a net sediment transport rate formulation for the instantaneous beach load in the swash zone which was further generalized by Madsen (1993). Larson et al. (2004) improved this formulation, which is widely used to model net sediment transport in the swash zone. Part of the improvement was that Larson et al. (2004) integrated the dimensionless bed shear stress over a single swash cycle at a specific location which results in a mean net sediment transport rate formulation, equation 2. Furthermore, Larson et al. (2004) neglected the critical bed shear stress.

$$\frac{q_s}{\sqrt{(s-1)gd^3}} = \frac{8I_U}{1 + \frac{dh/dx}{\tan(\phi_m)}} - \frac{8I_B}{1 - \frac{dh/dx}{\tan(\phi_m)}} \quad (2)$$

$$\begin{aligned} I_U &= \frac{1}{T} \int_{t_s}^{t_m} (|\theta(t)|)^{3/2} dt \\ I_B &= \frac{1}{T} \int_{t_m}^{t_e} (|\theta(t)|)^{3/2} dt \end{aligned} \quad (3)$$

Where:

$q_s$ : Net sand transport rate [ $m^3/m/s$ ]

$s$ : Relative density of sediment [-]

$g$ : Gravitational force [ $9.81 m/s^2$ ]

$d$ : Sediment diameter,  $d_{50}$  [ $m$ ]

$\frac{dh}{dx}$ : Local beach slope [-]

$\phi_m$ : Friction angle for a moving grain [ $30^\circ$ ]

$T$ : Wave period [ $s$ ]

$\theta$ : Shields parameter [-]

$t_i$ : Moments during the swash cycle, s = start, m = change between uprush and backwash and e = end [ $s$ ]

Equation 2 is based on the Shields parameter (non-directional bed shear stress) during uprush and backwash. This Shields parameter (equation 4) is depended on the bed shear stress (equation 1), which can be calculated with the velocity. The Shields parameter need to be integrated over the uprush and backwash period to obtain the time-averaged Shield parameter during uprush ( $I_U$ ) and backwash ( $I_B$ ). In general, if the time-averaged Shields parameter during uprush is larger than during backwash, sediment will be transported onshore and vice versa. However, the time-averaged Shields parameter are first correct for the bed slope effect before they are subtracted from each other, as can be seen in the denominators of equation 2.

$$\theta = \tau_b / (\rho_s - \rho)gd \quad (4)$$

### 2.3.2 Formulations of Larson: Run-up limit

The second formulation of Larson et al. (2004) is a simplification of the bed shear stress formulation of Larson et al. (2004) of the previous section. This new formulation is based on: the run-up limit, beach slope, friction angle, and dimensionless coefficient  $K_c$  (equation 5). This coefficient needs to be calibrated every time the formulation is used for a specific condition. Which means that data is needed to obtain the  $K_c$ -value before it can be used to research the swash zone development. Resulting in that the formulation can only be used after an experiment and not for the full data set.

Calibration coefficient  $K_c$  is introduced in the formulation to replace the unknown friction coefficient and  $\Gamma$ , which characterizes the non-dimensional velocity variation in time at all locations in the swash zone. With introduction of  $K_c$  the formulation could be used without the unknown parameters, however the calibration of  $K_c$  against field data becomes essential. In this research a  $K_c$ -value of  $1.6 \times 10^{-3}$  will be used. This value is based on the four experiments of Larson et al. (2004).

$$q_{b,net} = -K_c 2\sqrt{2g}R^{3/2} \left(1 - \frac{z}{R}\right)^2 \times \frac{\tan(\phi_m)}{\tan^2(\phi_m) - \left(\frac{dh}{dx}\right)^2} \left(\frac{dh}{dx} - \tan \beta_{eq}\right) \quad (5)$$

Where:

$q_s$ : Net sediment transport in the swash zone [ $m^3/m/s$ ]

$K_c$ : Dimensionless coefficient [ $1.6 \times 10^{-3}$ ]

$g$ : Gravitational force [ $9.81 m/s^2$ ]

$R$ : Run-up limit, [ $m$ ]

$z$ : The elevation above the location where  $x = x_s$  ( $z$  is pointing upwards) [ $m$ ]

$\phi_m$ : Friction angle [ $30^\circ$ ] (Nam, Larson, Hanson, et al., 2009)

$\frac{dh}{dz}$ : Local beach slope [-]

$\beta_e$ : Equilibrium beach slope [-]

The direction of the calculated net sediment transport rates is determined by the difference between the local and equilibrium bed slope. If the local bed slope is steeper than the equilibrium bed slope, this part becomes positive causing a negative net sediment transport rate, which indicates onshore directed sediment transport. The amount of the net transport rate depends on the run-up limit, elevation, and local bed slope.

### 2.3.3 SANTOSS formulations

The two formulations of Larson et al. (2004) do not calculate the net sediment transport perfect (Larson et al., 2004). Therefore, another approach will be tested, the SANTOSS formulation. This formulation is not developed for the swash zone. However, the formulation has acceptable net sediment transport rates for non-breaking waves and currents. The SANTOSS formulations does not have a calibration coefficient which is an advantage over the formulation of Larson et al. (2004) based on the run-up limit.

The processes which are included in SANTOSS formulation are the bed shear stress, ripple height, sheet flow layer thickness, wave speed, peak orbital velocity and settling velocity. However, some processes are not included, which are important for the swash zone. The missing processes are the bed slope effects, groundwater, bore turbulence and swash-swash interaction. Because, the SANTOSS formulation is never used for the swash zone, it is unknown how the results will be for the swash zone.

$$\vec{\Phi} = \frac{\vec{q}_s}{\sqrt{(s-1)gd^3}} = \frac{\sqrt{|\theta_c|T_c \left( \Omega_{cc} + \frac{T_c}{2T_{cu}} \Omega_{tc} \right) \frac{\vec{\theta}_c}{|\theta_c|} + \sqrt{|\theta_t|T_t \left( \Omega_{tt} + \frac{T_t}{2T_{tu}} \Omega_{ct} \right) \frac{\vec{\theta}_t}{|\theta_t|}}}{T} \quad (6)$$

Where (Van der A et al., 2013):

$\Phi$ : Non-dimensional sand transport rate [-]

$q_s$ : Net sand transport rate [ $m^3/m/s$ ]

$s$ : Relative density of sediment [-]

$g$ : Gravitational force [ $9.81 m/s^2$ ]

$d$ : The sediment diameter,  $d_{50}$  [ $m$ ]

$\theta_i$ : Shields parameter for the wave crest (i=c) and trough (i=t) [-]

$T$ : Wave period [ $s$ ]

$T_i$ : Wave period for crest (i=c) and wave period for trough (i=t) [ $s$ ]

$T_{iu}$ : Time length of accelerating part of wave crest (i=c) and trough (i=t) [ $s$ ]

$\Omega_{cc}$ : The sand load that enters during the wave crest and is transported during the crest [-]

$\Omega_{tc}$ : The sand load that enters during the wave crest and is transported during the trough [-]

$\Omega_{ct}$ : The sand load that enters during the wave trough and is transported during the trough [-]

$\Omega_{tt}$ : The sand load that enters during the wave trough and is transported during the crest [-]

The SANTOSS formulation is based on the non-dimensional bed shear stress, the Shields parameter (equation 4). This Shield parameter is used as input for the formulation and to calculate the sand load which enters during each half-cycle  $\Omega_i$  by using equation 7. The equation shows that when the critical Shield parameter ( $\theta_{cr}$ ) is higher than the Shield parameter, the sand load is zero, else the sand load can be determined using coefficient  $m$  and  $n$  (Ribberink, 2011). Subsequently,  $\Omega_i$  can be used in equation 9 to determine the sediment transported in combination with how much sediment remains in suspension and will be transported by the next half-cycle. But besides  $\Omega_i$  a phase lag parameter ( $P_i$ ) is required. This phase lag parameter is depended on the bed regime (ripple or sheet flow) and can be calculated by using equation 8 (Nomden, 2011). In this equations,  $\alpha$  represents a calibration coefficient,  $\eta$  the ripple height,  $\delta_{si}$  the sheet flow layer thickness,  $\xi$  is calibration factor,  $c_w$  is the wave speed,  $\hat{u}_i$  is the peak orbital velocity and  $W_s$  is the settling velocity (Van der A et al., 2013).

$$\Omega_i = \begin{cases} 0 & \text{if } |\theta_i| \leq \theta_{cr} \\ m(|\theta_i| - \theta_{cr})^n & \text{if } |\theta_i| > \theta_{cr}. \end{cases} \quad \text{with } i=c,t \quad (7)$$

$$P_i = \begin{cases} \alpha \left( \frac{1+\xi \hat{u}_i}{c_w} \right) \frac{\eta}{2(T_i - T_{iu})w_s} & \text{if } \eta > 0 \text{ (ripple regime)} \\ \alpha \left( \frac{1+\xi \hat{u}_i}{c_w} \right) \frac{\delta_{si}}{2(T_i - T_{iu})w_s} & \text{if } \eta = 0 \text{ (sheet flow regime)} \end{cases} \quad \text{with } i=c,t \quad (8)$$

$$\begin{aligned} & \text{if } P_c \leq 1 \quad \Omega_{cc} = \Omega_c \text{ and } \Omega_{tc} = 0 \\ & \text{if } P_c > 1 \quad \Omega_{cc} = \frac{1}{P_c} \Omega_c \text{ and } \Omega_{tc} = \left( 1 - \frac{1}{P_t} \right) \Omega_t \\ & \text{if } P_c \leq 1 \quad \Omega_{tt} = \Omega_c \text{ and } \Omega_{ct} = 0 \\ & \text{if } P_c > 1 \quad \Omega_{tt} = \frac{1}{P_t} \Omega_t \text{ and } \Omega_{ct} = \left( 1 - \frac{1}{P_c} \right) \Omega_c \end{aligned} \quad (9)$$

## 2.4 Suitable data sets

There are different data sets available to develop, verify and validate sediment transport formulations for the coastal zone. However, not all the data sets are suitable for the swash zone. This can be, for example, due to limited data availability in the swash zone. Three recent (within last ten years) experimental data sets, collected in wave flumes, are applicable to the swash zone: BARDEX II (Masselink et al., 2013), RESIST (Eichentopf et al., 2019) and the new data set Shaping the Beach (van der Werf et al., 2019). For Shaping the Beach and BARDEX II, irregular wave conditions are used (erosive and accretive), while for RESIST, bichromatic wave conditions are used. Furthermore, the RESIST and Shaping the Beach data sets are collected in the CIEM flume in Spain, while the BARDEX II data set is collected in the Delta flume in the Netherlands. More information about the data sets, including measurement equipment, can be found in section 3.1.

### 3 Methodology

The research is carried out in three phases corresponding to the three research questions in section 1.5. In the first phase, wave conditions were selected. Also, in this phase, the selected wave conditions were analysed and the required input data for the formulations are obtained. In the second phase, the essential processes and parameters which influence the net sediment transport rates are listed per formulation and the net sediment transport formulations are analysed. Furthermore, the formulations are used to predict the net sediment transport rates and the results are compared. At last, the "best" formulation is chosen to improve in the third phase. In this third phase, the formulation for improvement is analysed to check the most important parameters. Subsequently, these most important parameters are improved and tested. At last, the improvements are analysed how they can be implemented. These steps are discussed in more detail below.

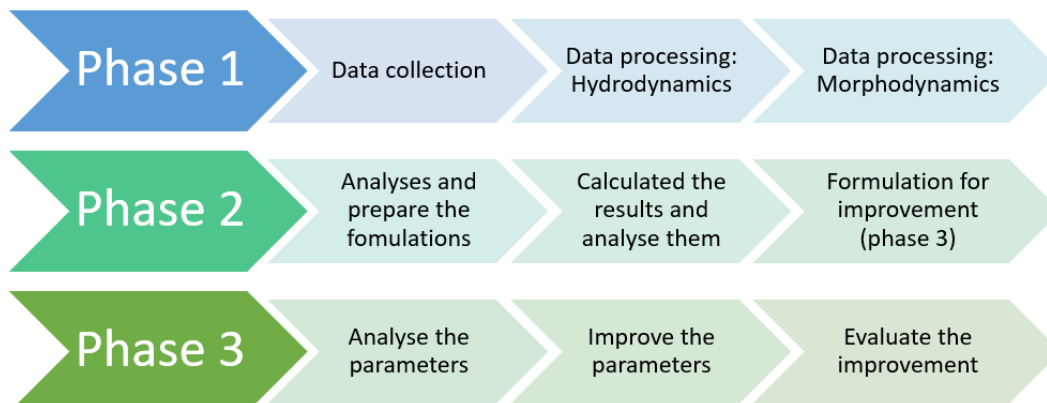


Figure 3.1: The three phases of the research

#### 3.1 Data collection and analysing

In this research three data sets are used: Shaping the Beach, RESIST and BARDEX II. For the Shaping the Beach and RESIST data sets, the experiments are carried out at the CIEM flume in Barcelona. While BARDEX II is carried out at the Delta flume in the Netherlands. Each of these data set consist of multiple wave conditions. From the wave conditions are there two selected per data set, one erosive wave and one accretive wave, resulting in six wave conditions. The wave conditions are selected on when they are applied in the experiment.

##### Shaping the Beach

The Shaping the Beach experiment is carried out in the CIEM flume in Barcelona, Spain. This flume is 100 m long, 3 m wide and 4.5 m deep (Eichentopf et al., 2019). At the start of the wave conditions, a 1:15 beach slope was build-up out-off medium sand,  $D_{50} = 0.25 \text{ mm}$ . In the Shaping the Beach experiment, four different irregular wave conditions are performed in order E1, A1, E2 and E3 (van der Werf et al., 2019). This research focuses on erosive wave condition 1 (E1) and accretive wave condition 1 (A1). The data/characteristics of these two wave conditions are shown in table 3.1.

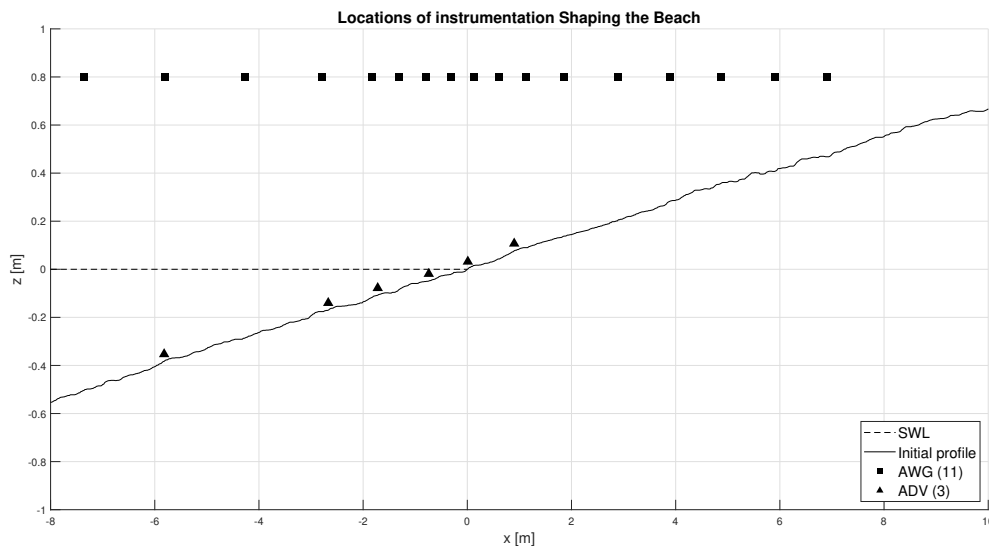
Table 3.1: Shaping the Beach irregular wave characteristics,  $b$  = benchmark,  $E$  = erosive wave condition and  $A$  = accretive wave condition

| Name  | Wave type | $H_s$ [m] | $T_p$ [s] | $W_s$ [m/s] | $\Omega$ [-] | Time [min] | Initial profile | Equilibrium profile |
|-------|-----------|-----------|-----------|-------------|--------------|------------|-----------------|---------------------|
| StB-b | Irregular | 0.42      | 4.0       | 0.034       | 3.09         | 1x15       | 1:15            | 1:15.2              |
| StB-E | Irregular | 0.45      | 3.5       | 0.034       | 3.78         | 6x30       | StB-b           | 1:17.6              |
| StB-A | Irregular | 0.25      | 5.2       | 0.034       | 1.41         | 10x60      | StB-E           | 1:10.2              |

The swash zone starts one meter seaward from the original coastline. To collect the data in the swash zone eleven Acoustic Wave Gauges (AWG) and four Acoustic Doppler Velocimeters (ADV) were used. AWGs were used to measure the water level elevation and the ADVs were used to measure the velocity in three dimensions, where the focus in this research is on the cross-shore velocity. The x-locations of the AWGs and ADVs are shown in table 3.2 and the measurement setup in figure 3.2. The profiles were measured after each run with a wheel which rolls over the bed and measures the profile.

**Table 3.2:** *Shaping the beach locations of the AWG and ADV*

| Instrument | $N^\circ$ | Cross-shore location, $x=0$ at the initial shoreline [m]                 |
|------------|-----------|--|
| AWG        | 11        | -1.31, -0.80, -0.32, 0.12, 0.61, 1.12, 1.85, 2.90, 3.89, 4.87, 5.9, 6.91 |
| ADV        | 4         | -1.72, -0.74, 0.01, 0.90 (3 cm above the bed)                            |

**Figure 3.2:** *Swash zone instrumentation Shaping the Beach*

## RESIST

For RESIST, the same wave flume as for Shaping the Beach is used with the same beach slope and grain size,  $D_{50} = 0.25 \text{ mm}$ . In contrast to the Shaping the Beach experiment, for RESIST five bichromatic wave conditions (E1, E2, A1, A2 and A3) are used in three sequences of multiple wave conditions (Eichentopf, Van der Zanden, Cáceres, Baldock, & Alsina, 2020). In this research, only wave condition E1 of sequence three and wave condition A1 of sequence one are used. The details of these preformed wave conditions can be found in table 3.3 (Eichentopf et al., 2019).

**Table 3.3:** *RESIST bichromatic wave characteristics, b = benchmark, E = erosive wave condition and A = accretive wave condition*

| Name  | Wave type   | $H_s$ [m] | $T_p$ [s] | $W_s$ [m/s] | $\Omega$ [-] | Time [min] | Initial profile | Equilibrium profile |
|-------|-------------|-----------|-----------|-------------|--------------|------------|-----------------|---------------------|
| RES-b | Bichromatic | 0.42      | 4.0       | 0.034       | 3.09         | 30         | 1:15            | 1:15.2              |
| RES-E | Bichromatic | 0.64      | 3.7       | 0.034       | 5.09         | 240        | Rest-b          | 1:19.4              |
| RES-A | Bichromatic | 0.32      | 4.7       | 0.034       | 2.00         | 600        | Rest-E (seq. 1) | 1:12.2              |

The swash zone of the RESIST experiment starts at one meter seaward from the original coastline, based on the water level measurements. Within the swash zone the water level elevation and velocities are measured with nine AWGs and five ADVs. The locations can be found in table 3.4 and for the measurement setup, see figure 3.3 (Eichentopf et al., 2019). For the profile measurement is the same technique is applied as for Shaping the Beach.

**Table 3.4:** *RESIST locations of the AWG and ADV*

| Instrument | $N^\circ$ | Cross-shore location, $x=0$ at the initial shoreline [m] |
|------------|-----------|--|
| AWG        | 9         | -1.57, -0.52, 0.47, 1.25, 2.31, 3.5, 4.55, 5.56, 6.51    |
| ADV        | 5         | -1.54 -0.53, 0.07, 0.15, 0.20 (3 cm above the bed)       |

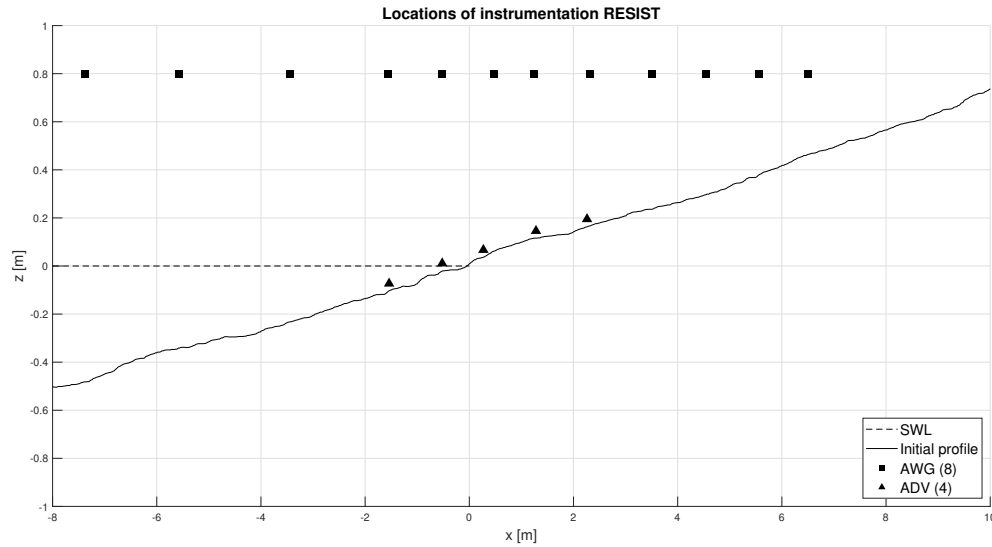


**Figure 3.3:** Swash zone instrumentation RESIST

## BARDEX II

The experiments of BARDEX II were carried out in the Delta Flume, the Netherlands. The flume dimensions are 300 m long, 5 m wide and 9.5 m deep (Wenneker, Hoffmann, & Hofland, 2016). Just like the other two data sets, BARDEX II contains multiple irregular wave conditions. This research focuses on wave condition A1 an erosive wave and wave condition A6 an accretive wave (Masselink et al., 2016). The beach was constructed with medium-sized sand ( $D_{50} = 0.42$  mm) and a 1:15 initial bed slope (Masselink et al., 2013). The details of wave conditions A1 and A6 can be found in table 3.5.

**Table 3.5:** BARDEX II irregular wave characteristics

| Name   | Wave type | $H_s$ [m] | $T_p$ [s] | $W_s$ [m/s] | $\Omega$ [-] | Time [min] | Initial profile | Equilibrium profile |
|--------|-----------|-----------|-----------|-------------|--------------|------------|-----------------|---------------------|
| BAR-A1 | Irregular | 0.8       | 8         | 0.046       | 2.2          | 300        | 1:15            | 1:12.8              |
| BAR-A6 | Irregular | 0.6       | 12        | 0.046       | 1.1          | 255        | BAR-A5          | 1:9.0               |

For BARDEX II different instrumentation is used than for the Shaping the Beach and RESIST campaigns. For BARDEX II pressure transducers (PT), Vectrinos (VEC) and electromagnetic current meter (EM) were used. The x-locations of the instrumentation are shown in table 3.6 and figure 3.4. The PTs were used to measure the pressure; this pressure signal is converted to a water level elevation. The VECs and EMs were used to measure the velocities in three directions (Masselink, Conley, & Ruju, 2012). In this research, only the cross-shore velocity is used. Further, for the profile measurement is a wheel used, just like the Shaping the Beach and RESIST data set.

**Table 3.6:** BARDEX II locations of the EMs, VECs and PTs

| Instrument | $N^{\circ}$ | Cross-shore location and between brackets the z location. x,z are 0 at the initial shoreline [m].                |
|------------|-------------|--|
| EM         | 9           | -19 (-1.17), -19 (-0.97), -19 (-0.77), -14 (-0.84), -14 (-0.64), -14 (-0.44), -9 (-0.50), -9 (-0.30), -9 (-0.10) |
| VEC*       | 2           | A1: 0.27 and 1.80, A6: 1.62 and 3.08   |
| PT         | 4           | -19, -14, -9, 2.5  |

\*VEC's have different locations for A1 and A6.

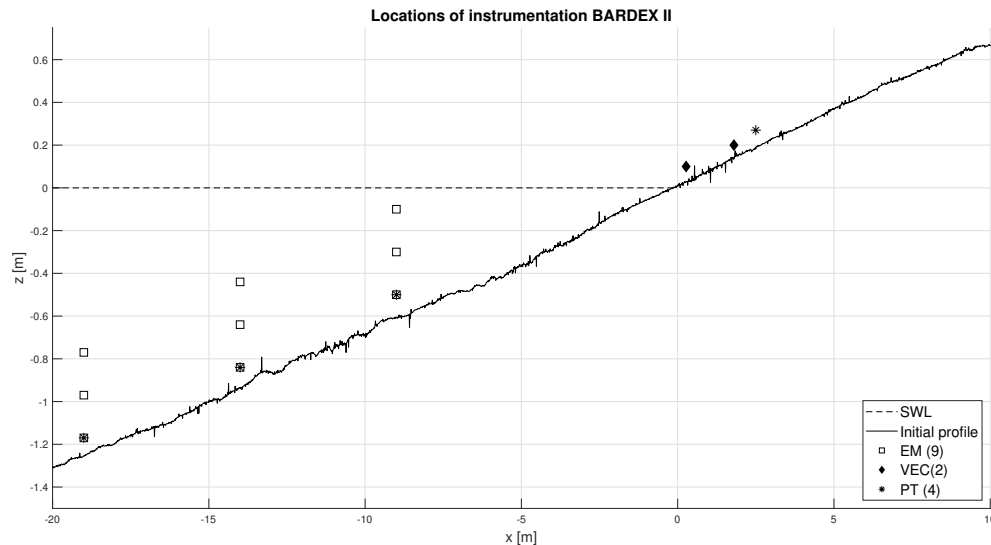


Figure 3.4: *Deltares instrumentation BARDEX II*

## 3.2 Data processing

For understanding the six wave conditions and to obtain the required input data for the formulations the hydrodynamics and morphodynamics were analysed.

### 3.2.1 Hydrodynamics

The wave sequences in the wave flume are generated based on the peak period ( $T$ ) and significant wave height ( $H_s$ ). However, this does not mean that the wave has exactly these characteristics. Further, the wave height differs over the length of the flume. Therefore, the wave period and significant wave height are calculated at different locations in the flume for each run separately and for the total wave condition. For the wave period, a spectral analysis (Fast Fourier Transform) is applied to the measured water level elevation data. The spectral analysis results in a periodogram with the wave energy density for different frequencies (Hegge & Masselink, 1996). The highest peak in this periodogram represents the wave period. The significant wave height is determined by using the 0th spectral moment ( $m_0$ ), equation 10. This 0th spectral moment is obtained by the summation of the energy density (the frequency bands ( $S(f)$ ) multiplied with the bandwidth ( $d(f)$ )) from the lowest frequency ( $f_l$ ) to the highest frequency ( $f_u$ ) (Horstman et al., 2014). After that, the significant wave height is calculated with equation 11.

$$m_0 = \sum_{f_l}^{f_u} (S(f) \times d(f)) \quad (10)$$

$$H_s = 4 \times \sqrt{m_0} \quad (11)$$

### Velocity signal

Each wave condition of a data set has a different period and wave height, which are analysed as described above. Due to the different wave characteristics and changing bed slope, are the velocities different for each wave condition. For each wave condition, the highest onshore (maximum), mean and highest offshore (minimum) velocity is determined. The mean velocity is collected from the velocity signal from the measurement equipment after applying a low pass filter of 3 hz to remove the outliers. The maximum and minimum velocity are more challenging to obtain because the maximum and minimum velocity varies over time. Therefore, a representative velocity and acceleration signal is created by using the method of Abreu, Silva, Sancho, and Temperville (2010) and Ruessink, Ramaekers, and Van Rijn (2012) (Appendix A). With this method equation 12 is used for the representative velocity signal ( $U(t)$ ) and equation 13 is used for the representative acceleration signal ( $a(t)$ ).

$$U(t) = U_{rms} \sqrt{2} f \frac{\left[ \sin(\omega t) + \frac{r \sin(\phi)}{1 + \sqrt{1 - r^2}} \right]}{[1 - r \cos(\omega t + \phi)]} \quad (12)$$

$$a(t) = U_{rms} \sqrt{2} f \frac{\left[ \cos(\omega t) - r \cos(\phi) - \frac{r^2}{1 + \sqrt{1 - r^2}} \sin(\phi) \sin(\omega t + \phi) \right]}{[1 - r \cos(\omega t + \phi)]^2} \quad (13)$$

Where  $U_{rms}$  is the orbital velocity amplitude and  $f$  is a dimensionless factor.  $\omega$  is the angular frequency,  $\phi$  the phase and  $r$  a non-linearity index, the formulations for  $f$ ,  $\phi$  and  $r$  can be found in appendix A.

### 3.2.2 Morphodynamics

For understanding the changes in morphodynamics and net sediment transport rates, the equilibrium bed slope is determined. This bed slope is based on the Dean number ( $\Omega$ ), which follows from the wave height, fall velocity ( $W_s$ ) and period, equation 14 (Dean et al., 1973). According to Wright and Short (1984) a higher Dean number represents dissipative beaches and a lower Dean number reflective beaches. In combination with data from several beach studies Masselink (1993) determined the best fit relation to estimate the equilibrium beach slope ( $\beta_{eq}$ ), equation 15.

$$\Omega = \frac{H_s}{W_s \times T} \quad (14)$$

$$\tan(\beta_{eq}) = 0.116 * \Omega^{-1/2} \quad (15)$$

Furthermore, the net sediment transport rates ( $q_s$ ) are calculated for the active part of the profile. For the net sediment transport rates, the mass conservation technique in equation 16 is used. To obtain the correct net sediment transport rates, the transport rates are calculated from the left-hand side (wave paddle) and right-hand side (end of the flume). The net sediment transport rates calculated from left-hand side and right-hand side have the same pattern but do not result in the same quantity, as can be seen in figure 3.5. Also, the reliability of the net sediment transport rates reduces with distance from the boundary condition. Therefore, the calculated transport rates from the left-hand side and right-hand side are combined to obtain a weighted function. This weighted net sediment transport rate gives the highest validity (Posanski, 2018). The weighted net sediment transport rates does not start at the boundary condition; it starts after the sum curve of the absolute values of change in transport exceeds a threshold of  $4 \times 10^{-6} \text{ m}^2/\text{s}$  (Posanski, 2018).

$$q_s(i) = q_s(i - 1) - \frac{(1 - \varepsilon_0) \times (z_{final}(i) - z_{begin}(i)) \times \Delta x}{\Delta t} \quad (16)$$

In which ( $\varepsilon_0$ ) is the porosity.  $z_{final}$  and  $z_{begin}$  refer to the elevation of the final and begin profile.  $\Delta x$  is the space in x direction between two data point and  $\Delta t$  is the duration of the applied wave condition.

However, for RESIST, this was not possible because the profiles are not fully measured. The measurement profile reaches from 2/3 of the beach slope till the onshore end of the flume. Therefore, the net sediment transport rates for RESIST are only calculated from the right-hand side (end of the flume).

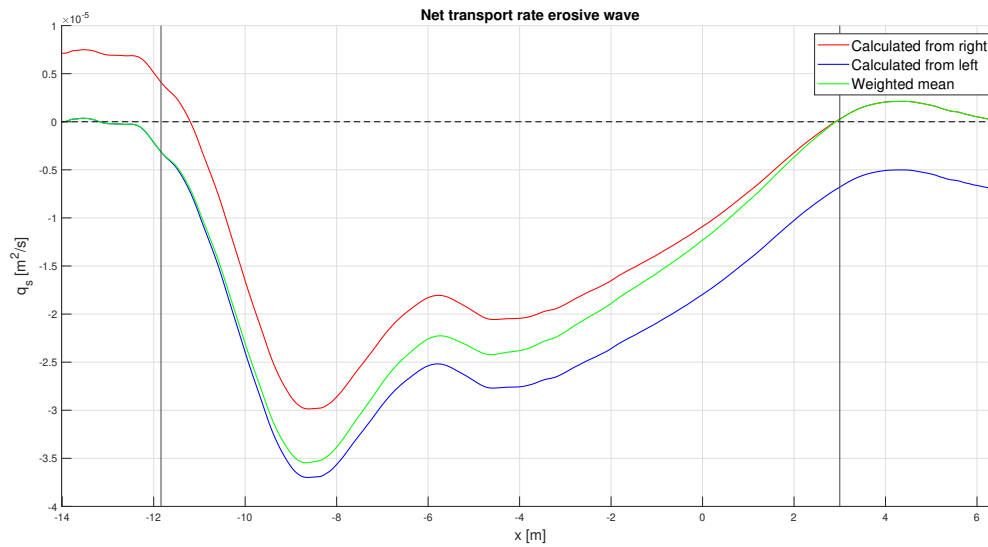


**Figure 3.5:** Weighted mean of left and right-hand side net sediment transport rates

## Sediment losses

The profiles are measured at one cross-shore location. Due to this, it is possible that the mass balance is not closed. Therefore, the losses of each run are determined to know how much sediment is missing or gained. The lost or added sediment is calculated by subtracting the start profile from the final profile for each run.

The error is reduced by using the weighted mean, as described above. For RESIST the error is corrected by shifting the final profile with the mean difference between the start and final profile (van der Zanden, personal communication, March 5, 2020), the so called long-shore correction. This method is also tested for the other data set. However, this does not show a significant difference in losses and/or transport rate (as can be seen in figure 3.6). Therefore, the weighted mean is applied for Shaping the Beach and BARDEX II because this gives a higher validation.

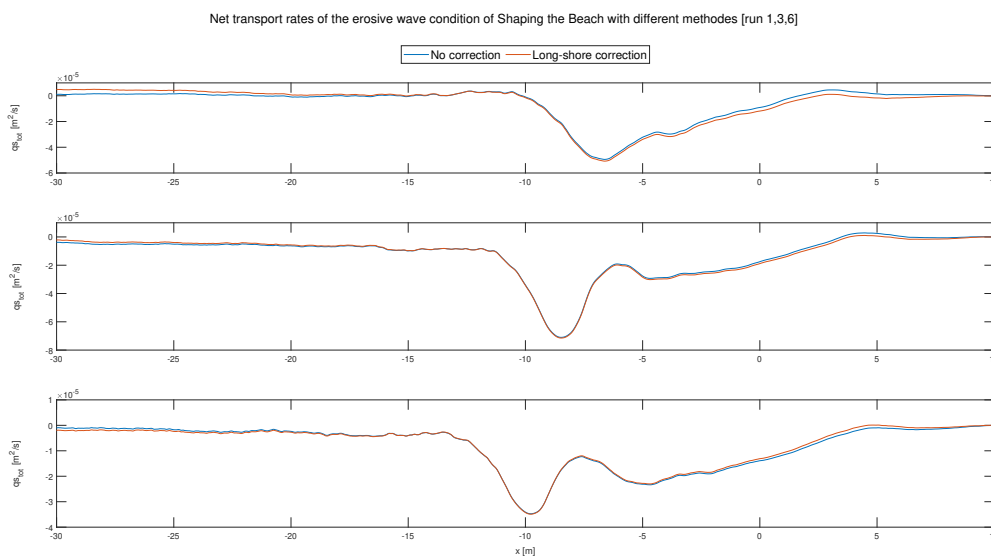


**Figure 3.6:** Difference between no profile correction and long-shore correction for the erosive wave condition of Shaping the Beach

### 3.3 The net sediment transport formulations

The morphodynamics in the swash zone are complex and therefore a challenge to predict for coastal engineers (J. A. Puleo, Lanckriet, Conley, & Foster, 2016). To understand the complex morphodynamics in the swash zone the essential processes and parameters are analysed to see how they influence the sediment transport. Therefore, a distinction is made between onshore transport, offshore transport and general (depending on the value the transport is on- or offshore directed). These essential processes and parameters are obtained by doing a literature review.

#### 3.3.1 Net sediment transport formulations

After understanding the essential processes and parameters which drive the sediment transport in the swash zone, three formulations are used:

- The SANTOSS formulation (Ribberink, 2011; Van der A et al., 2013)
- Formulation of Larson et al. (2004) based on the bed shear stress
- Formulation of Larson et al. (2004) based on the run-up limit

#### Program

The SANTOSS formulation was already programmed in MATLAB. However, before it could be used, the script is prepared for the input data and some parameters must be set, for example, if mix sediment is used or a mean  $D_{50}$ . The formulations of Larson et al. (2004) were not programmed yet. Therefore, these formulations are programmed in MATLAB.

#### Data preparation

The formulations calculate the net sediment transport rate at one specific location. Therefore, different locations in the swash zone have been selected that correspond to the locations of the instrumentation. Because at these locations, the most reliable data is available, if other locations are selected interpolation is needed, which makes the data more unreliable (for the locations of the instrumentation see section 3.1). Which means that for the different data sets the locations of calculated net sediment transport rate are different, as can be seen in table 3.7. For Shaping the Beach, three locations are selected, for RESIST four locations and for BARDEX II two locations. These locations are chosen because at these locations in the swash zone all the data was available.

At these locations, the required data is collected. Part of the data followed from the first phase among which the velocities, acceleration, wave height and net sediment transport rate. Furthermore, the formulations needed data from the bathymetry. The local bed slopes are obtained by taken the elevation ten centimeters before and after the location. Followed by dividing the difference with the distance. For the local slope the elevation is obtain from the measured profiles at the start of each run or wave condition, depended on the calculation purpose (one run or total wave condition).

**Table 3.7:** *Used locations for the net sediment transport rates*

| Data set           | Location with respect to the shoreline [m] |
|--------------------|--|
| Shaping the Beach  | -0.70, 0.01, 0.9                           |
| RESIST             | -0.53, 0.28, 1.26, 2.28                    |
| BARDEX II wave A1* | 0.27, 1.80                                 |
| BARDEX II wave A6* | 1,62, 3.08                                 |

\*Instrumentation is replaced for the different wave conditions.

#### Hypothesis

Every formulation is based on a different combination of processes and parameters. Some of them determine only the amount of the net sediment transport rate. However, all three formulations include a process which determines if the sediment is transported on- or offshore. Based on these processes and parameters (amount and direction) for every calculation a hypothesis is formed. These hypotheses include the amount of the net sediment transport rate (high or low) and the direction. The hypotheses help to understand the formulation and to see if the results match the theory.

## Results

The results of the three formulations are plotted against the measured net sediment transport rates of the first phase. This is done for each wave condition of the three data sets, so six figures (three erosive and three accretive). The plots also include an 1:1-line. Due to the line, it is easier to see how close the results of the formulations are compared to the measured net sediment transport rates. Because if the points are around the 1:1-line the formulation show promising results (left side of figure 3.7) and if the points are spread the results are not the same as measured (right side of figure 3.7).

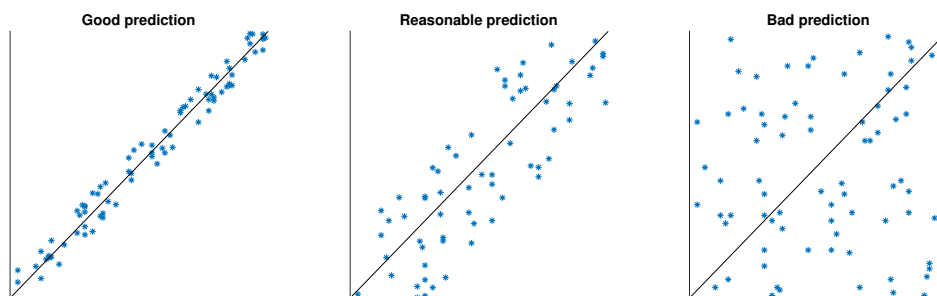


**Figure 3.7:** *Example good, reasonable and bad prediction*

Furthermore, the sediment transport is calculated for a total wave condition. The total wave conditions are calculated by two methods. For the first method the mean velocities and accelerations from each run of a wave condition is used in combination with the conditions (slope, run-up limit, etc.) at the start of the wave condition. With this input, the net sediment transport rates are calculated for the total wave condition. The second method is based on the individual results of each run. From each run within a wave condition the calculated and measured net sediment transport rates are averaged to result in the mean net sediment transport rate. The results of both methods are plotted in the same way as for each run.

### 3.3.2 Formulation for improvement

The formulations are analysed at four points: visual, Root-Mean-Square-Error (RMSE), correlation coefficients and the potential to improve the formulation. The visual aspect is based on the plots made from the results. For this visual aspect, the calculated net transport rates are analysed and the strong and weak points of the formulations are mentioned. This is done for both the amount of sediment transported and the direction. Furthermore, the RMSE is an often used method to analyse the error of a model or formulation. The RMSE is based on the difference between the measured and calculated results, as shown in equation 17. Where  $n$  is the number of observations and  $x$  and  $y$  are the results.

$$RMSE = \sqrt{\frac{\sum_{i=1}^n (x_i - y_i)^2}{n}} \quad (17)$$

Another way to check how accurate the formulations are is by using a correlation coefficient. There are multiple correlation coefficients. However, the Spearman rank correlation coefficient and Pearson product-moment correlation coefficient are mostly used correlations (de Winter, Gosling, & Potter, 2016). The Spearman correlation, equation 18, is based on the ranks of the data points (Spearman, 1961). The correlation is used for monotonic relationships and does not take the distance between the measured and calculated data into account. Because the Spearman correlation does not take the distance into account, the correlation is used mainly for the direction.

$$r_{Spearman} = 1 - \frac{6 \sum_{i=1}^n d_i^2}{n^3 - n} \quad (18)$$

Where  $d_i$  is the difference between two rankings (the ranked net sediment transport rates),  $x_i$  and  $y_i$  are the individual sample points indexed with  $i$  and  $n$  the sample size.

The Pearson correlation, equation 19, is based on the difference between the calculated and measured transport rate, which can result in a low correlation due to one large outlier (Artusi, Verderio, & Marubini, 2002; Benesty, Chen, Huang, & Cohen, 2009). The Pearson correlation can be used to find linear relationships. For both the correlation coefficients is the best possible correlation one and zero means there is no correlation. At last are the formulations assessed on potential to be improved. The potential to improve the formulation is determined by looking at which important processes are missing and if the formulation can be fit to the results by changing a parameter or process.

$$r_{Pearson} = \frac{\sum_{i=1}^n (x_i - \bar{x})(y_i - \bar{y})}{\sqrt{\sum_{i=1}^n (x_i - \bar{x})^2 \sum_{i=1}^n (y_i - \bar{y})^2}} \quad (19)$$

### 3.4 Improvement of the net sediment transport formulation

The run-up limit formulation of Larson et al. (2004), which is chosen for improvement, has different input parameters and/or data. Due to limited time it is not possible to investigate them all. Therefore first, the formulation is analysed which parameters have the most significant influence on the net sediment transport rate and which parameters can be changed because some data input is can not be changed, for example the grain size and friction angle. From these parameters the most important ones are chosen to see if they can be improved. To check if the results are an improvement, the same method is applied as is used to choose the formulation for improvement (paragraph 3.3.2), visual, RMSE and correlation coefficients. The results are compared with the situation without the improvement to check if the improvement really shows a better result and to quantify the improvement. Followed by a recommendation about the improvement, if the improvement should be used or not and how it eventually can be used in the formulation to predict the net sediment transport rate.

#### 3.4.1 Input data

The run-up limit turns out to be an important parameter for the calculations of the net sediment transport rate. For the improvement of the run-up limit, first a literature study is carried out to see which other methods there are to obtain the run-up limit. Form the literature two methods are selected to calculate the run-up limit. Both run-up limit formulations are tested and analysed to see if they give better results, as described above.

#### 3.4.2 Calibration coefficient

The second important parameter is the calibration coefficient. The calibration coefficient is calibrated based on the RMSE, as shown in figure 3.8. If the RMSE decreases, the results are an improvement. Based on this, new  $K_c$ -values are obtained with better results than with the original  $K_c$ -value. The calibration is carried out for the wave conditions of Shaping the Beach and RESIST because these wave conditions consist of more than 16 data point where BARDEX II A1 only has ten data point and BARDEX II A6 only five reliable data point which is too small to obtain a conclusion. Also the  $K_c$ -value is not calibrated for the total wave conditions. Because, according to Larson et al. (2004) has the  $K_c$ -value a correlation with the wave period and swash period. These periods are for every wave condition different, which means that there is not one optimal  $K_c$ -value for the total wave conditions.

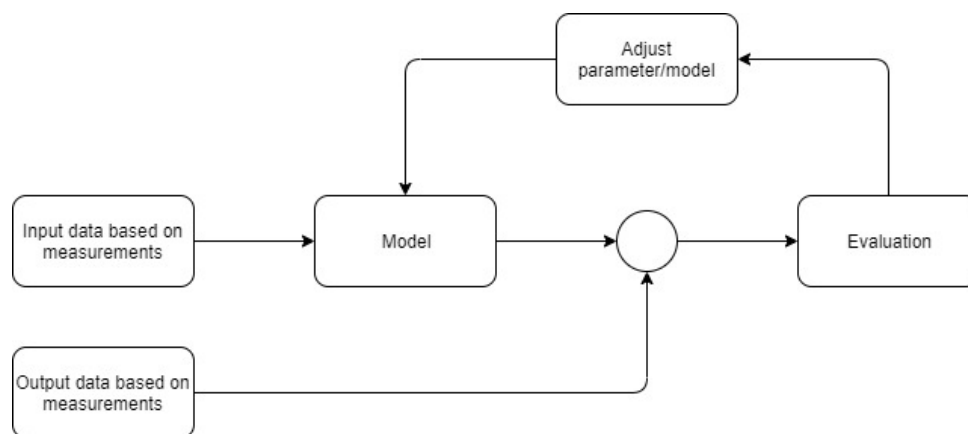


Figure 3.8: Calibration diagram for a formulation (Milivojević et al., 2009)

## 4 Results of the wave conditions

The hydrodynamics (4.1) and morphodynamics (4.2) of Shaping the Beach, RESIST and BARDEX II will be processed and compared.

### 4.1 Wave hydrodynamics

In this section, the wave hydrodynamics are analysed. The wave hydrodynamics are analysed for each of the selected wave conditions of the three data sets. First, the Shaping the Beach data set is analysed followed by RESIST and BARDEX II. The hydrodynamics are analysed to get an overview of the differences between the wave conditions and to prepare the data to use as input for the formulations in section 5.

#### 4.1.1 Shaping the Beach

The periods of the erosive and accretive wave of the Shaping the Beach data set are respectively 3.5 s (0.286 Hz) and 5.2 s (0.192 Hz) (Dionísio António et al., 2020). To check if the actual periods are the same as the used periods on paper, the wave periods are calculated with a spectral analysis. The periods from the spectral analysis match the input period as can be seen in figure 4.1 and 4.2. The decreasing wave heights in the flume is shown in figure 4.3 and 4.4 together with the water level elevation (at 3 locations) and the start and final profile of the wave condition.

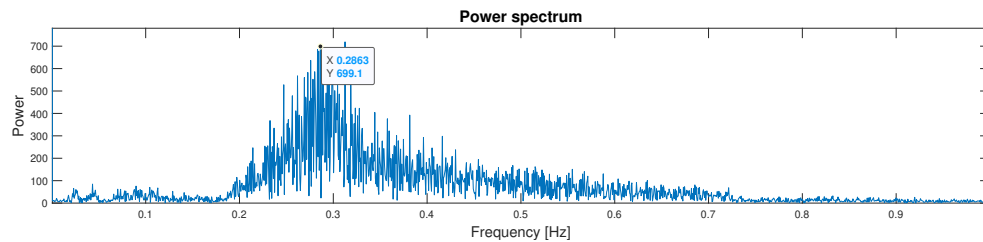


Figure 4.1: Spectral analysis from the erosive wave in deep water at  $x=-52.05$  m, Shaping the Beach

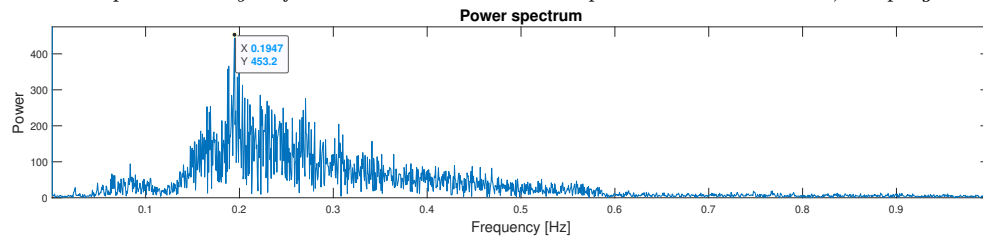


Figure 4.2: Spectral analysis from the accretive wave in deep water at  $x=-52.05$  m, Shaping the Beach

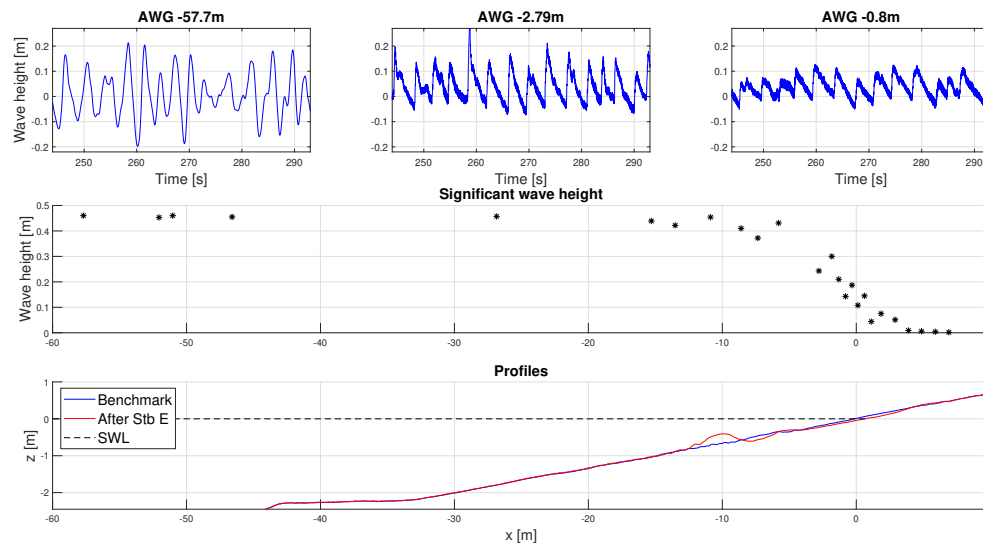
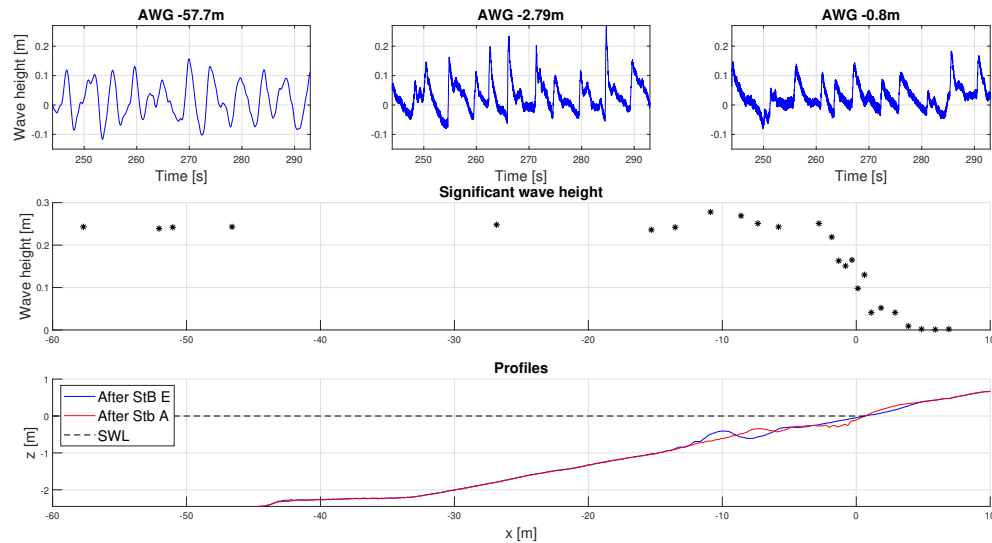


Figure 4.3: Average wave heights and profiles erosive wave, Shaping the Beach



**Figure 4.4:** Average wave heights and profiles accretive wave, Shaping the Beach

## Velocity

The velocity, in combination with acceleration, are important characteristics which influence the net sediment transport rates in the swash zone (Chardón-Maldonado et al., 2015). The mean, highest and lowest velocity for Shaping the Beach, are plotted in figure 4.5. The velocities are the average velocities over the entire wave condition (erosive or accretive). In figure 4.5, it is visible that the mean velocity is always offshore directed, with the exception of the most landward ADV of the erosive wave condition. The difference between the erosive and accretive case at  $x=-5.82$  m is small. However, the velocities and the acceleration in the swash zone is much higher during the erosive wave condition. This is due to that the waves of the erosive wave condition are more energetic (Waters, 2008).

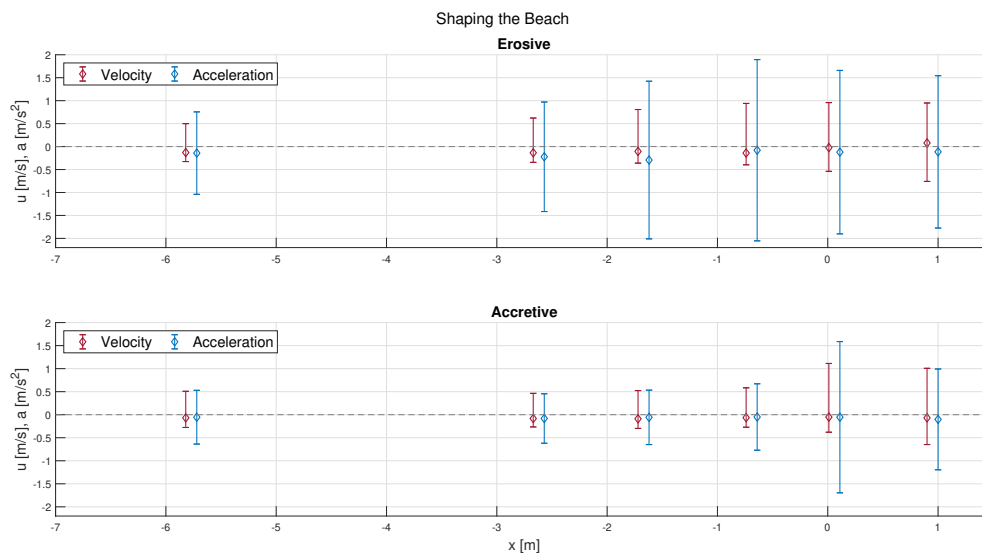


**Figure 4.5:** Mean, maximum and minimum velocities, Shaping the Beach

### 4.1.2 RESIST

For the RESIST data set, bichromatic wave conditions are used. Bichromatic wave conditions means that there are two superimposed (sinusoidal) waves. Therefore, the spectral analyses also should show two peaks. The peaks of the erosive wave are at 0.237 Hz and 0.304 Hz (4.2 s and 3.3 s), as can be seen in figure 4.6. The wave height in deep water for the erosive wave is 0.64 m, figure 4.8. These frequencies and wave heights correspond with the applied wave conditions (Eichentopf et al., 2019).

The peaks of the spectral analysis of the accretive wave condition, as shown in figure 4.7, are at 0.198 Hz and 0.227 Hz (5.1 s and 4.4 s). The wave height in deep water is 0.32 m and declines when the waves enter the surf zone (figure 4.9). These results also match the applied wave conditions (Eichentopf et al., 2019).

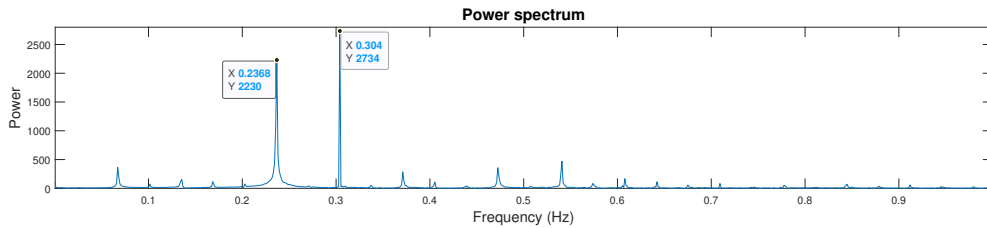


**Figure 4.6:** Spectral analysis from the erosive wave in deep water at  $x=-56.04$  m, RESIST

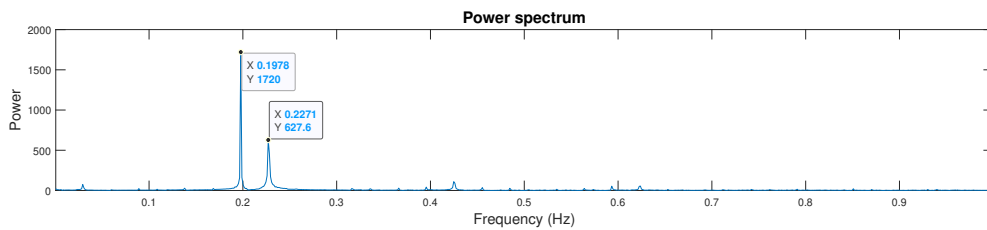


**Figure 4.7:** Spectral analysis from the accretive wave in deep water at  $x=-56.04$  m, RESIST

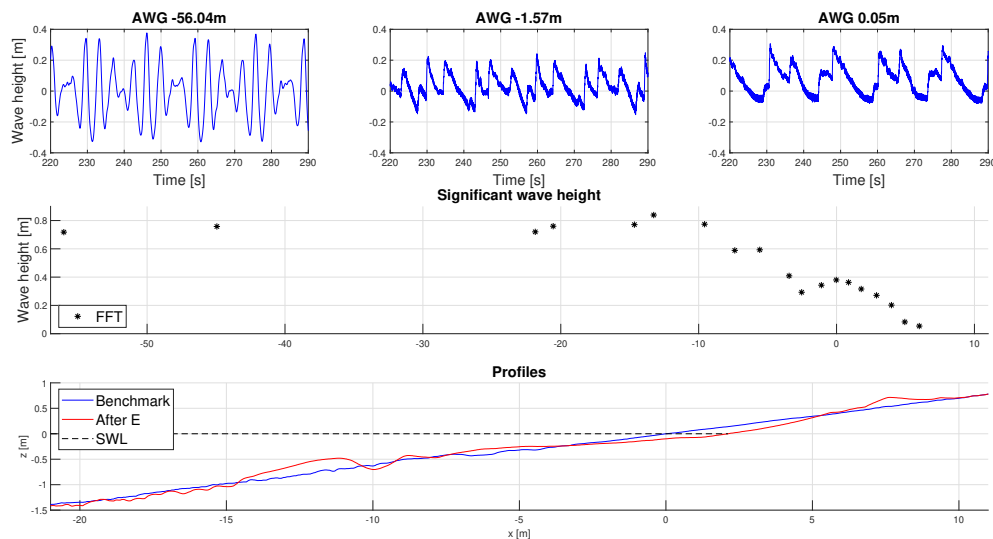


**Figure 4.8:** Average wave heights and profiles erosive wave, RESIST

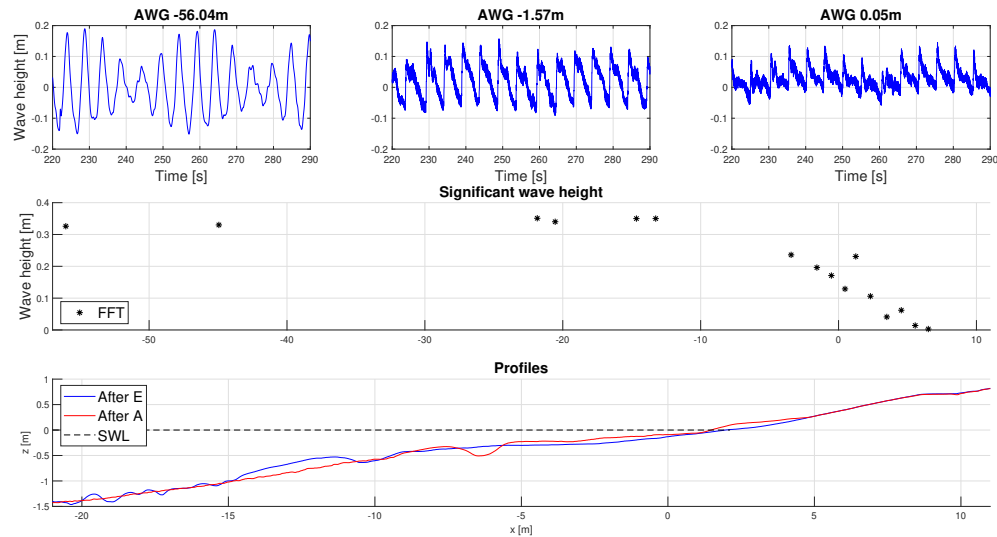


Figure 4.9: Average wave heights and profiles accretive wave, RESIST

## Velocity

The velocities during the erosive wave are higher than the accretive wave (note the range of the y-axis). This is due to the higher potential energy of the erosive wave (Waters, 2008). Further, both cases show a higher onshore velocity than offshore velocity. However, figure 4.10 shows that the mean velocities for both wave conditions are in the offshore direction, which can be explained due that the backwash lasts longer than the uprush. The acceleration is, just like the velocity, higher during the erosive wave than the accretive wave. The data of the ADV at location  $x=-4.72$  for the erosive wave is missing because this data was not available. This does not influence the research because it is outside the swash zone.

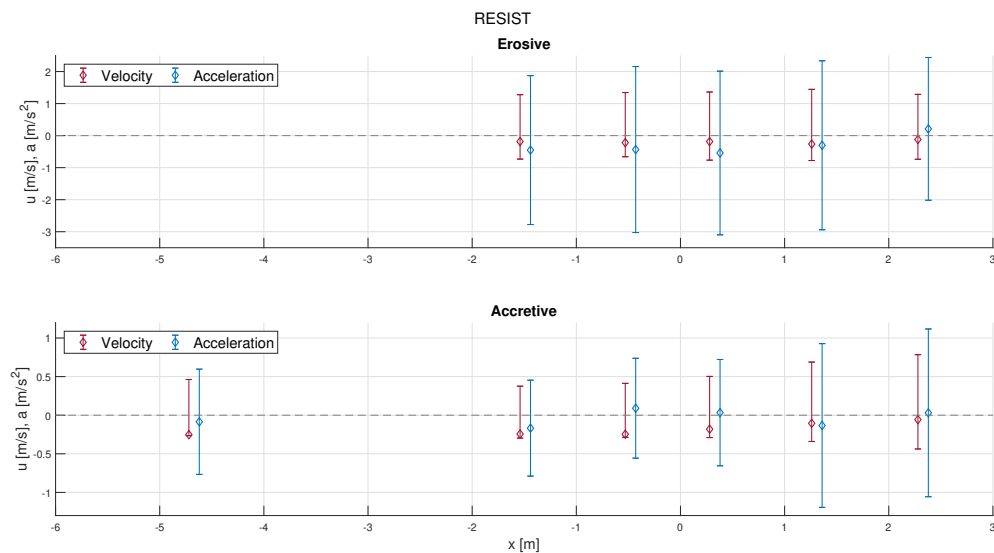


Figure 4.10: Mean, maximum and minimum velocities, RESIST

### 4.1.3 BARDEX II

The spectral analysis in figure 4.11 shows a period of 8 s (0.1245 Hz), which corresponds with the used periods of wave condition A1 (Turner et al., 2013). The obtained wave height for wave condition A1 is approximately 4 cm lower than what it should be. For wave condition A6 the wave height is 5 cm lower. The spectral analysis of wave condition A6, shows a period of 12.8 s (0.07813 Hz). This wave period is longer as the wave period initial proposed. According to the data storage report of Masselink et al. (2012) the measured wave period is indeed longer than the initially proposed wave periods.

Figure 4.11 and 4.12 show the spectral analysis of cases A1 and A6. Figure 4.13 and 4.14 shows the wave evolution and wave height in the flume for cases A1 and A6.

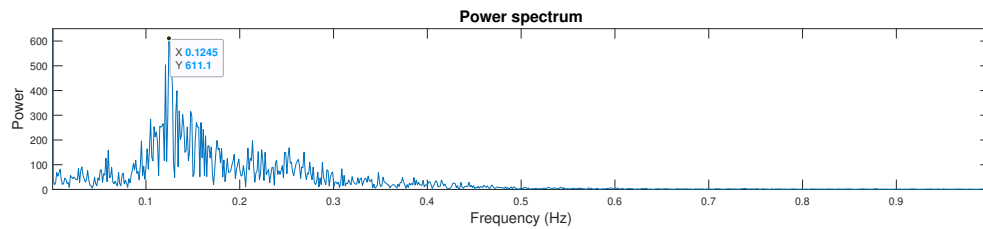


Figure 4.11: Spectral analysis from the erosive wave in deep water at  $x=-50.3$  m, BARDEX II

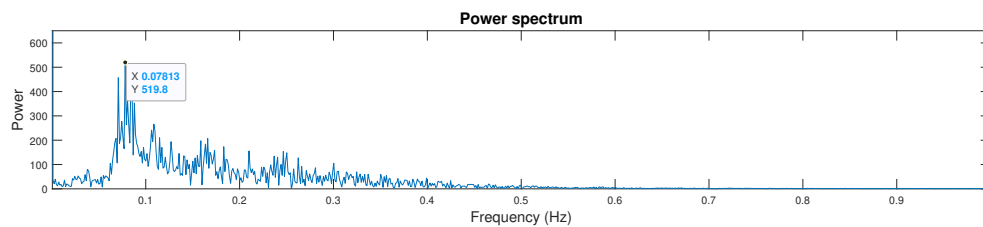


Figure 4.12: Spectral analysis from the accretive wave in deep water at  $x=-50.3$  m, BARDEX II

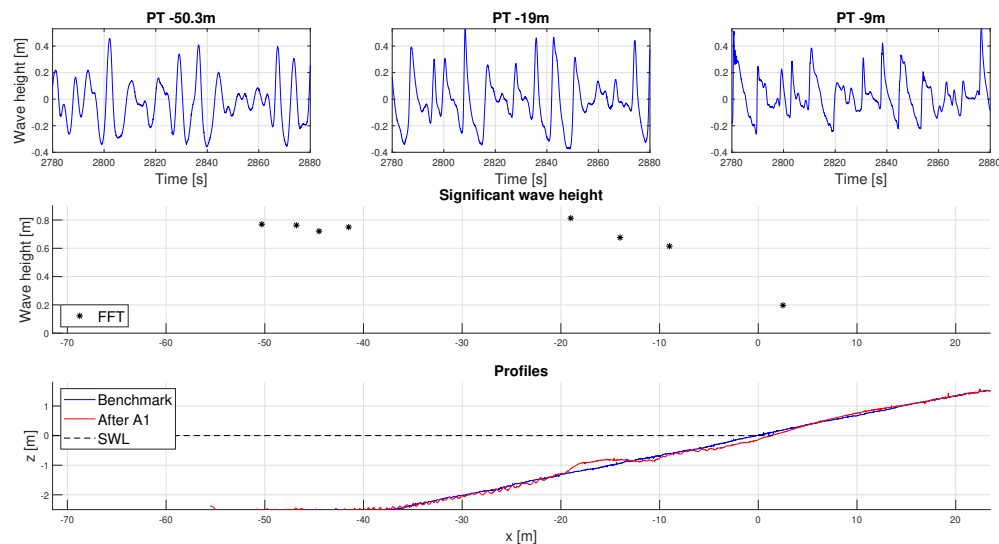


Figure 4.13: Average wave heights and profiles erosive wave, BARDEX II

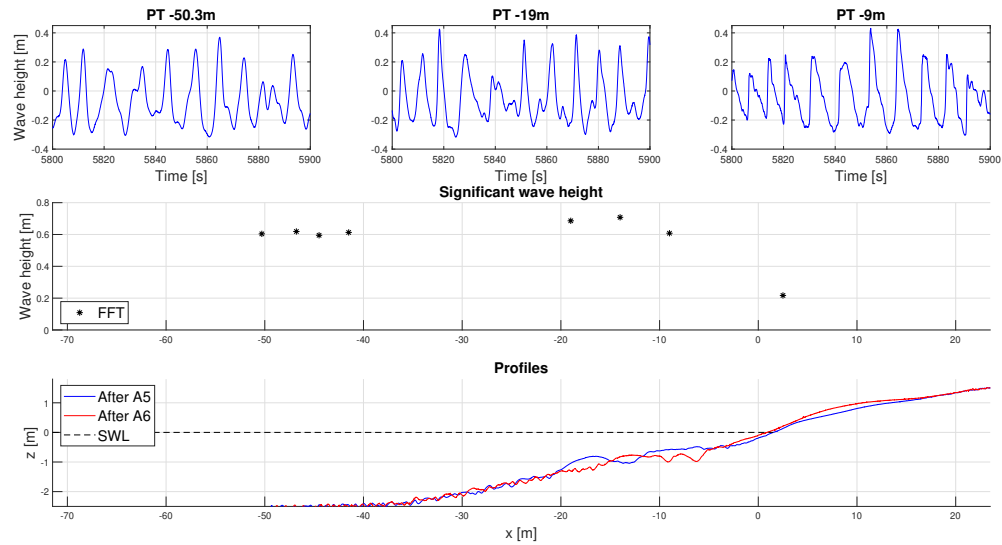


Figure 4.14: Average wave heights and profiles accretive wave, BARDEX II

### Velocity

The velocities of wave condition A1 and A6 do not differ much. Onshore directed velocities are around 1 m/s and 0.78 m/s in the swash zone. At the same time, the offshore velocities vary between 0.5 m/s and 0.9 m/s with a velocity of around 0.8 m/s in the swash zone. The mean velocities are, just like the other four wave conditions of Shaping the Beach and RESIST, in offshore direction except for the most landward Vectrino for both wave conditions.

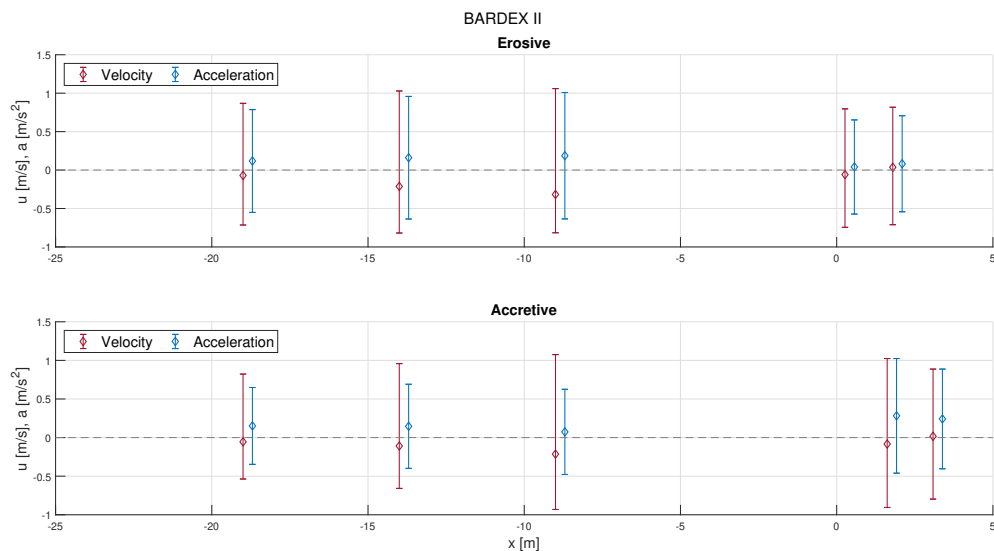


Figure 4.15: Mean, maximum and minimum velocities, BARDEX II

## 4.2 Morphodynamics

In this chapter, the sediment transport rates, and sediment losses will be analysed. This is done to see how the sediment transport rates are in the flume and to use them for comparison with the results of the formulations.

### 4.2.1 Shaping the Beach

The top plot of figure 4.16 shows the bed evolution during the erosive wave condition of Shaping the Beach. During this wave condition erosion occurs in the swash zone and a bar is developed in the surf zone which slowly migrates in the offshore direction. The bottom plot of figure 4.16 shows the corresponding net sediment transport rates for each run. In this plot, it can be seen that the net sediment transport rates in the swash zone are higher in the beginning. Figure 4.17 shows the same plots for the accretive cases. The profiles show that the opposite of the erosive wave is happening in the swash zone. Instead of erosion, sediment is deposited which causes accretion in the swash zone. At the seaside of the shoreline erosion occurs. The erosion before the shoreline and the accretion in the swash causes a steeper slope at the shoreline. The erosion before the shoreline and the accretion in the swash causes a steeper slope at the shoreline. The created bar by the erosive cases is flattened. The net sediment transport rates also show accretion in the swash zone, erosion from  $x=0$  m till  $x=-4$  m and the flattening of the bar.

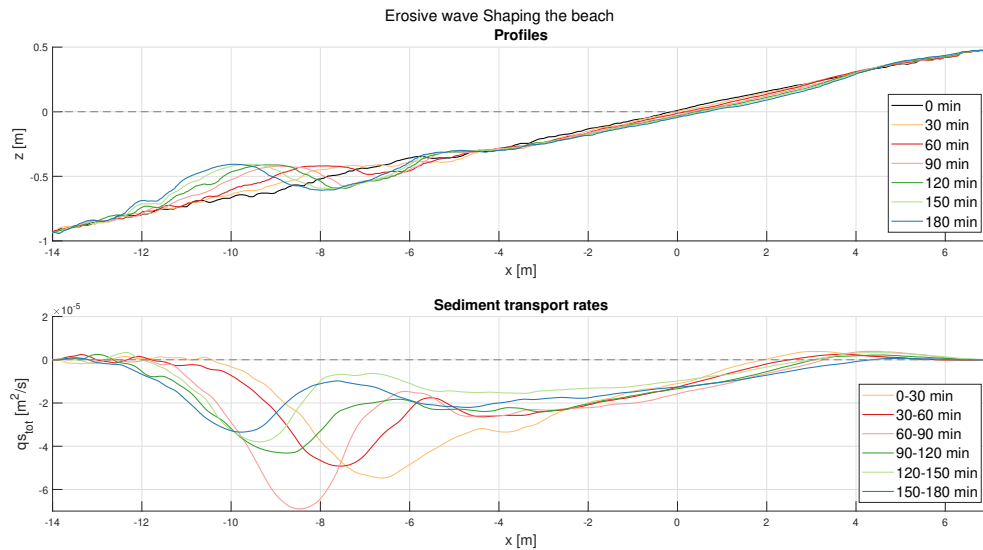


Figure 4.16: Net sediment transport rates, Erosive wave Shaping the Beach

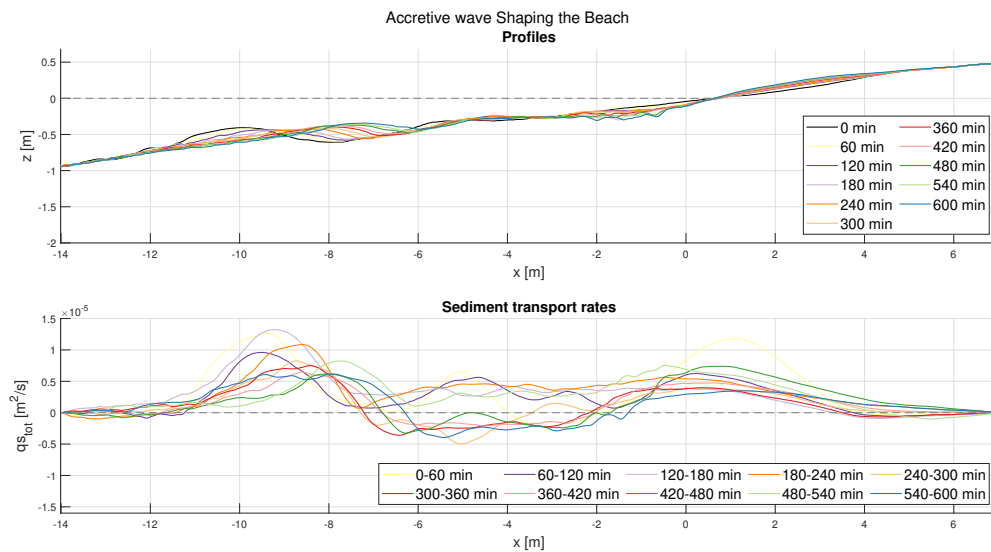


Figure 4.17: Net sediment transport rates, Accretive wave Shaping the Beach

The profiles are measured at one cross-shore location in the wave flume. Therefore, sediment can be lost due to longshore transport, measurement errors, compaction, and erosion/accretion around measurement instrumentation. During the erosive wave, the total amount of sediment within the profile increased with  $0.12 \text{ m}^2$ . During the accretive wave, the profile sediment amount decreased with  $0.07 \text{ m}^2$ . The difference in sediment for each run can be found in table 4.1 and 4.2. Figure 4.18 shows a slowly retreating shoreline during the erosive wave condition. During the accretive wave condition, the shoreline is stable.

**Table 4.1:** *Difference in sediment during each run (30 min) of the erosive wave of Shaping the beach*

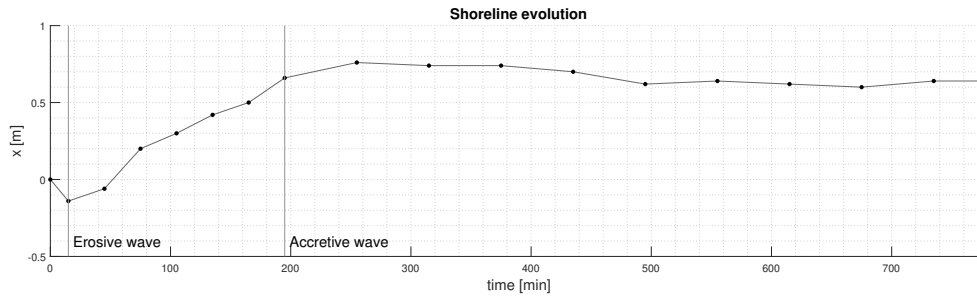
| Run                   | 3                 | 4                 | 6                 | 7                 | 8                 | 9                  |
|-----------------------|-------------------|-------------------|-------------------|-------------------|-------------------|--------------------|
| $\text{m}^2$          | 0.0463            | 0.0122            | 0.00192           | 0.0470            | 0.0329            | -0.0203            |
| $\text{m}^2/\text{s}$ | $2.572\text{e-}5$ | $0.680\text{e-}5$ | $0.107\text{e-}5$ | $2.609\text{e-}5$ | $1.830\text{e-}5$ | $-1.129\text{e-}5$ |

**Table 4.2:** *Difference in sediment during each run (60 min) of the accretive wave of Shaping the beach*

| Run                   | 10                | 11                 | 12                 | 13                | 14                |
|-----------------------|-------------------|--------------------|--------------------|-------------------|-------------------|
| $\text{m}^2$          | 0.0211            | -0.0440            | -0.0596            | 0.0537            | 0.0282            |
| $\text{m}^2/\text{s}$ | $0.586\text{e-}5$ | $-1.222\text{e-}5$ | $-1.657\text{e-}5$ | $1.492\text{e-}5$ | $0.784\text{e-}5$ |

| Run                   | 15                 | 16                | 17                | 18                 | 19                |
|-----------------------|--------------------|-------------------|-------------------|--------------------|-------------------|
| $\text{m}^2$          | -0.0537            | 0.0046            | 0.0480            | -0.1201            | 0.0500            |
| $\text{m}^2/\text{s}$ | $-1.492\text{e-}5$ | $0.129\text{e-}5$ | $1.333\text{e-}5$ | $-3.335\text{e-}5$ | $1.389\text{e-}5$ |



**Figure 4.18:** *Shoreline evolution Shaping the Beach*

#### 4.2.2 RESIST

Figure 4.19 shows the profile evolution and net sediment transport rates of the erosive wave condition of RESIST. Within the first 120 minutes, the bed rapidly evolves and then stabilizes. The net sediment transport rates show the same pattern as Shaping the Beach with decreasing rates while the bed stabilizes. The profiles and net sediment transport rates clearly show that sediment from the swash zone is eroded and stored higher on the beach. Additionally, the profiles show the development of two bars in the surf zone. van der Zanden et al. (2019) researched the same erosive wave condition and found the same results. The accretive wave in figure 4.20 has a lower run-up limit, the waves reach till  $x=5 \text{ m}$  and during the erosive wave condition the run-up limit was  $8 \text{ m}$ . In addition, the accretive wave condition causes a gentle slope in the surf zone and accretion in the swash zone. This is also visible in the net sediment transport rates, which are lower than for the erosive wave.

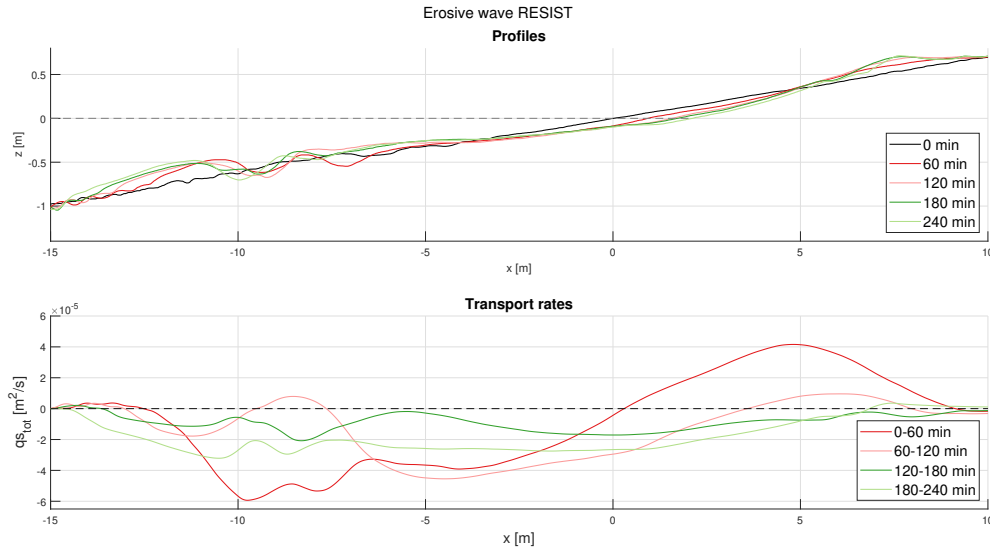


**Figure 4.19:** Net sediment transport rates, Erosive wave RESIST

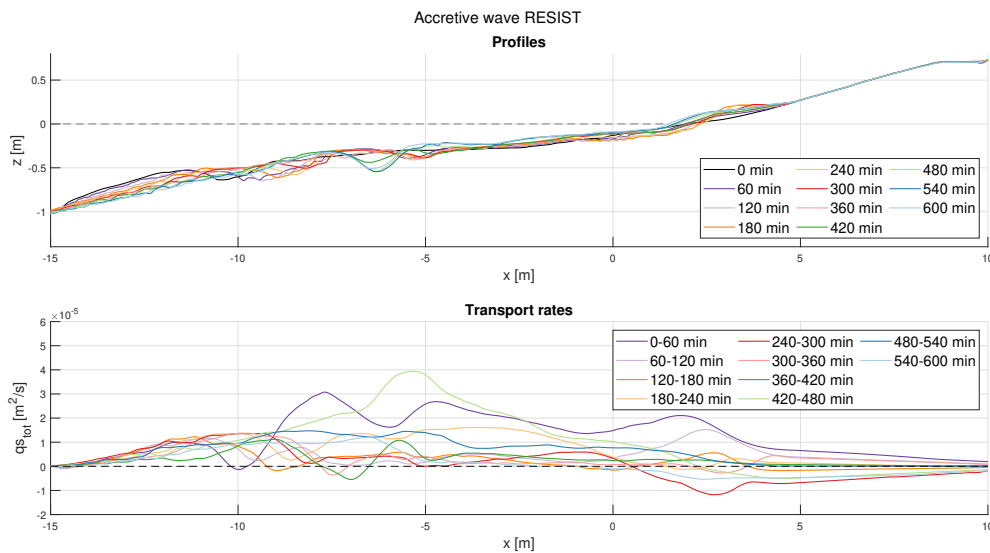


**Figure 4.20:** Net sediment transport rates, Accretive wave RESIST

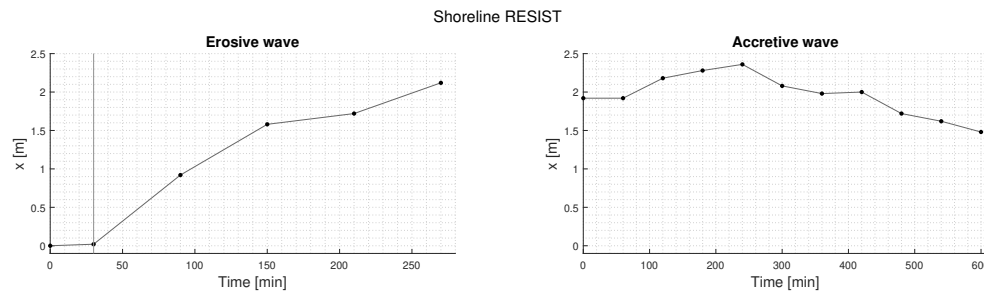
During the erosive wave,  $2.38 \times 10^{-15} \text{ m}^2$  of sediment is lost and during the accretive wave,  $4.01 \times 10^{-15} \text{ m}^2$  is gained. The difference in sediment for each run can be found in table 4.3 and 4.4. These values are significantly lower than Shaping the Beach. This is due to the different applied corrections on the profiles, as described in section 3.2.2. For RESIST the profiles are shifted to each other to reduce the added/lost sediment. While for Shaping the Beach, the profiles are not shifted because the result did not improve. Figure 4.21 shows the shoreline evolution during the erosive and accretive wave. During the first 120 minutes of the erosive wave, the shoreline is fast retreating, during the remainder of the wave condition the shoreline is retreating slower. The accretive wave causes that the shoreline first slowly retreats and then after 240 minutes the shoreline slowly migrates in a seaward direction.

**Table 4.3:** Difference in sediment during each run (60 min) of the erosive wave of RESIST

| Run                   | 88                        | 89                       | 90                        | 91                       |
|-----------------------|---------------------------|--------------------------|---------------------------|--------------------------|
| $\text{m}^2$          | $-0.2615 \times 10^{-15}$ | $0.4753 \times 10^{-15}$ | $-0.7991 \times 10^{-15}$ | $-1.792 \times 10^{-15}$ |
| $\text{m}^2/\text{s}$ | $-0.7264 \times 10^{-19}$ | $1.320 \times 10^{-19}$  | $-2.220 \times 10^{-19}$  | $-4.977 \times 10^{-19}$ |

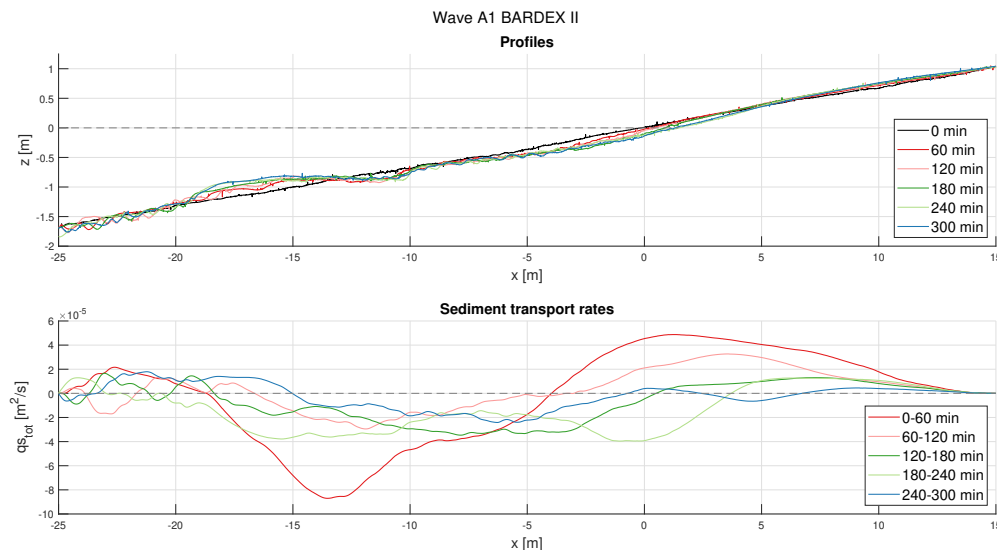
**Table 4.4:** Difference in sediment during each run (60 min) of the accretive wave of RESIST

| Run     | 24-25     | 26-27     | 28        | 29        | 30         |
|---------|-----------|-----------|-----------|-----------|------------|
| $m^2$   | 9.005e-16 | 4.819e-16 | 5.101e-16 | 7.818e-16 | 4.266e-16  |
| $m^2/s$ | 2.501e-19 | 1.339e-19 | 1.417e-19 | 2.171e-19 | 1.185e-19  |
| Run     | 31        | 32        | 33        | 34        | 35         |
| $m^2$   | 4.130e-16 | 4.153e-16 | 0.366e-16 | 2.162e-16 | -1.723e-16 |
| $m^2/s$ | 1.147e-19 | 1.154e-19 | 0.102e-19 | 0.601e-19 | -0.478e-19 |

**Figure 4.21:** Shoreline evolution RESIST

### 4.2.3 BARDEX II

Figure 4.22 shows the bed evolution of wave condition A1. The profiles show that around the shoreline erosion occurs and there is bar development in the surf zone. The net sediment transport rates are the highest in the first 60 minutes, which also results in the largest bed changes. After the first 60 minutes, the transport rates become smaller, especially in the swash zone. Wave condition A6 causes accretion in the swash zone, flattening of the berm and erosion occurs between  $x=-11$  and  $x=-5$  m (figure 4.23). The net sediment transport rates of wave condition A6 are lower than wave condition A1. Further, show the bed the same morphodynamic changes as wave condition A6.

**Figure 4.22:** Net sediment transport rates, Wave A1 BARDEX II

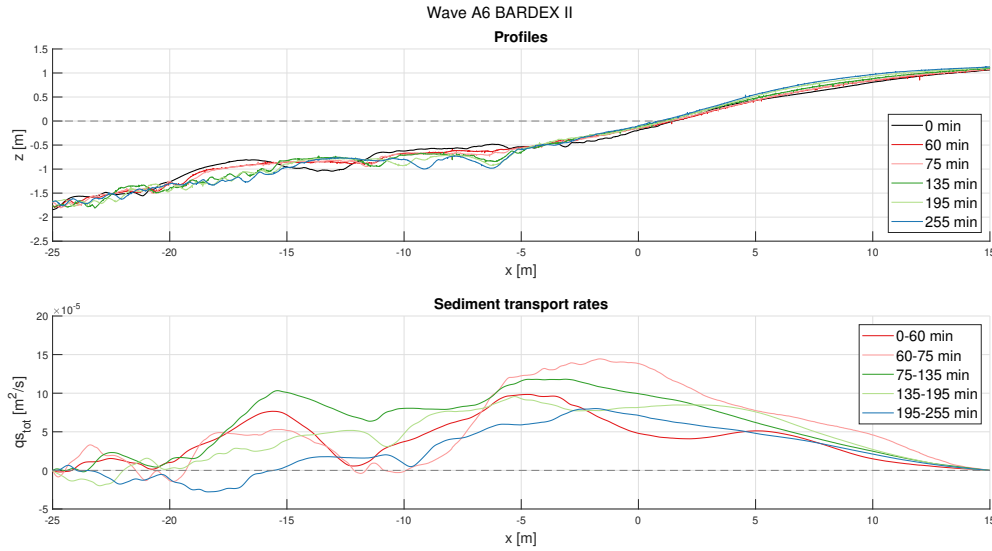


**Figure 4.23:** Net sediment transport rates, Wave A6 BARDEX II

Both wave conditions of BARDEX II show a loss in sediment. During wave condition A1 and A6 respectively  $0.127 \text{ m}^2$  and  $0.493 \text{ m}^2$  of sediment is lost. These values are so high due to that the losses are only calculated for the active part of the beach (x -25 till 15 m). So, it could be that sediment is transported outside the active part. How much sediment is lost or added per run can be found in table 4.5 and 4.6. Furthermore, the shoreline shows the same pattern as Shaping the Beach and RESIST, with a retreating shoreline during wave condition A1 (erosive) and slowly migration in seaward direction during wave condition A6 (accretive), figure 4.24.

**Table 4.5:** Difference in sediment during each run (60 min) of wave condition A1 of BARDEX II

|                       |           |           |          |           |           |
|-----------------------|-----------|-----------|----------|-----------|-----------|
| Run                   | 1-4       | 5-6       | 7        | 8         | 9         |
| $\text{m}^2$          | -0.293    | 0.155     | 0.089    | -0.127    | -0.028    |
| $\text{m}^2/\text{s}$ | -1.626e-4 | 0.860e-4  | 0.495e-4 | -0.703e-4 | -0.155e-4 |
| Run                   | 10        | 11        | 12       | 13        | 14        |
| $\text{m}^2$          | 0.113     | -0.172    | 0.114    | -0.053    | 0.078     |
| $\text{m}^2/\text{s}$ | 0.629e-4  | -0.954e-4 | 0.633e-4 | -0.295e-4 | 0.434e-4  |

**Table 4.6:** Difference in sediment during each run (60 min) of wave condition A6 of BARDEX II

|                       |           |           |           |           |           |
|-----------------------|-----------|-----------|-----------|-----------|-----------|
| Run                   | 34-36     | 37-38     | 39        | 40        | 41        |
| $\text{m}^2$          | -0.194    | 0.114     | -0.170    | -0.230    | -0.0437   |
| $\text{m}^2/\text{s}$ | -1.078e-4 | 0.634e-4  | -1.889e-4 | -1.276e-4 | -0.243e-4 |
| Run                   | 42        | 43        | 44        | 45        |           |
| $\text{m}^2$          | 0.117     | -0.186    | 0.066     | 0.034     |           |
| $\text{m}^2/\text{s}$ | 0.650e-4  | -1.035e-4 | 0.365e-4  | 0.190e-4  |           |

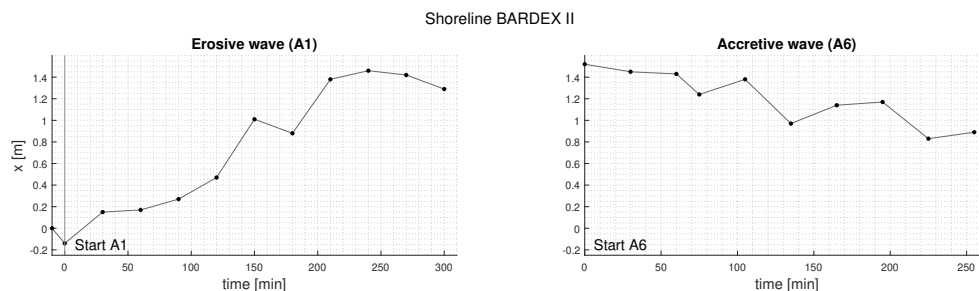


**Figure 4.24:** Shoreline evolution BARDEX II

### 4.3 Data sets comparison

In this section the difference in the hydrodynamics and morphodynamics between Shaping the Beach, RESIST and BARDEX II for are listed.

#### 4.3.1 Hydrodynamics

For Shaping the Beach and BARDEX II, irregular waves are applied while for RESIST bichromatic wave are used. This means that for RESIST the same group of waves occur after each other. For the Shaping the Beach and BARDEX II there is no consistent repetition of a set group of waves. The used wave period of Shaping the Beach and RESIST do not differ much from each other. This can be explained because Shaping the Beach had the idea to reproduce relatable random waves. But the used wave heights for RESIST are higher than Shaping the Beach. The wave characteristics of BARDEX II are totally different. For BARDEX II longer periods and higher wave heights are used. This is possible because for BARDEX II a bigger flume is used, the Delta flume in the Netherlands. An overview of the hydrodynamics can be found in table 4.7.

**Table 4.7:** Overview of the hydrodynamics of the three data sets

| Condition       | Shaping the Beach |           | RESIST      |             | BARDEX II |         |
|-----------------|-------------------|-----------|-------------|-------------|-----------|---------|
|                 | Erosive           | Accretive | Erosive     | Accretive   | Wave A1   | Wave A6 |
| Wave type       | Random            | Random    | Bichromatic | Bichromatic | Random    | Random  |
| Period (s)      | 3.5               | 5.2       | 3.7         | 4.7         | 8         | 12.8    |
| Wave height (m) | 0.45              | 0.25      | 0.64        | 0.42        | 0.76      | 0.55    |
| Dean Number     | 3.78              | 1.41      | 5.09        | 2.00        | 2.20      | 1.10    |
| Grain size (mm) | 0.25              | 0.25      | 0.25        | 0.25        | 0.42      | 0.42    |

#### 4.3.2 Morphodynamics

The initial slope of the three data sets is the same, a 1:15 slope. However, they used a different grain size to build up the beach. Shaping the Beach and RESIST used a  $d_{50}$  of 0.25 mm while BARDEX II used larger grains with a  $d_{50}$  of 0.42mm. The net sediment transport rates of Shaping the Beach are the lowest, as can be seen in figure 4.25; this is due to the lower bed shear stresses. The net sediment transport rates of the erosive wave from RESIST and wave A1 from BARDEX II has the same magnitude. This shows that due to the larger grains, the higher waves of BARDEX II do not cause higher net sediment transport rates. The accretive wave from RESIST has higher transport rates than the accretive wave (wave A6) of BARDEX II. So, with the lower wave height of RESIST, more sediment is transported.

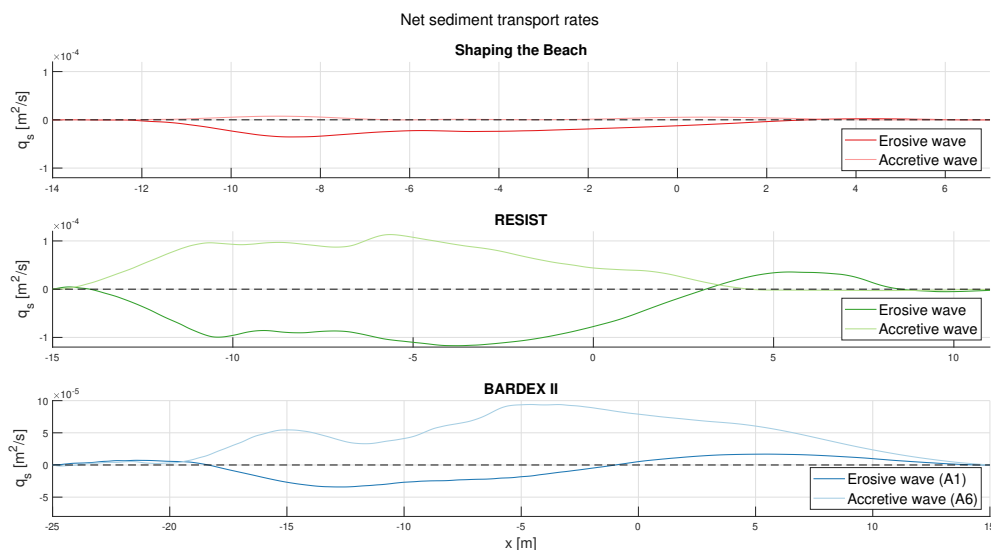


**Figure 4.25:** Total transport rates for the six wave conditions

## 5 Validation of the net sediment transport formulations

The results of the formulations are discussed in paragraph 5.1 till 5.3. Followed by the choice for the formulation for the improvement in paragraph 5.4.

### 5.1 SANTOSS formulation

#### 5.1.1 Hypothesis

The most important processes for the SANTOSS formulation are the wave skewness and asymmetry in combination with the maximum and minimum velocity of a single swash event. The formulation uses these parameters to determine the bed shear stresses. Based on these processes is for each run and total wave conditions a hypothesis is formed to estimate the net sediment transport rate (large/small and direction). These hypotheses help to understand to formulation and to see if the calculated transport rates are a logical result of the formulation.

The hypotheses for the total events are visible in table 5.1 and the hypotheses for each run are shown in appendix C.1. The hypotheses show that the sediment transport rates are always in the onshore direction. This can be explained due to the velocity skewness (and for BARDEX II A6 the acceleration skewness), higher velocities during the wave crest than during through, which cause higher bed shear stress during the uprush than during the backwash. However, this does not directly mean that, higher bed shear stresses cause more sediment transport during the uprush because there is a possible phase lag.

**Table 5.1:** *Hypotheses SANTOSS for the total wave conditions*

| Wave event | Wave skewness and asymmetry | Mean velocity | Mean bed shear stress | Hypothesis                     |
|------------|-----------------------------|---------------|-----------------------|--------------------------------|
| StB-E      | Velocity skewed             | Offshore      | Onshore               | Onshore sediment transport     |
| StB-A      | Velocity skewed             | Low offshore  | Onshore               | Onshore sediment transport     |
| RES-E      | Velocity skewed             | High offshore | Strong onshore        | Onshore sediment transport     |
| RES-A      | Velocity skewed             | Offshore      | Onshore               | Low onshore sediment transport |
| BAR-A1     | Sinus                       | Almost zero   | Weak onshore          | Almost no sediment transport   |
| BAR-A6     | Acceleration skewed         | Almost zero   | Weak onshore          | Onshore sediment transport     |

#### 5.1.2 Results

First, the tree erosive wave conditions are calculated and analysed, followed by the accretive wave conditions. As last are the transport rates calculated from the start of the wave condition till the end (total wave conditions) and is transport rate calculated for the whole based on the individual runs.

#### Erosive wave conditions

The calculated net sediment transport rates for the erosive wave conditions are shown in figure 5.1, 5.2 and 5.3. As can be seen in the figures are the calculated net sediment transport rates of the erosive condition from Shaping the Beach and RESIST meanly (94%) in the opposite direction as the measured net sediment. While the directions of wave condition A1 (BARDEX II) are for 70% in the same direction as the measured transport rates. The opposite direction of Shaping the beach and RESIST is caused by the high velocity skewness which is absent for BARDEX II.

Besides the direction the amount is important. The erosive wave conditions of the three data sets have all about the same range, from  $0.4 \times 10^{-4}$  till  $5.9 \times 10^{-4} m^2/s$ . However, the measured net sediment transport rates are between  $-0.5 \times 10^{-4}$  till  $0.5 \times 10^{-4} m^2/s$ . These, overestimation are probably caused due to the absent of the bed slope effect which drives sediment offshore and therefor would reduce the net sediment transport rates, because the calculate net sediment transport rates are onshore directed.

Furthermore, are the results in general better for the locations closer to the start of the swash zone than more to the end of the swash zone. Which is also visible in the correlation coefficient in table 5.5. This means that, for the erosive wave conditions, the SANTOSS formulation is better for locations that are longer covered than exposed by the incoming waves.

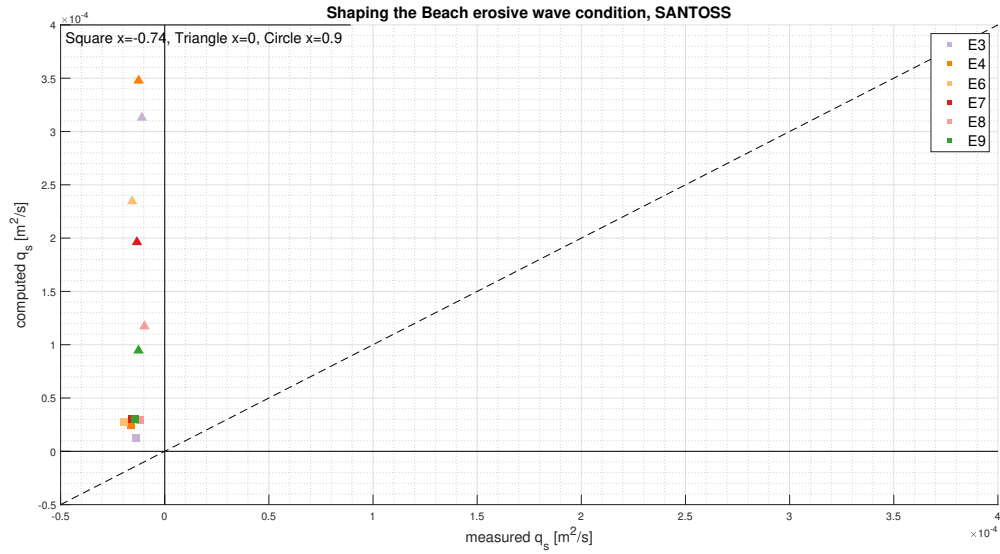


**Figure 5.1:** *Shaping the Beach erosive wave condition net sediment transport calculated using the SANTOSS formulation*

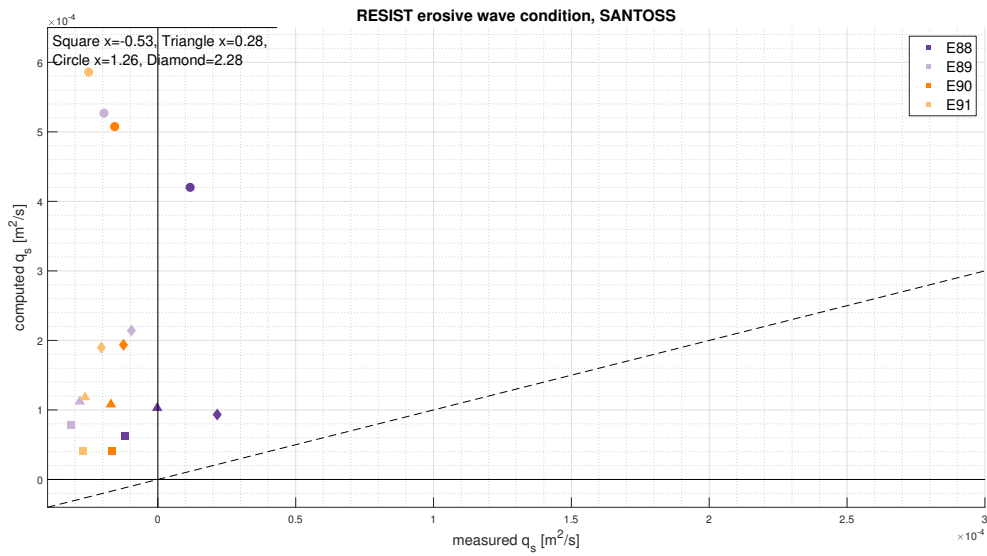


**Figure 5.2:** *RESIST erosive wave condition net sediment transport calculated using the SANTOSS formulation*

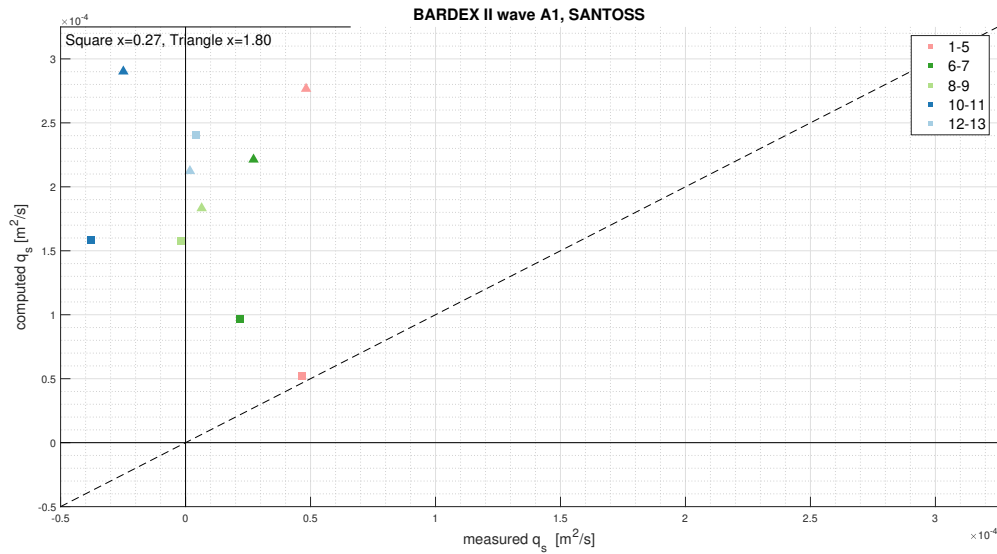


**Figure 5.3:** *BARDEX II erosive wave condition net sediment transport calculated using the SANTOSS formulation*

### Accretive wave conditions

For the accretive wave conditions are the calculated transport rates in general better than the erosive wave conditions, some of the points of Shaping the beach (figure 5.4 and RESIST (figure 5.5) are less than 10% off the 1:1-line. Especially the directions are better, because 78% of the directions are in the same direction as the measured direction. The 22% which is in the opposite direction is mainly caused by the accretive wave condition of RESIST where 35% is in the opposite direction as measured. This mainly onshore directed calculated net sediment transport rate can be explained due to the velocity skewness.

The net sediment transport rates for the accretive wave condition of BARDEX II (figure 5.6) are 10 times higher, as well for the calculated as measured transport rates (note the different scales). Further, is the height of the net sediment transport rates for the locations at the beginning of the swash zone closer to the 1:1-line than the location further in the swash zone. However, for 64 of the 77 locations are the transport rates overestimated. This is probably caused due to the missing bed slope effect.

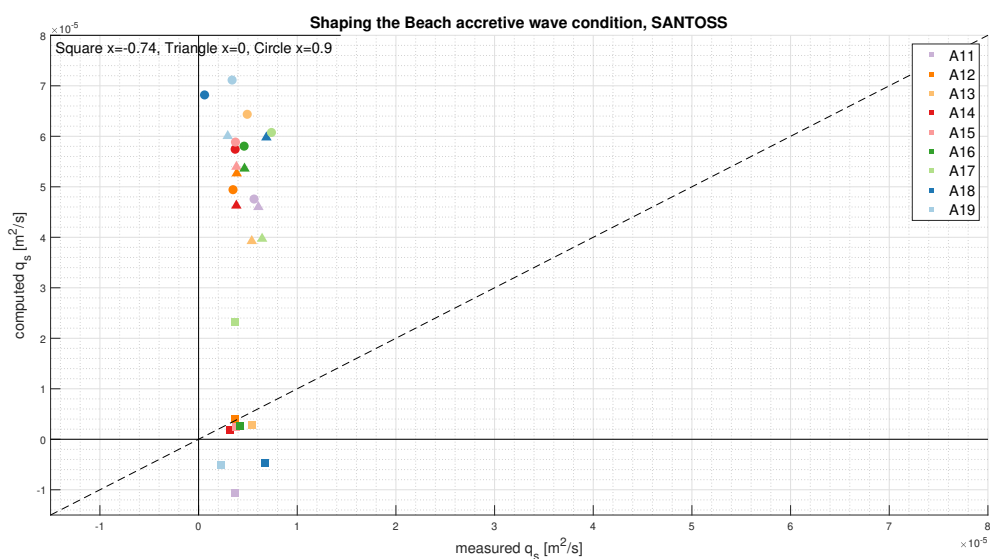


**Figure 5.4:** *Shaping the Beach accretive wave condition net sediment transport calculated using the SANTOSS formulation*

So, for the accretive wave conditions the SANTOSS formulations shows the same pattern as for the erosive wave conditions with meanly onshore calculated transport rates and overestimation transport rates. In combination with better results closer to the shoreline relative to the end of the swash zone.

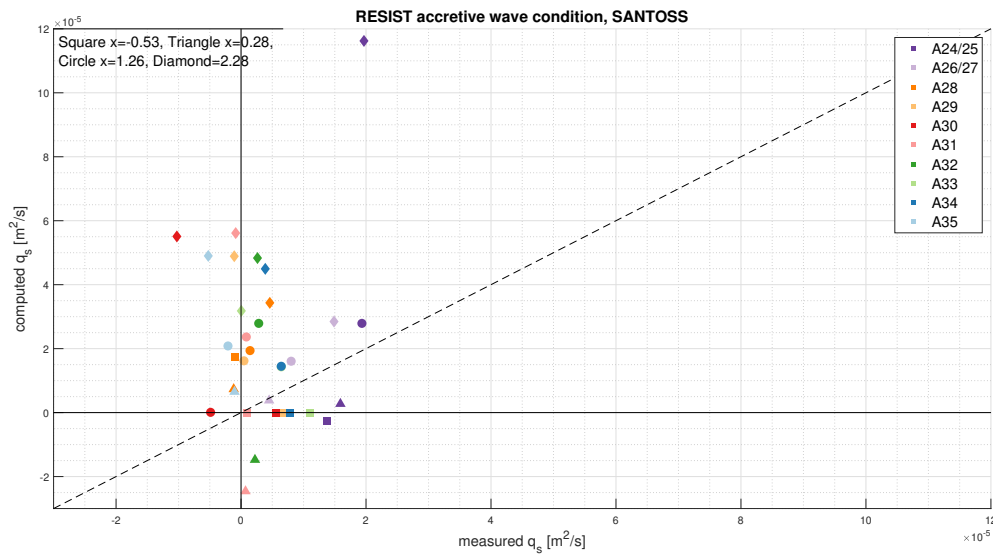


Figure 5.5: RESIST accretive wave condition net sediment transport calculated using the SANTOSS formulation

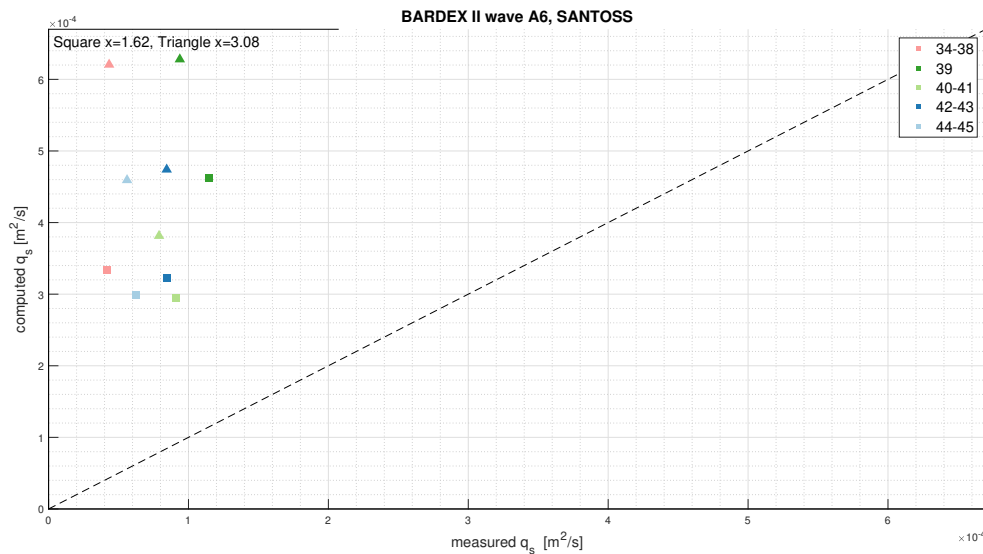
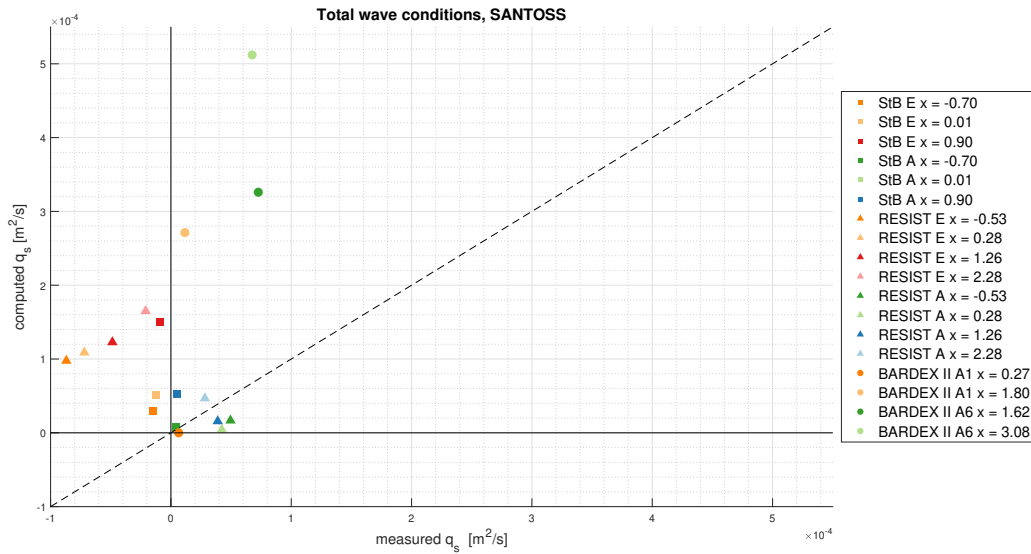


Figure 5.6: BARDEX II accretive wave condition net sediment transport calculated using the SANTOSS formulation

### Total wave conditions

The transport rates of the total wave conditions (figure 5.7) for the erosive wave condition are all, except for wave condition A1 of BARDEX II, in the opposite direction as the measured transport rate. The amount of net transported sediment is in the same magnitude as measured. For the accretive wave conditions, the calculated net sediment transport rates with the SANTOSS formulation are in the same direction as the measured transport rates and the amounts are not far over- or underestimated (maximum with a factor 2), by the exception of BARDEX II A6 where the quantity is far overestimated.



**Figure 5.7:** Total net sediment transport of the whole wave conditions of the three data sets calculated using the SANTOSS formulation

As can be seen in figure 5.8, the mean net sediment transport rate, which is the mean of the individual runs, are different in comparison with the total wave conditions (calculated for the total wave condition is one time). The first difference is the measured net sediment transport rates. The mean transport rate based on the measured transport rates of the runs is not exactly the same as when the transport rates measured for the total wave condition in one time (difference of maximum 5%). The difference could be explained due to that the mean transport rates are corrected for each run while the total transport rate of the whole wave condition is only one time correction. Furthermore, the calculated transport rates are different. This can be explained partly due to that the whole wave condition is based on the water depth at the start of the wave condition where the mean of the run as a different waterdepth for each run. Also, for the whole wave condition, the mean velocities are used, while for the mean of the runs, each run has a different velocity. By using the mean velocities, the higher velocities, in the beginning are decreased, which causes a big difference in the bed shear stress because the bed shear stress is proportional to the velocity squared.

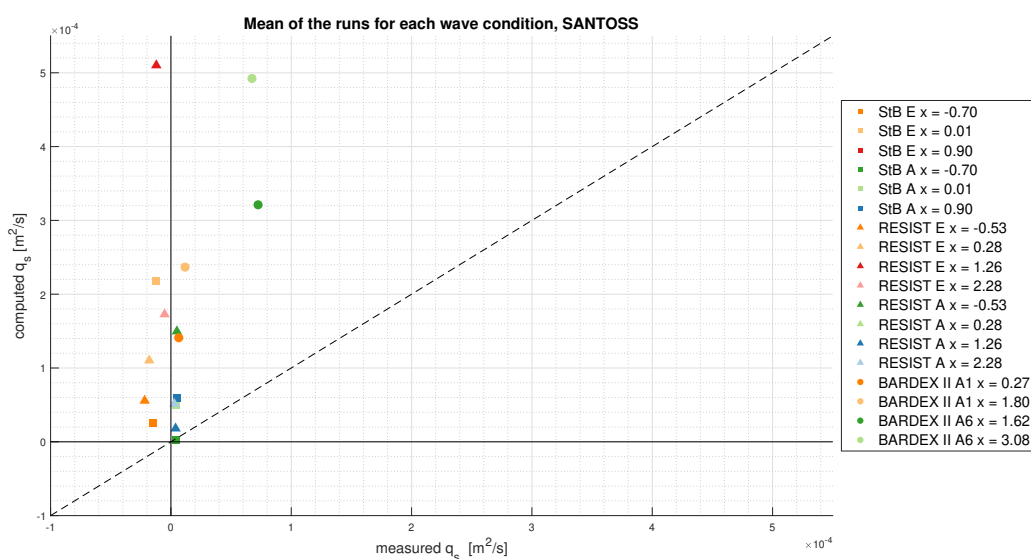


**Figure 5.8:** Total mean net sediment transport of the runs per wave conditions of the three data sets calculated using the SANTOSS formulation

## 5.2 Formulations of Larson: Bed shear stress

### 5.2.1 Hypothesis

The non-directional bed shear stress is higher during the uprush due to the higher velocities. Also, the time-averaged non-directional bed shear stress is higher during uprush. This difference causes onshore directed net sediment transport. The bed slope effects are depending on the steepness of the beach, but are in general not strong enough to drive net sediment transport offshore because the slope is not steep enough. Only if the difference between the bed shear stress during uprush and backwash is minimal. Based on these essential processes the hypotheses are formed. In table 5.2, the hypotheses can be found for the total wave conditions. For the hypotheses of each run see appendix C.2 the hypotheses for each run can be found.

**Table 5.2:** *Hypotheses Larson et al. (2004) based on bed shear stress for the total wave conditions*

| Wave event | Shields parameters difference       | Hypothesis                      |
|------------|-------------------------------------|---------------------------------|
| StB-E      | Multiple times higher during uprush | High onshore sediment transport |
| StB-A      | Multiple times higher during uprush | High onshore sediment transport |
| RES-E      | Three times higher during uprush    | Onshore sediment transport      |
| RES-A      | Three times higher during uprush    | Onshore sediment transport      |
| BAR-A1     | A little higher during uprush       | Weak onshore sediment transport |
| BAR-A6     | A little higher during uprush       | Weak onshore sediment transport |

### 5.2.2 Results

The results of the erosive wave conditions are analysed followed by the accretive and the total wave condition.

#### Erosive wave conditions

For the erosive wave conditions shows the bed shear stress formulation of Larson et al. (2004) the same results for the direction as the SANTOSS formulation. 77% of the directions is in the opposite direction as the measured net sediment transport rate, as can be seen in figure 5.9 till 5.11. This is caused by the higher time-averaged Shield parameter during the uprush period in comparison whit the backwash period. Which is a direct result of the velocity skewness.

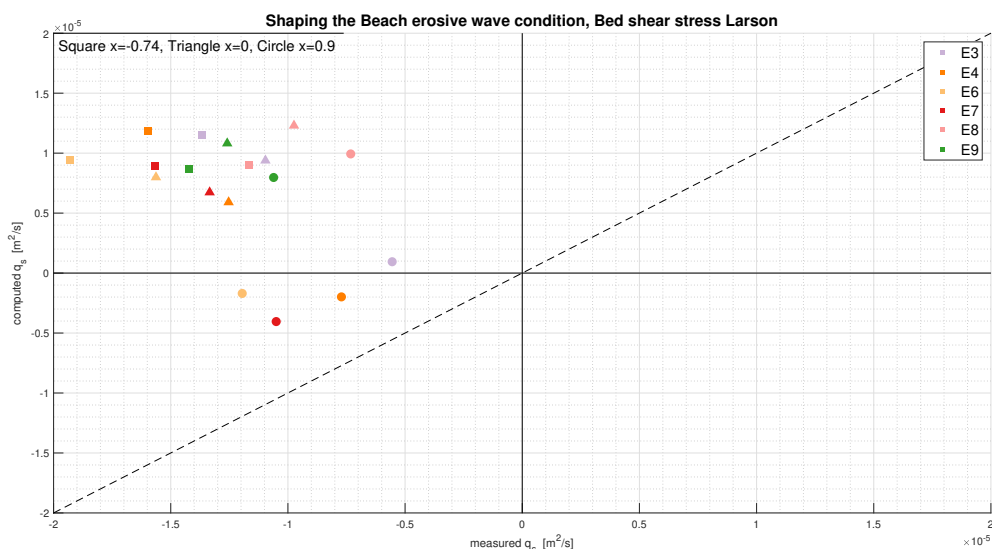


**Figure 5.9:** *Shaping the Beach erosive wave condition net sediment transport calculated using the formulation of Larson et al. (2004) based on the bed shear stress*

The height of the net sediment transport rates are the lowest for Shaping the beach and the highest for BARDEX II, for the calculated as well as the measured transport rates. For Shaping the beach the net sediment transport rates are underestimated with a factor two. Also the transport rates of BARDEX II are underestimated but way more, a factor of approximately 7. While for RESIST the results are two times overestimated. This difference is caused by the same reasons as for the directions.

Further, is the formulations of Larson et al. (2004) based on the bed shear stress designed for the swash zone, which results in higher correlations in the middle part of the swash zone where there are no other boundary conditions. The correlations are visible in in table 5.5.

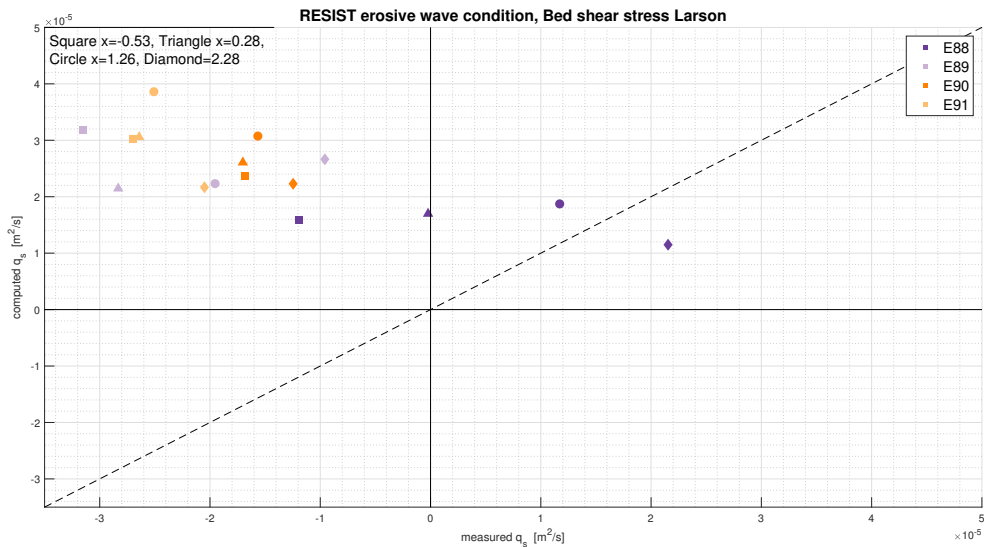


**Figure 5.10:** RESIST erosive wave condition net sediment transport calculated using the formulation of Larson et al. (2004) based on the bed shear stress

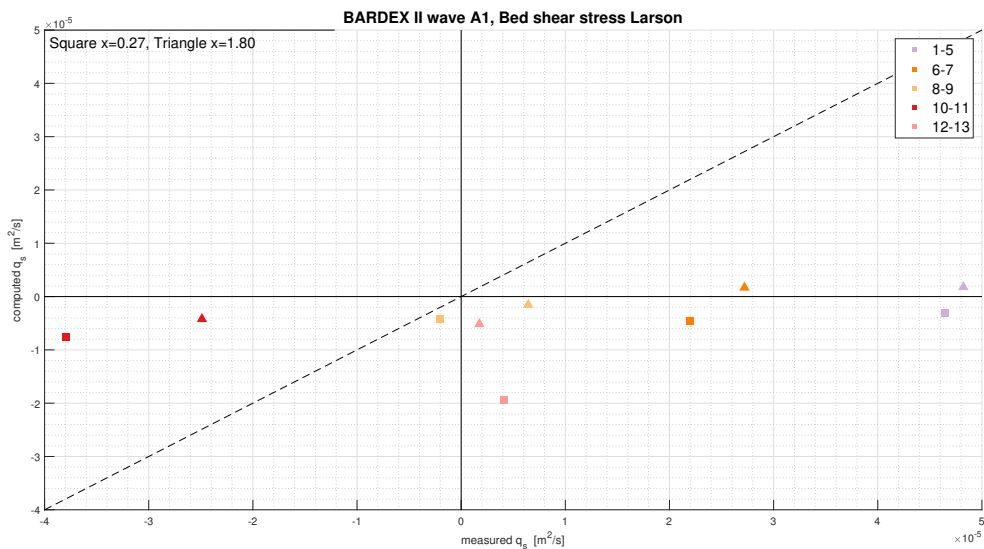


**Figure 5.11:** BARDEX II erosive wave condition net sediment transport calculated using the formulation of Larson et al. (2004) based on the bed shear stress

### Accretive wave conditions

The calculated directions for the accretive wave conditions of Shaping the Beach (figure 5.12) and RESIST (figure 5.13) are for, respectively, 93% and 75% in the same direction as the measured net sediment transport rates, which is better than for the erosive wave conditions. While for BARDEX II (figure 5.14) only 10% of the results has the same direction as measured. This is mainly due to the velocity skewness which results in a higher time-average Shields parameter during the uprush period than the backwash period (same as for the erosive wave conditions).

Wave condition A1 of BARDEX II has the highest measured net sediment transport rates of the three wave conditions. However, the calculated transport rates are approximately four times lower than the measured transport rates. This is due to small difference between the time-average Shield parameters of the uprush and backwash. For Shaping the beach and RESIST, half of the net sediment transport rates is underestimated while the other half is overestimated. The difference is probably caused by the variation in the representative velocity signal.

Another remark is that the run in the middle and end of the accretive wave condition of Shaping the Beach and RESIST have better results than the run at the beginning of the wave condition. This is because in the beginning the conditions are changing fast and the transport rates are high, probably the formulation is not designed for these conditions.

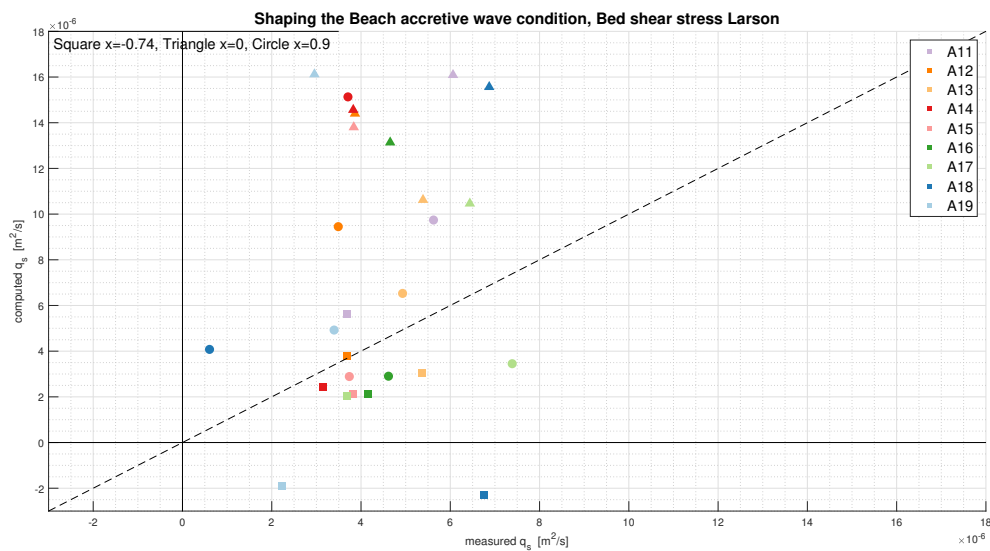


**Figure 5.12:** Shaping the Beach accretive wave condition net sediment transport calculated using the formulation of Larson et al. (2004) based on the bed shear stress

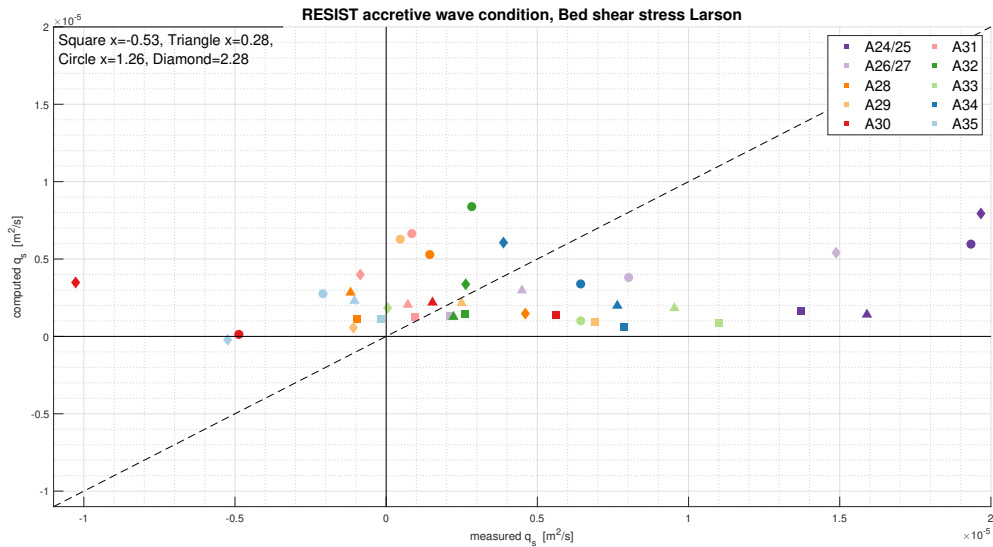


**Figure 5.13:** *RESIST accretive wave condition net sediment transport calculated using the formulation of Larson et al. (2004) based on the bed shear stress*

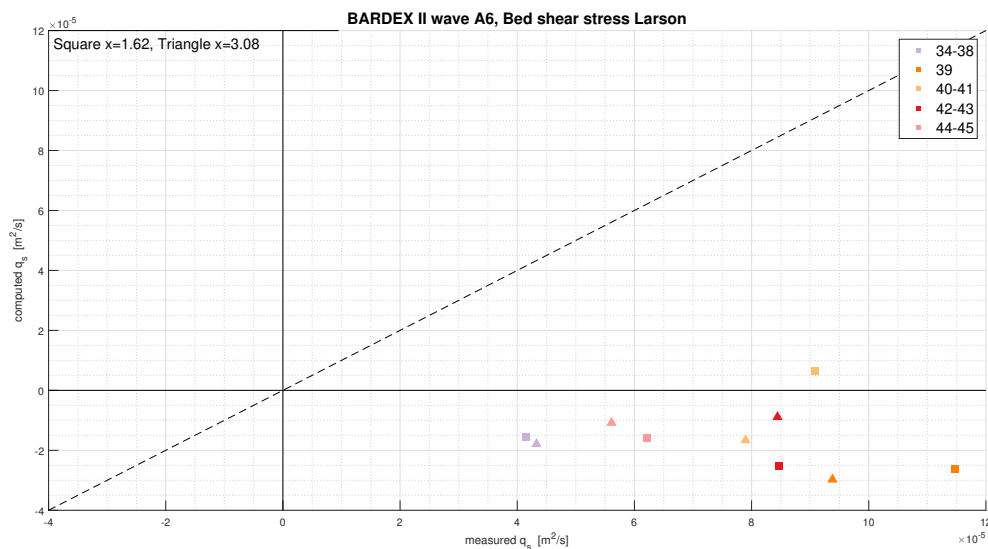


**Figure 5.14:** *BARDEX II accretive wave condition net sediment transport calculated using the formulation of Larson et al. (2004) based on the bed shear stress*

### Total wave conditions

The net sediment transport for the total wave conditions (figure 5.15) look very different in comparison with the mean net sediment transport rates in figure 5.16. However, the calculated net sediment transport rates do not change much. So, the difference in the figures is caused by the difference in measured net sediment transport rates, which is caused by the same reason as described in section 5.1.2. Which means that, for the calculated net sediment transport rates it does not matter if the mean bed shear stress of the runs is used to calculate the net sediment transport rate or that the mean net transport rates of each run is used.

The results (from both methods) for Shaping the Beach are closer to the 1:1-line than the other two data sets. Especially, wave condition A6 of BARDEX II is far off. Furthermore, for all the erosive cases, the direction is opposite as the measured direction, while for the accretive wave conditions only for wave condition A6 is the calculated net sediment transport rate in the opposite direction as measured. This is due to the above explained reasons (difference in bed shear stress and bed slope effect).

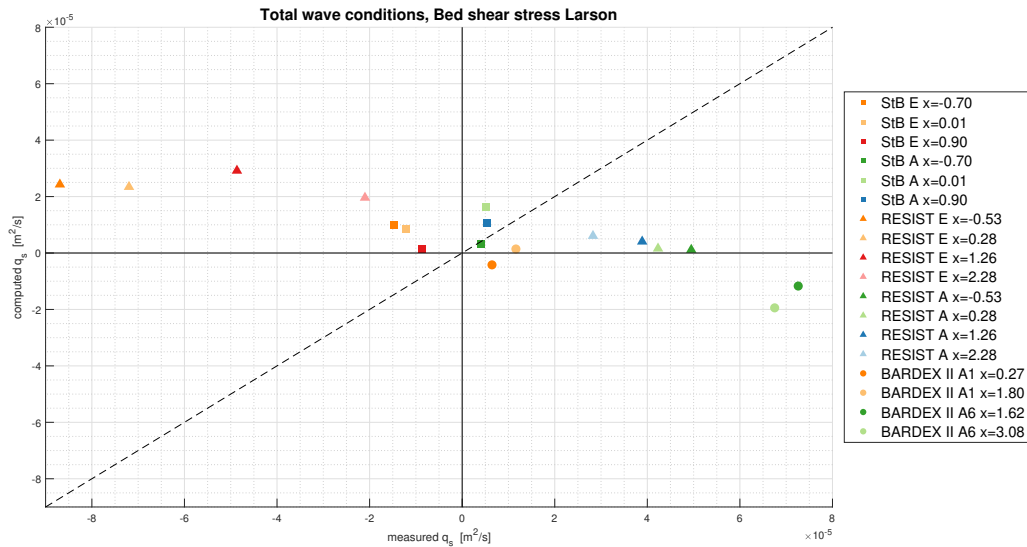


**Figure 5.15:** Total net sediment transport of the whole wave conditions of the three data sets calculated using the formulation of Larson et al. (2004) based on the bed shear stress

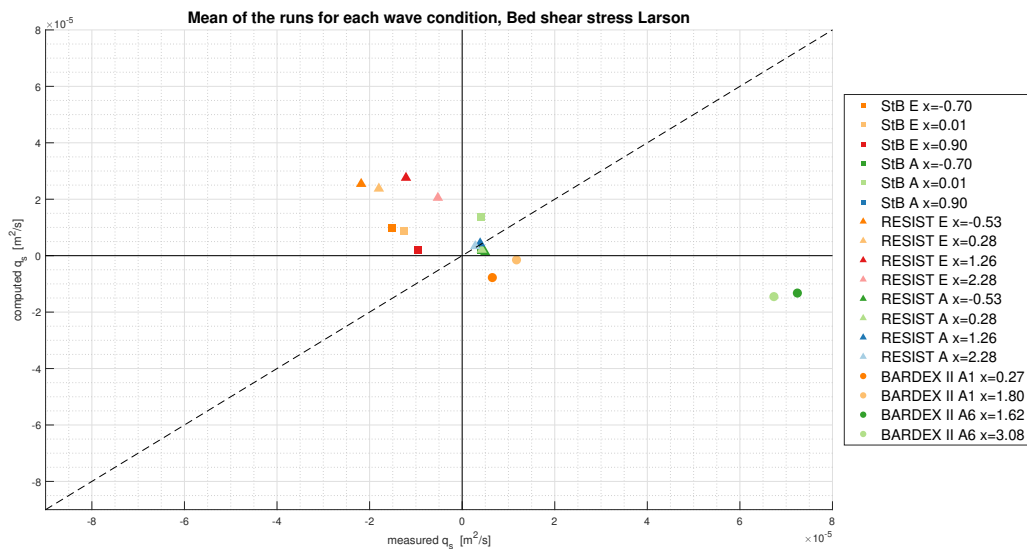


**Figure 5.16:** Total net sediment transport of the whole wave conditions of the three data sets calculated using the formulation of Larson et al. (2004) based on the bed shear stress

### 5.3 Formulations of Larson: Run-up limit

#### 5.3.1 Hypothesis

For the hypotheses, three parts of equation 5 are important: run-up limit, elevation, and local vs equilibrium slope. The run-up limit is constant for one wave condition, while the elevation is different for the different used locations (depending on the data set). Based on these three parts, the hypotheses for the total wave conditions are formulated in table 5.2 and for each run in appendix C.3.

**Table 5.3:** Hypotheses Larson et al. (2004) based on the run-up limit for the total wave conditions

| Wave event | Run-up limit | Elevation per location*        | Equilibrium slope | Local slope vs Equilibrium slope         | Hypothesis                  |
|------------|--------------|--------------------------------|-------------------|--|-----------------------------|
| StB-E      | 0.52m        | 0.017m, 0.074m, 0.149m         | 1:17.6            | Local slope steeper as equilibrium slope | Offshore sediment transport |
| StB-A      | 0.49m        | 0.017m, 0.069m, 0.132m         | 1:10.2            | Equilibrium slope steeper as local slope | Onshore sediment transport  |
| RES-E      | 0.78m        | 0.035m, 0.093m, 0.164m, 0.229m | 1:19.4            | Local slope steeper as equilibrium slope | Offshore sediment transport |
| RES-A      | 0.44m        | 0.023m, 0.079m, 0.138m, 0.206m | 1:12.2            | Equilibrium slope steeper as local slope | Onshore sediment transport  |
| BAR-A1     | 1.12m        | 0.149m, 0.264m                 | 1:12.8            | Equilibrium slope steeper as local slope | Onshore sediment transport  |
| BAR-A6     | 1.65m        | 0.430m, 0.645m                 | 1:9.0             | Local slope steeper as equilibrium slope | Offshore sediment transport |

\*The elevation is the vertical distance from the start of the swash zone till the location.

#### 5.3.2 Results

The results will be discussed in the order: erosive wave conditions, accretive wave conditions and the total wave conditions.

##### Erosive wave conditions

Larson et al. (2004) formulation based on the run-up limit uses the difference between the equilibrium slope and local slope to determine the direction of the net sediment transport rate. Resulting in that, for the erosive wave conditions, 77% of the calculated runs are in the same direction as measured, which is meanly directed offshore. For the erosive wave conditions of Shaping the beach (figure 5.17) it is even 100%.

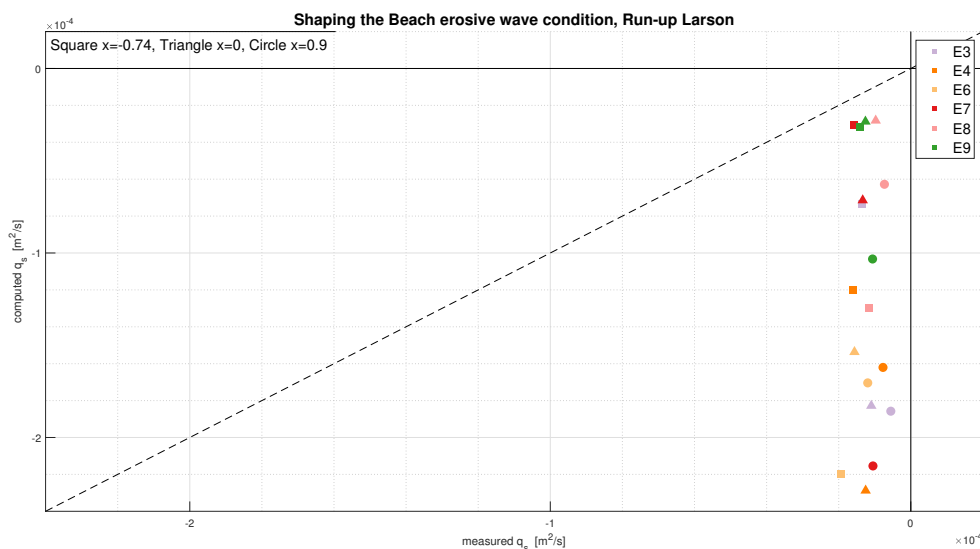


**Figure 5.17:** Shaping the Beach erosive wave condition net sediment transport calculated using the formulation of Larson et al. (2004) based on the run-up limit

Further, are the results vertical spread which is caused by an overestimation of the calculated transport rates. The erosive wave condition of RESIST (figure 5.18) and BARDEX II (figure 5.19) are on average thirty times overestimated. While for Shaping the Beach this overestimation is on average ten times. This probably caused by an overestimation of the run-up limit and due to a  $K_c$ -value which is too high for these wave conditions. Another reasons can be the missing onshore directed processes sediment response time and groundwater effects. Theses two processes can reduce the offshore directed transport rates resulting in a lower net sediment transport rates. So, the formulation has better results for the direction than for the amount of the transport sediment.

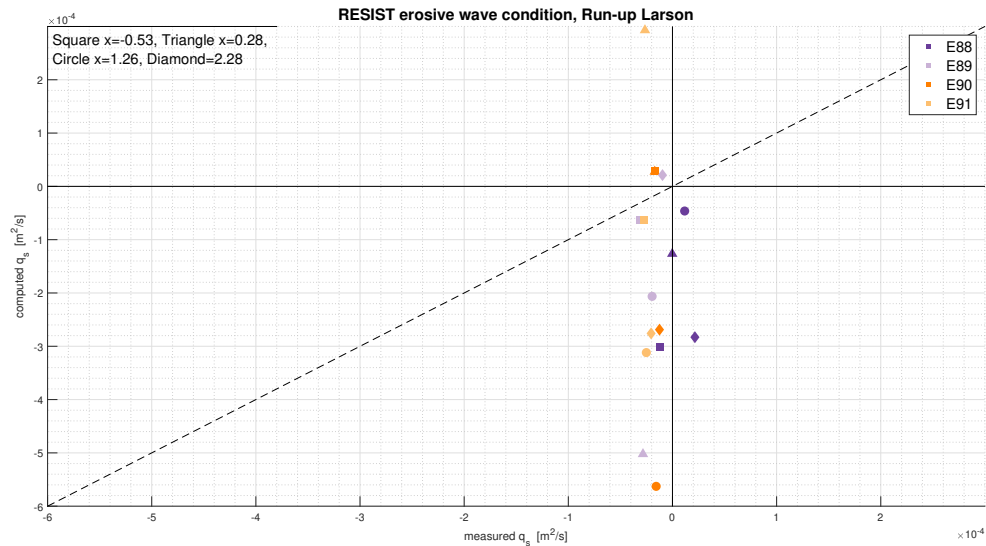


**Figure 5.18:** RESIST erosive wave condition net sediment transport calculated using the formulation of Larson et al. (2004) based on the run-up limit

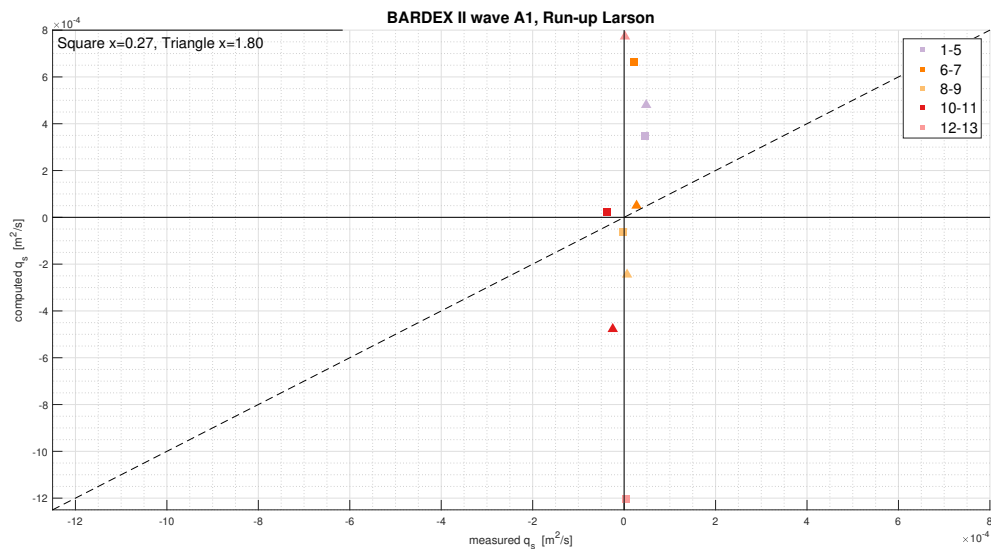


**Figure 5.19:** BARDEX II erosive wave condition net sediment transport calculated using the formulation of Larson et al. (2004) based on the run-up limit

### Accretive wave conditions

Where for the other two formulations the accretive wave conditions show better directions than for the erosive wave condition is this not the case for the run-up limit based formulation of Larson et al. (2004). For the accretive wave condition only 47% of the direction is in the same direction as measured, which is mainly directed onshore corresponding to an accretive wave condition. The opposite direction is caused by a local slope which turns out to be steeper than the equilibrium slope, causing offshore directed transport rates with the run-up limit formulation of Larson et al. (2004)

The amount of calculated and measured transport rates of Shaping the Beach and RESIST are in the same range, while both the transport rates of BARDEX II are higher. Further, is it visible in figures 5.20, 5.21 and 5.22, that the sediment transport rates are far overestimated. This overestimation results in a almost vertical line of the the calculated net sediment transport rates. The overestimation are caused by the same reasons as described for the erosive wave condition above.

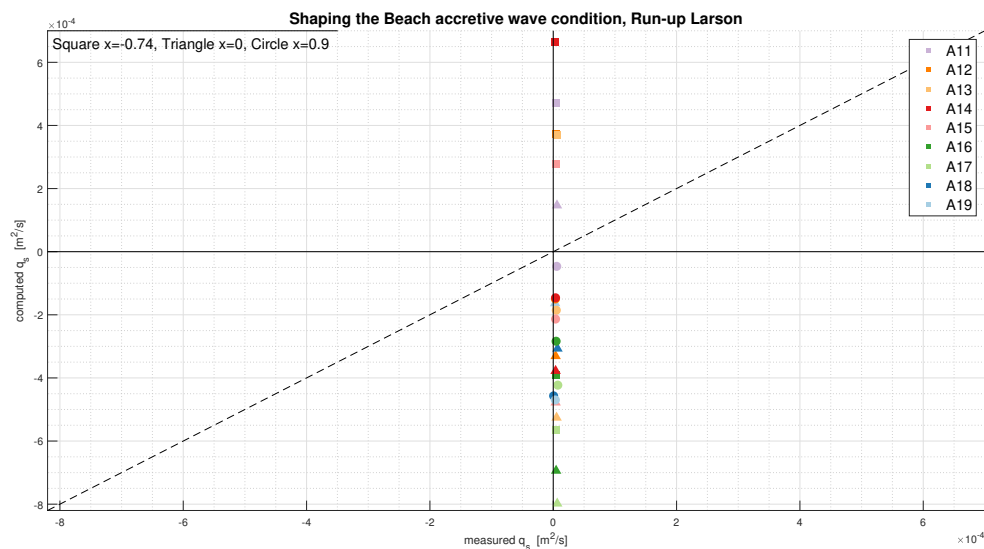


**Figure 5.20:** *Shaping the Beach accretive wave condition net sediment transport calculated using the formulation of Larson et al. (2004) based on the run-up limit*

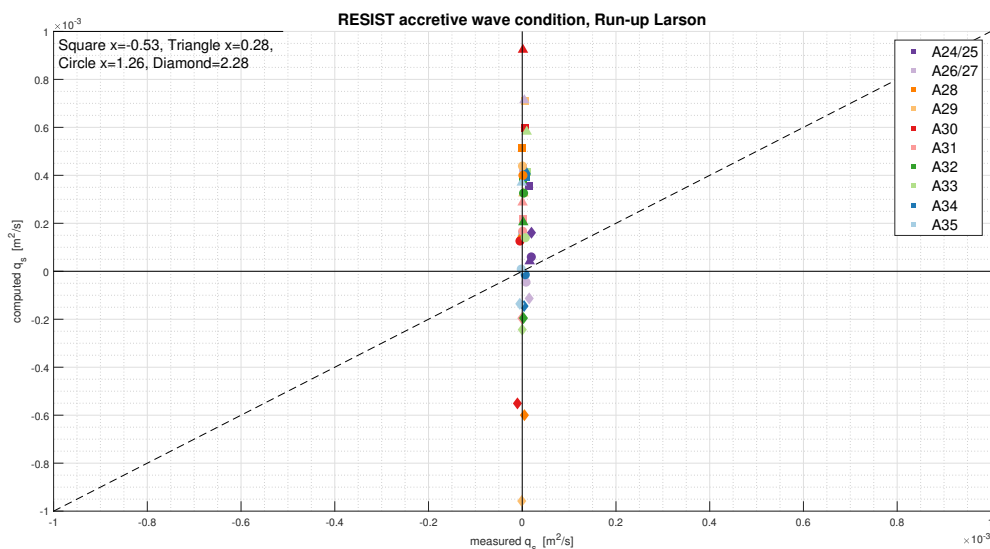


**Figure 5.21:** *RESIST accretive wave condition net sediment transport calculated using the formulation of Larson et al. (2004) based on the run-up limit*

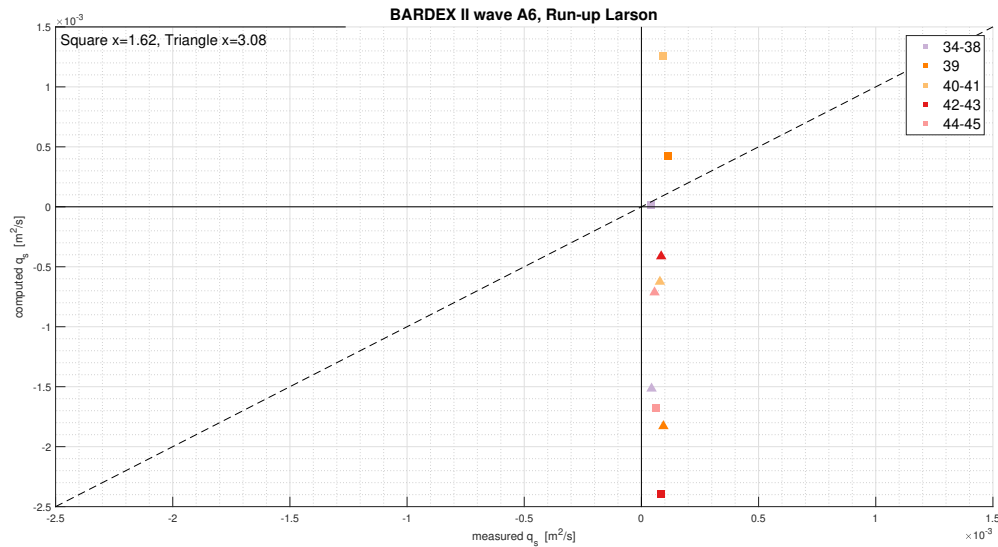


**Figure 5.22:** *BARDEX II accretive wave condition net sediment transport calculated using the formulation of Larson et al. (2004) based on the run-up limit*

### Total wave conditions

The calculated net sediment transport rates of the total wave conditions, based on the conditions at the start of the wave condition, are shown in figure 5.23. Figure 5.24 shows the mean of the different runs. The difference in measured transport rates is caused by the same reason as for SANTOSS formulation and the other formulation of Larson et al. (2004). The difference in calculated net sediment transport rate can be explained due to the change in bed slope and elevation. For the total wave condition, the bed slope and elevation are used from the start of the wave condition. Where for the mean of the runs the elevation and bed slope is used at the beginning of each run, which causes that the elevation and bed slope changes for each run during a wave condition.

The calculated direction of the net sediment transport rates for the total wave condition are better than the direction based on the mean of the runs. The calculation for total wave condition calculated all the directions correct (except BARDEX II A6  $x=3.08$ ), while for the mean method only 33% of the directions are in the same direction as measured. By way of contrast, the amount of transported sediment is in the same range, between  $x=-1.25 \times 10^{-4}$  and  $1.20 \times 10^{-4} m^2/s$ , except BARDEX II wave condition A6.

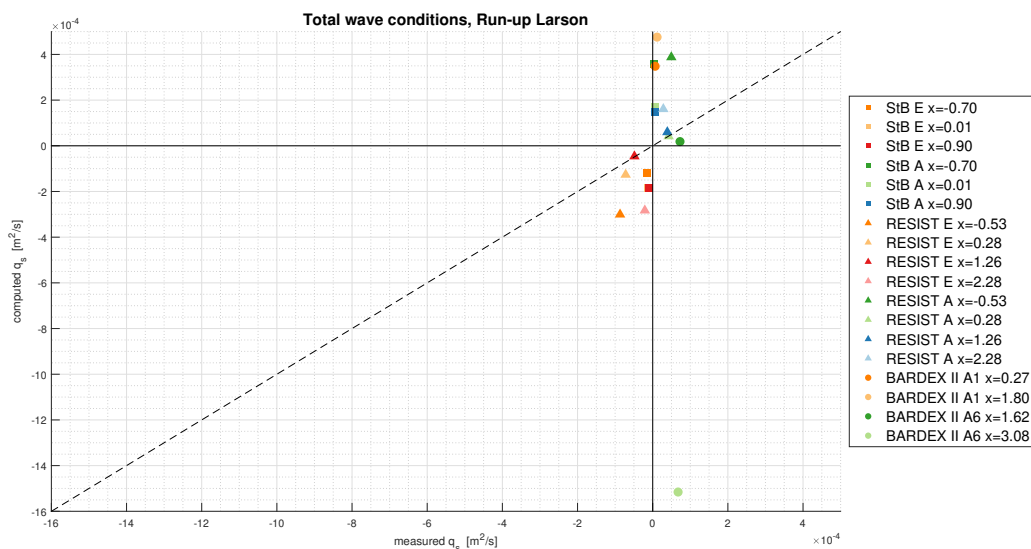


**Figure 5.23:** *Total net sediment transport of the whole wave conditions of the three data sets calculated using the formulation of Larson et al. (2004) based on the run-up limit*

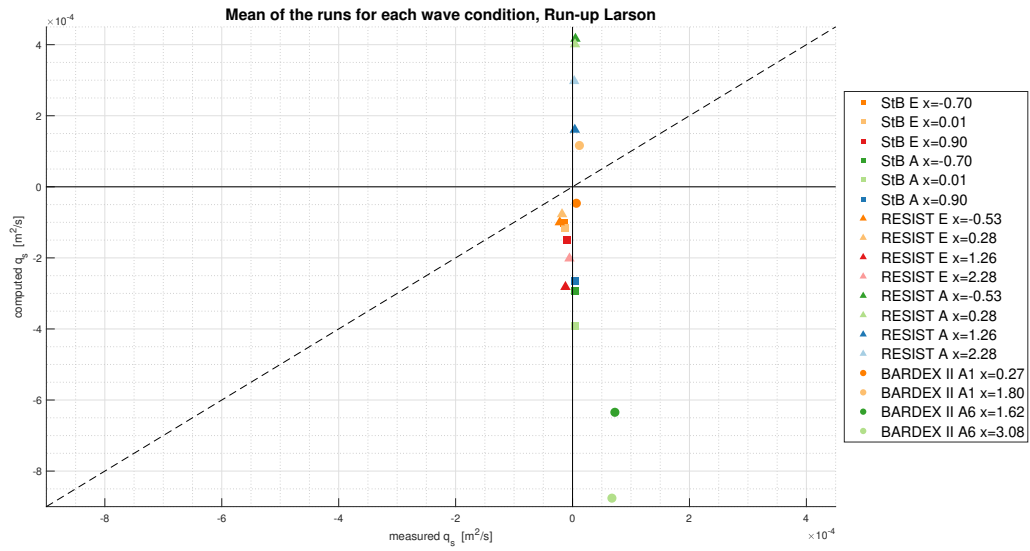


**Figure 5.24:** Total net sediment transport of the whole wave conditions of the three data sets calculated using the formulation of Larson et al. (2004) based on the run-up limit

## 5.4 Formulation assessment

Before choosing the formulation for the improvement, the strengths and weaknesses of the SANTOSS formulation and the two formulations of Larson et al. (2004) are discussed and showed in table 5.4. Followed by an analysis of the error statistics.

### 5.4.1 Strong and weak points of the formulations

The SANTOSS formulation, which is originally developed for deeper water, calculated the height of the transport rates better for the start of the swash zone than for the end of the swash zone, this is due to that these locations are covered by waves for a longer period. However, the directions for the erosive wave condition at these locations are in the opposite as the measured transport rates. The calculated rates are onshore directed, while the measured transport rates are offshore directed. For the other locations, on the beachside of the shoreline, the SANTOSS formulation overestimates the net sediment transport rates up to a factor twenty. Furthermore, the transport rates are in general onshore directed, while the measured direction is offshore for the erosive wave conditions. This onshore directed sediment transport is caused by the high velocity or acceleration skewness. Also, the absence of the bed slope effect, which drives the sediment offshore, could cause the high onshore sediment transport rates.

For shaping the Beach and RESIST the bed shear stress formulation of Larson et al. (2004) is better for the accretive than the erosive wave conditions. Because due to the velocity skewness 80% of the calculated transport rates (erosive and accretive) are onshore directed, while for the erosive wave conditions the measured transport rates are mainly offshore directed. On the other hand, the amounts of transported sediment are better than for the SANTOSS formulation, as well for the erosive as the accretive wave conditions. Furthermore, the calculated transport rates increase with the increasing distance from the shoreline. For the total wave conditions and means of the wave conditions, the accretive conditions are better.

The net sediment transport rates of BARDEX II data set are underestimated with the bed shear stress formulation of Larson et al. (2004). This can be due to the absence of velocity skewness for the BARDEX II data set which causes that the difference between the time-average Shields parameter during uprush and backwash is very small. The direction for the run-up based formulation of Larson et al. (2004) is depended on the difference between equilibrium slope and local slope. For the erosive wave condition, the formulation calculated the net sediment transport directions mainly in the same direction as measured. The height of the net sediment transport rate are overestimated varying from a factor ten till thirty. For the accretive wave conditions, the calculated transport rates are less accurate. Most of the calculated sediment transport rates are far overestimated, resulting in a vertical line with calculated net sediment transport rates. This could be due to three reasons: 1. the absence of any velocity input which could drive the sediment offshore or onshore depending on the skewness and asymmetry, 2. the dimensionless coefficient  $K_c$  is too high for accretive cases or 3. maybe an overestimated run-up limit because a lower run-up limit results directly in a lower sediment transport rate (see formulation 5). The formulation show some promising results for the total wave condition. The directions are all, except A6 of BARDEX II, in the same direction as measured and the amount are on average 3 times overestimated. While for the mean of the runs, the formulation works less well. So, it looks like the formulation calculate the transport rates better for a longer period, not for individual run of 30-60 min but for total wave conditions of multiple hours.

**Table 5.4:** Overview of the results of the formulations based on the direction and amount of the net sediment transport rate. with a - for disagree, -/+ for mid term and + for agree

| Wave   | SANTOSS   |        | Bed Shear Stress |        | Run-up limit |        |
|--------|-----------|--------|------------------|--------|--------------|--------|
|        | Direction | Amount | Direction        | Amount | Direction    | Amount |
| StB_E  | -         | -      | -                | +      | +            | -/+    |
| StB_A  | +         | -      | +                | -/+    | -            | -      |
| RES_E  | -         | -      | -                | +      | -/+          | -      |
| RES_A  | -/+       | -/+    | +                | -/+    | -/+          | -      |
| BAR_A1 | -/+       | -      | -/+              | -      | -/+          | -      |
| BAR_A6 | +         | -      | -                | -      | -/+          | -      |
| Total  | -/+       | -/+    | -/+              | -/+    | +            | +      |
| Mean   | -/+       | -      | -/+              | +      | +            | -/+    |

### 5.4.2 Error statistics

To test the correlation between the calculated and measured data two correlations are applied, the Spearman and Pearson correlation (as described in section 3.3.2). The results of the correlation are shown in table 5.5. With the Spearman correlation, the run-up limit formulation of Larson et al. (2004) has for nine locations the best correlation. While the bed shear stress formulations of Larson et al. (2004) and SANTOSS have respectively five and four times the best correlation. Also for the Pearson correlation, the Run-up limit based formulation of Larson et al. (2004) has most of the times the best correlation (ten times). Where the other two formulations only have two (bed shear stress Larson et al. (2004)) and eight locations (SANTOSS formulations) with the best correlation. For the total wave condition, the SANTOSS formulation has three times the best correlation and the run-up limit based formulation of Larson et al. (2004) one time.

Furthermore, the RMSE is calculated for the different wave conditions and formulations. The bed shear stress formulation from Larson et al. (2004) turns out to have the lowest RMSE (see table 5.5). However, this method has one remark because the RMSE is sensitive for outliers (Chai & Draxler, 2014; Pontius, Thontteh, & Chen, 2008). This explains why the bed shear stress formulation of Larson et al. (2004) has the lowest RMSE because the net calculated sediment transport rates are the lowest and there are almost no outliers.

**Table 5.5:** Error statistics for the three formulations where one is the best possible correlation, in bold the best correlation. *S* = SANTOSS formulation, *B* = Bed shear stress formulation Larson et al. (2004) and *R* = Run-up limit formulation Larson et al. (2004)

| Wave             | x-loc. | Spearman     |             |              | Pearson      |             |              | RMSE    |         |         |
|------------------|--------|--------------|-------------|--------------|--------------|-------------|--------------|---------|---------|---------|
|                  |        | S            | B           | R            | S            | B           | R            | S       | B       | R       |
| StB_E            | -0.70m | 0.09         | -0.26       | <b>0.20</b>  | -0.10        | -0.06       | <b>0.51</b>  | 4.16E-5 | 2.51E-5 | 1.07E-4 |
|                  | 0.01m  | 0.03         | <b>0.49</b> | 0.14         | -0.15        | <b>0.59</b> | 0.25         | 2.48E-4 | 2.14E-5 | 1.29E-4 |
|                  | 0.90m  | 0.14         | <b>0.26</b> | 0.03         | <b>0.44</b>  | 0.21        | 0.13         | 1.80E-3 | 1.20E-5 | 1.50E-4 |
| StB_A            | -0.70m | <b>0.20</b>  | -0.14       | -0.31        | <b>-0.08</b> | -0.21       | -0.22        | 9.32E-6 | 3.63E-6 | 9.96E-4 |
|                  | 0.01m  | -0.37        | -0.30       | <b>-0.15</b> | -0.35        | -0.27       | <b>-0.08</b> | 4.59E-5 | 9.37E-5 | 4.78E-4 |
|                  | 0.9m   | -0.35        | -0.07       | <b>0.37</b>  | -0.36        | -0.02       | <b>0.24</b>  | 5.60E-5 | 4.93E-6 | 3.04E-5 |
| RES_E            | -0.53m | <b>-0.20</b> | -1.00       | -0.40        | <b>-0.30</b> | -0.97       | -0.49        | 8.00E-5 | 4.93E-5 | 1.48E-4 |
|                  | 0.28m  | -0.80        | -0.40       | <b>0.20</b>  | -0.87        | -0.67       | <b>0.04</b>  | 1.29E-4 | 4.44E-5 | 2.94E-4 |
|                  | 1.26m  | -1.00        | -0.80       | <b>0.40</b>  | -0.96        | -0.75       | <b>0.60</b>  | 5.27E-4 | 4.48E-5 | 3.24E-4 |
|                  | 2.28m  | -0.20        | -0.20       | -0.20        | -0.91        | -0.85       | <b>-0.19</b> | 1.88E-4 | 3.32E-5 | 2.37E-4 |
| RES_A            | -0.53m | -0.51        | -0.03       | <b>0.12</b>  | -0.18        | -0.06       | <b>0.23</b>  | 7.05E-4 | 6.04E-6 | 4.40E-4 |
|                  | 0.28m  | -0.16        | -0.54       | <b>0.12</b>  | <b>0.04</b>  | -0.50       | -0.16        | 7.35E-4 | 5.78E-6 | 4.73E-4 |
|                  | 1.26m  | 0.16         | <b>0.18</b> | -0.35        | <b>0.49</b>  | 0.24        | -0.33        | 1.59E-5 | 6.30E-6 | 2.29E-4 |
|                  | 2.28m  | -0.31        | <b>0.59</b> | 0.50         | 0.40         | 0.39        | <b>0.54</b>  | 5.30E-5 | 6.97E-6 | 4.22E-4 |
| BAR_A1           | 0.27m  | -0.70        | 0.50        | 0.50         | -0.60        | 0.27        | <b>0.30</b>  | 1.28E-4 | 3.04E-5 | 6.27E-4 |
|                  | 1.80m  | -0.10        | <b>0.90</b> | 0.40         | -0.04        | <b>0.86</b> | 0.52         | 2.68E-4 | 9.84E-5 | 4.85E-4 |
| BAR_A6           | 1.62m  | 0.10         | -0.40       | <b>0.50</b>  | <b>0.61</b>  | -0.12       | 0.25         | 2.68E-4 | 9.84E-5 | 1.46E-3 |
|                  | 3.08m  | <b>0.30</b>  | -0.10       | 0.00         | -0.13        | -0.36       | <b>0.04</b>  | 4.53E-4 | 9.09E-5 | 1.22E-3 |
| Total waves      |        | -0.08        | -0.83       | <b>0.41</b>  | <b>0.29</b>  | -0.86       | -0.03        | n/a     | n/a     | n/a     |
| Mean of the runs |        | <b>0.16</b>  | -0.71       | -0.12        | <b>0.08</b>  | 0.00        | -0.56        | n/a     | n/a     | n/a     |

### 5.4.3 Formulation for improvement

The formulation for improvement is the run-up limit formulation from Larson et al. (2004). This formulation has the best correlation based on the Spearman correlation and the Pearson correlation. Further, are the calculated net sediment transport rates most of the times in the same directions as the measured net sediment transport rate, while this is not the case for the other formulations. Furthermore, has this formulation a high potential to be improved with the coefficient  $K_c$  and an option to implement missing processes (the velocity or/and wave/swash period). Also, this formulation uses input data which can directly be measured (slopes, run-up limit and elevation) which is not the case for the Shields parameter. This run-up limit based formulation is also the formulation proposed by Larson et al. (2004) to use for the calculation of the net sediment transport rate in the swash zone.

## 6 Improve the net sediment transport formulation

The formulation of Larson et al. (2004) based on the run-up limit uses different input data. However, only three parameters need to be obtained before the experiment. These parameters are the equilibrium slope, run-up limit and calibration coefficient  $K_c$ . The equilibrium slope does not have a significant influence amount of net transported sediment. Therefore, the run-up limit and  $K_c$  value will be studied to find an improvement. To see if there is an improvement first, the results of the individual runs will be calculated, including the correlation coefficients and RMSE. Subsequently, the total wave condition will be calculated.

### 6.1 Run-up limit

The run-up limit in section 5.3 is based on the final profiles of each run. However, when the formulation would be used to predict the net sediment transport rate, it is not possible to determine the run-up limit based on the final profiles. To determine the run-up limit Larson et al. (2004) used equation 20 (Hughes, 1992), which is based on the velocity at the start of the swash zone ( $u_s$ ) and the gravitational force ( $g$ ).

$$R = \frac{u_s^2}{2g} \quad (20)$$

Mase and Iwagaki (1985) developed another formulation to estimate different run-up limits based on field experiments. The run-up limits can be estimated with equation 21. This formulation is based on the deepwater wave height ( $H_0$ ), surf similarity parameter ( $\xi$ ) and coefficients a and b. For the run-up limit the values a = 0.88 and b = 0.69 are used (Mase & Iwagaki, 1985).

$$R = H_0 \times a\xi^b \quad (21)$$

#### 6.1.1 Individual runs

In general, the calculated net sediment transport rates with the calculated run-up limits are lower than the transport rates with the measured run-up limit, which causes less overestimated results. This is due to a lower calculated run-up limit with the method of Hughes (1992) and Mase and Iwagaki (1985) than the measured run-up limit (appendix D). This can be explained because the measured run-up limit is determined as where the profile does not change anymore, while the calculated run-up limits are an approximation of the run-up limit.

Appendix E contains the figures of the new calculated net sediment transport rates. It can be seen that the figures based on the method of Hughes (1992) show better results. Especially for the erosive wave condition the results are closer to the 1:1-line. The results of the accretive wave conditions are still overestimated, which causes a that the results are vertical spread. The calculated net sediment transport rates based on Mase and Iwagaki (1985) are less good but better than when the measured run-up limit is used.

Further, as explained above, the calculated net sediment transport rates are, in general, lower than the transport rates based on the measured run-up limit. This also causes that the RMSE for the calculated run-up limits is lower than for the measured run-up limit. On the other hand, the Pearson and Spearman correlation coefficients do not improve significantly as can be seen in table 6.1. For some of the locations for a selective wave condition the correlation improves, for example, for erosive wave condition of Shaping the beach at x=-0.7m. While for other locations/wave conditions, the correlation decreases. For example, for BARDEX II, where the correlations are the same or worse.

**Table 6.1:** Error statistics for the different methods to determine the Run-up limit.  $R$  = based on the beach profiles,  $U$  = based on the velocity (Hughes, 1992) and  $W$  = based on the deep water wave conditions. A correlations of one is the best possible correlation (Mase & Iwagaki, 1985)

| Wave   | x-loc. | Spearman |       |       | Pearson |       |       | RMSE    |         |         |
|--------|--------|----------|-------|-------|---------|-------|-------|---------|---------|---------|
|        |        | R        | U     | W     | R       | U     | W     | R       | U       | W       |
| StB_E  | -0.70m | 0.20     | 0.43  | 0.49  | 0.51    | 0.38  | 0.60  | 1.07E-4 | 1.37E-5 | 2.29E-5 |
|        | 0.01m  | 0.14     | 0.03  | -0.03 | 0.25    | -0.29 | 0.23  | 1.29E-4 | 1.49E-5 | 2.63E-5 |
|        | 0.90m  | 0.03     | 0.31  | -0.14 | 0.13    | 0.16  | 0.03  | 1.50E-4 | 1.97E-5 | 1.90E-5 |
| StB_A  | -0.70m | -0.31    | -0.27 | -0.17 | -0.22   | -0.33 | -0.27 | 9.96E-4 | 1.52E-5 | 6.38E-4 |
|        | 0.01m  | -0.15    | 0.18  | -0.47 | -0.08   | 0.13  | -0.38 | 4.78E-4 | 8.81E-6 | 1.91E-4 |
|        | 0.9m   | 0.37     | -0.37 | 0.28  | 0.24    | -0.28 | 0.45  | 3.04E-4 | 3.05E-5 | 1.27E-4 |
| RES_E  | -0.53m | -0.40    | -0.20 | -0.20 | -0.49   | -0.17 | -0.55 | 1.48E-4 | 2.15E-5 | 3.01E-5 |
|        | 0.28m  | 0.20     | 0.40  | 0.20  | 0.04    | 0.26  | -0.03 | 2.94E-4 | 2.09E-5 | 4.19E-5 |
|        | 1.26m  | 0.40     | 0.40  | 0.40  | 0.60    | -0.20 | 0.51  | 3.24E-4 | 2.65E-5 | 2.68E-5 |
|        | 2.28m  | -0.20    | 0.40  | -0.40 | -0.19   | 0.56  | -0.36 | 2.37E-4 | 2.29E-5 | 2.03E-5 |
| RES_A  | -0.53m | 0.12     | -0.44 | 0.22  | 0.23    | -0.26 | 0.05  | 4.40E-4 | 7.11E-6 | 2.44E-4 |
|        | 0.28m  | 0.12     | -0.35 | -0.12 | -0.16   | -0.22 | -0.17 | 4.73E-4 | 9.48E-6 | 3.72E-4 |
|        | 1.26m  | -0.38    | 0.11  | -0.63 | -0.33   | 0.01  | -0.57 | 2.29E-4 | 9.69E-6 | 5.66E-5 |
|        | 2.28m  | 0.50     | -0.61 | -0.05 | 0.54    | -0.57 | 0.41  | 4.22E-4 | 4.21E-4 | 2.21E-4 |
| BAR_A1 | 0.27m  | 0.50     | -0.50 | 0.50  | 0.30    | -0.34 | 0.29  | 6.27E-4 | 3.43E-5 | 1.70E-4 |
|        | 1.80m  | 0.40     | -0.40 | 0.40  | 0.52    | -0.57 | 0.51  | 4.58E-4 | 4.59E-5 | 9.63E-5 |
| BAR_A6 | 1.62m  | 0.50     | -0.50 | 0.50  | 0.25    | -0.24 | 0.22  | 1.46E-3 | 9.44E-5 | 7.33E-4 |
|        | 3.08m  | 0.00     | 0.00  | -0.10 | 0.04    | -0.19 | -0.07 | 1.22E-3 | 6.15E-5 | 4.44E-4 |

### 6.1.2 Total wave condition

For the total wave condition, the same two methods are used as before, a calculation for the total wave condition and a mean of the runs. The results based on the run-up limit of Hughes (1992) shows a little improvement when the mean of the run is used (figure 6.2). The results are closer to the 1:1-line, which also results in higher correlations, as shown in table 6.2. The other results for the method of Hughes (1992) based on the calculation of the net sediment transport rates for the whole wave condition are worse. The transport rates are almost zero (figure 6.1) and the correlation is negative/low.

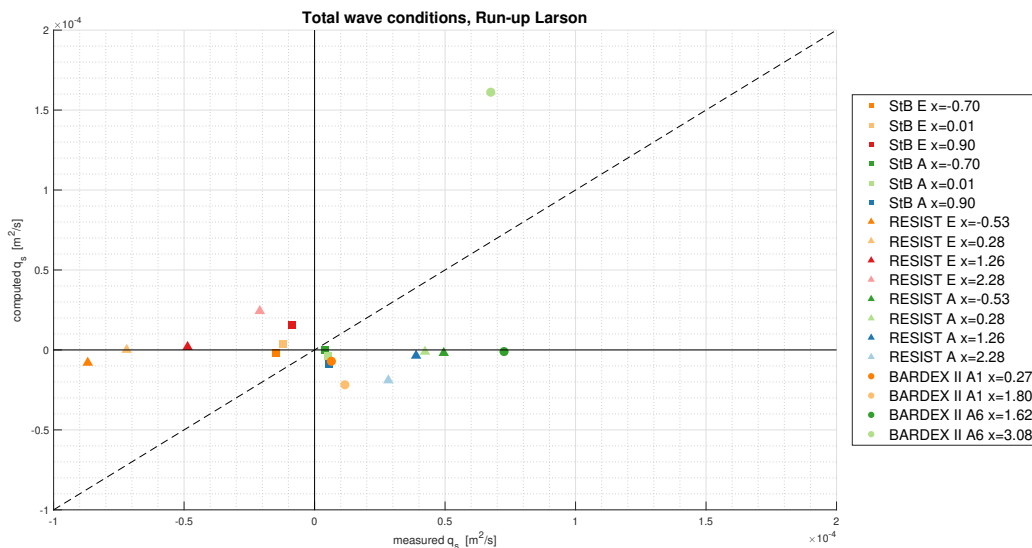


**Figure 6.1:** The net sediment transport rates of the total wave condition calculated using the run-up limit based on the velocity

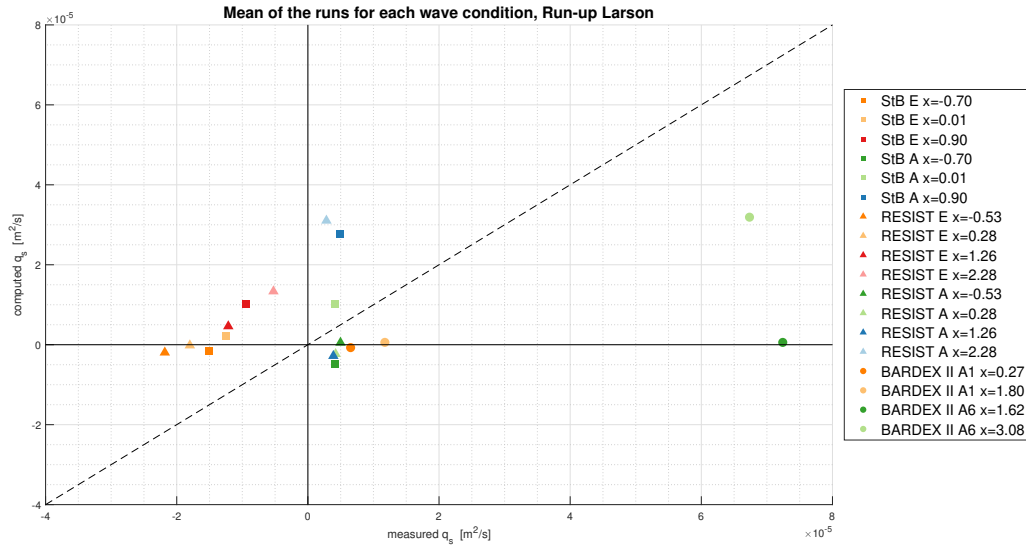


**Figure 6.2:** The mean net sediment transport rates of the individual runs calculated using the run-up limit based on the velocity

The calculation of the run-up limit with the method of Mase and Iwagaki (1985) based on the deepwater wave conditions shows promising results for the total wave condition (neglecting point  $x=3.08\text{m}$  of BARDEX II). The results, in figure 6.3, are similar to the ones based on the measured run-up limit. Also, the error coefficients are higher or almost the same. For the method of Mase and Iwagaki (1985) the net sediment transport are less overestimated for the erosive wave conditions based on the mean of the different runs, as can be seen in figure 6.4. However, for the accretive wave the results are more overestimated and still not in the same direction as measured.

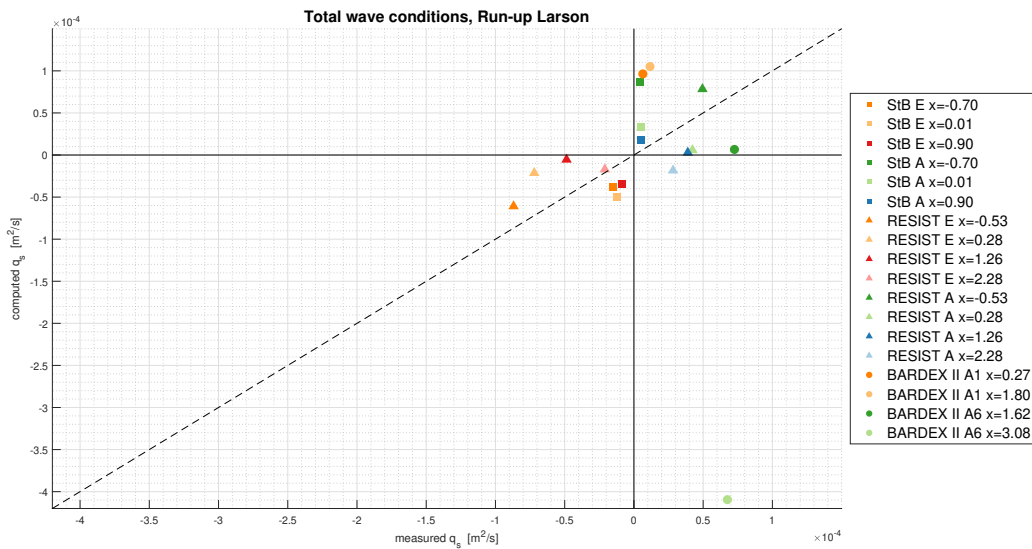


**Figure 6.3:** The net sediment transport rates of the total wave condition calculated using the run-up limit based on the deep water wave conditions

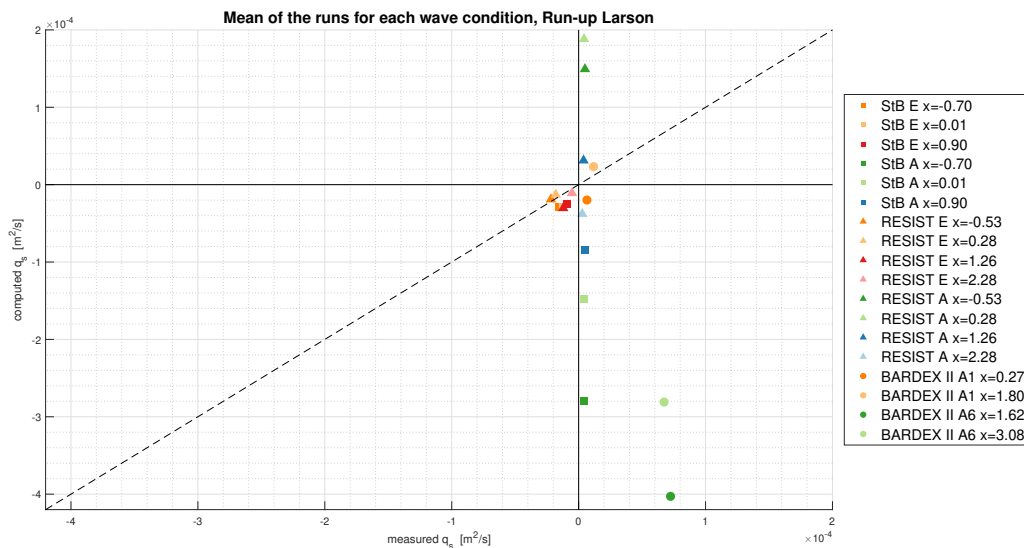


**Figure 6.4:** The mean net sediment transport rates of the individual runs calculated using the run-up limit based on the deep water wave conditions

**Table 6.2:** Error coefficient of the total wave condition.  $R$  = based on the beach profiles,  $U$  = based on the velocity (Hughes, 1992) and  $W$  = based on the deep water wave conditions (Mase & Iwagaki, 1985)

| Method | Spearman |       |       | Pearson |      |       |
|--------|----------|-------|-------|---------|------|-------|
|        | R        | U     | W     | R       | U    | W     |
| Total  | 0.41     | -0.14 | 0.37  | -0.03   | 0.31 | -0.14 |
| Total* | 0.65     | n/a   | 0.60  | 0.55    | n/a  | 0.45  |
| Mean   | -0.12    | 0.17  | -0.19 | -0.56   | 0.31 | -0.66 |

\*With the outlier BARDEX II  $x=3.08\text{m}$  neglected

### 6.1.3 Conclusion Run-up limit

For the individual runs are the calculated net sediment transport rates with the method of Hughes (1992) less overestimated than with the measured run-up limit, especially for the erosive wave conditions. This is because the calculated run-up limits are on average ten times lower. However, the calculated run-up limits are probably too low to be correct. This can be due to too low velocities at the start of the swash zone. The results of the individual runs with the calculated run-up limit with the method of Mase and Iwagaki (1985) are overestimated. The correlations coefficients for both methods are for some runs better and for some runs worse, which causes that it is not possible to conclude if one of the methods is better than the measured run-up limit.

For the total wave condition are the calculated net sediment transport rates with the method of Mase and Iwagaki (1985) quite similar to the results based on the measured run-up limit. The net sediment transport rates have the same direction as measured and are not far off the 1:1-line. While for the mean net sediment transport based on the runs, the results still are off. The Hughes (1992) method is less suitable for the total wave condition, as while for the mean of the run as for the total wave condition.

## Conclusion

In general, it cannot be concluded that the calculated run-up limits are an improvement of the calculated net sediment transport rates because the directions and amount of transported sediment are sometimes better and sometimes worse than with the measured run-up limit. However, when the calculated run-up limits are used, the formulation can be used to predict the net sediment transport rates instead of calculating them after the experiment. Therefore, if the formulation of Larson et al. (2004) based on the run-up limit is used after an experiment or field test, it is better to use the measured run-up limit. While if the net sediment transport must be predicted, it is better to use the run-up limit calculated with the method of Mase and Iwagaki (1985). Because the formulations works better for longer periods (total wave conditions) and the run-up limit of Mase and Iwagaki (1985) has almost the same results as when the measured run-up limit is used.

## 6.2 Calibration coefficient

The Larson et al. (2004) formulation based on the run-up limit includes a calibration coefficient  $K_c$ . Larson et al. (2004) found a  $K_c$  value of  $1.6 \times 10^{-3}$ . This value is based on four field experiments at Hasaki Beach (Japan) between 1990 and 1997. The field experiments of Larson et al. (2004) had a wave period between 8.5 and 14.1 s and a wave height of +/- 0.6 m. The beach contains grains with a size of 0.18 mm and a initial slope of 1:10. Which means that the  $K_c$ -value is calibrated for these conditions. For the individual runs of Shaping the Beach and RESIST it is founded in section 5.3.2 that the  $K_c$ -value is probably to high resulting in overestimated net sediment transport rates.

### 6.2.1 Results

For the calibration of the  $K_c$ -value the erosive and accretive wave conditions of Shaping the Beach and RESIST are used. Because, these wave conditions consist of at least 16 data points, while BARDEX II only consist of ten data points. Based on these four wave conditions, the  $K_c$ -value should be lower, as can be seen in figure 6.5. The results show that with a  $K_c$ -value of  $1.6 \times 10^{-3}$  the RMSE is high and with decreasing  $K_c$ -values the RMSE becomes better (smaller). Only for the erosive wave condition of RESIST the RMSE do not change much.

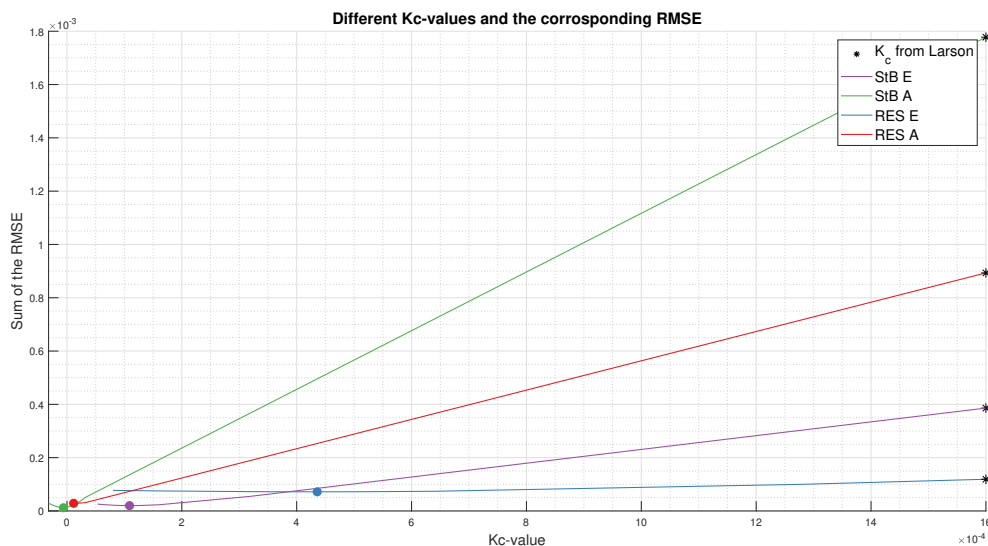


**Figure 6.5:** The RMSE with different  $K_c$ -value, started from the  $K_c$ -value founded by Larson et al. (2004) of  $1.6 \times 10^{-3}$ . The optimal  $K_c$ -values are indicated with the dots.

The optimal  $K_c$ -values are shown in table 6.3. It can be seen that the  $K_c$ -values for the erosive wave conditions are higher than for the accretive wave conditions. Further, the  $K_c$ -value for the accretive wave condition of Shaping the Beach is negative; this is due to that most of the calculated net sediment transport rates have the opposite direction than the measured direction. This is due to the equilibrium slope and local slope and not the  $K_c$ -value, as described in paragraph 5.3.2.

**Table 6.3:** Optimal  $K_c$ -values for Shaping the Beach and RESIST

| Wave condition                    | $K_c$ -value          |
|-----------------------------------|-----------------------|
| Erosive wave Shaping the Beach    | $1.1 \times 10^{-4}$  |
| Erosive RESIST                    | $4.4 \times 10^{-4}$  |
| Accretive wave Shaping the Beach* | $-5.8 \times 10^{-6}$ |
| Accretive wave RESIST             | $1.2 \times 10^{-5}$  |

\*The RMSE is lower when the net sediment transport rates are in the opposite direction

### 6.2.2 Conclusion calibration coefficient

Based on the results of Shaping the Beach and RESIST should the  $K_c$ -value for the erosive wave conditions be in the order of  $10^{-4}$ . Which is ten times lower than the value founded by Larson et al. (2004). For the accretive wave condition, the  $K_c$ -value should be even lower. How much exactly is not clear because for Shaping the Beach, a negative value is found while for RESIST a positive value is found. Also, the magnitude is different for the two data sets. But in general, it is found that the  $K_c$ -value should be lower for Shaping the Beach and RESIST.

The results for the  $K_c$ -value in combination with the results of the field experiment of Larson et al. (2004) show a small tendency between the wave period and the  $K_c$ -value, as can be seen in table 6.4. The results showed a tendency of decreasing wave period with decreasing  $K_c$ -value. Larson et al. (2004) found the same trend in combination with the swash period, although the number of wave conditions is limited (only eight wave conditions). More data are needed to find a relationship for the  $K_c$ -value. For now, if you want to do a calculation, I will recommend using the  $K_c$ -value which corresponding to your wave period for individual runs. For the total wave conditions the  $K_c$ -value is not calibrated. So for the total wave conditions i recommend to use the  $K_c$ -value found by Larson et al. (2004) of  $1.6 \times 10^{-3}$ . Despite this value is calibrated for field data and not lab data.

**Table 6.4:** *Optimal  $K_c$ -values for Shaping the Beach and RESIST*

|              | StB     |           | RESIST  |           | Larson et al. (2004) |        |        |        |
|--------------|---------|-----------|---------|-----------|----------------------|--------|--------|--------|
|              | Erosive | Accretive | Erosive | Accretive | HA92                 | HA95   | HA96   | HA97   |
| Period       | 3.5s    | 5.2s      | 3.7s    | 4.7s      | 13.5s                | 8.5s   | 14.1s  | 12.9s  |
| Wave height  | 0.45m   | 0.25m     | 0.64m   | 0.32m     | 0.40m                | 0.62m  | 0.58m  | 0.53m  |
| $K_c$ -value | 1.1E-4  | -5.8E-6   | 4.4E-4  | 1.2E-5    | 1.0E-3               | 2.1E-3 | 2.3E-3 | 1.2E-3 |

## 7 Discussion

The research is carried out in three phases; every phase has limitations and points that could be discussed. Therefore, each phase is discussed separately.

### 7.1 Phase 1: Processing the data of the wave conditions

For the research, three different data set were selected: Shaping the Beach, RESIST and BARDEX II. Each data set consist of multiple wave conditions. However, only two wave condition, one erosive and one accretive, were selected. This means that there was more data available, but due to time limitations, these data are not used. The used wave conditions consists of multiple runs with different time lengths. These time lengths are not the same for every wave condition. Further, the data sets used a different instrument which means that data is obtained in a different way which causes that the data is not the same and contains different errors for each data set. Besides the various instruments, the location and number of instruments are also not the same. This can influence the comparison between the data set.

Additionally, the data are obtained in wave flumes and are not field data (a simplification). This means that some processes that occur in the field are not included in the data. For example, all the waves are straight on the coast and not under an angle. Also, longshore sediment transport does not occur in a wave flume. These processes affect the net sediment transport rate, which means that if the formulation has perfect results for the wave flume, it does not mean that it also has perfect results for field data.

#### Hydrodynamics

The hydrodynamics (wave height, period and velocity) are calculated for the individual runs. However, these runs do not have all the same duration, the runs vary between 15 minutes and 60 minutes. This causes that the calculated hydrodynamics are not calculated over the same time period for each run. This can influence the results because the shorter the run the more sensitive it is for outliers. However, when the hydrodynamics were calculated the outliers were removed.

The velocity signal from the ADV's and VEC's contained a lot of noise which makes it unavailable to use directly for the formulations. Therefore, the signal is converted to a representative velocity signal for one swash cycle. Subsequently, this signal is used to obtain the velocities. During this conversion, some data is lost and the maximum and minimum are lower because it is a mean signal for the whole run.

#### Morphodynamics

During the analyses of the profiles of the wave conditions, it was founded that the volume of the profiles is not the same. This means that sediment is lost or gained during a run. The loss or gain of sediment should not be possible because the flume is a closed system, but it was the case. Because it was not clear how the difference arose, it was decided not to adjust the profiles. Further, it was notable that the net sediment transport rates calculated from the right and left are not the same. Therefore, a weighted mean is applied to correct for this error. This weighted mean starts after a threshold is reached. This threshold also influences the results, a different threshold gives different results. This causes that the net sediment transport rates are maybe not exactly correct. Further, for RESIST, it was remarkable that the available profiles were only measured until 2/3 of the wave flume. This means that it was not possible to calculate the net sediment transport rate from the left and right side. Therefore, for RESIST the net sediment transport rates are only calculated from the right-hand side, which give a small difference in transport rate. The method with the weighed mean gives a smaller error therefore is this method used for the other two data sets. Also after calculating the net sediment transport rates, wave condition A1 of BARDEX II turn-out to be an accretive wave condition, which was unexpected.

### 7.2 Phase 2: Working with the net sediment transport formulations

Three net sediment transport formulations are used to calculate the net sediment transport rate in the swash zone. The first formulation is the SANTOSS formulation. The SANTOSS formulation is not developed for the swash zone. This is also visible in the results. The results of SANTOSS do not match the measured net sediment transport rates. This is due to that the formulation misses some processes which are essential for the swash zone (bed slope and swash-swash interaction). This formulation was a trial to test if it maybe has some positive results and can be used with some adjustments. This was not the case, the results are not acceptable and too many adjustments are needed to improve the formulation for the swash zone.

From the paper of Larson et al. (2004); two formulations are used in this research. Both formulations do not make a distinction between the bed and suspended load. The transport loads are calculated as one total load, which makes the formulations easier to use but less accurate. The formulations are easier to use because less data is needed and a distinction between bed and suspended load is not needed. The first formulation is based on the integrated non-dimensional bed shear stress for one swash cycle. The bed shear stress is then based on the representative velocity for over one swash cycle. This means that if the velocity signal is under- or overestimated, this will have a directed influence on the net sediment transport rate. Further, the direction of the sediment transport is determined by the difference between the integrated bed shear stress during backwash and uprush. This means that the formulation does not take into account a delay in transport or swash-swash interaction. Overall, this means that the transport rates are very depending on the velocities and that the formulation is very sensitive for an error in the velocity measurements or the processing of the velocity signal. As the velocities are first converted there is a change that the net sediment transport rates are under- or overestimated. This is probably why the sediment transport rates are so different for each wave condition and the directions are most the times in the opposite direction as measured.

The second formulation of Larson et al. (2004) is based on the local and equilibrium slope, run-up limit and a calibration coefficient. The direction is determined by the difference between the equilibrium slope and the local slope. First, the equilibrium slope is difficult to determine, the research about this topic is limited and there are different formulation to determine the equilibrium slope depending on the data that is used. For the research, the best fit formulation of Masselink (1993) is used, which based on data with the same wave conditions. For the local slope is not fixed how it must be determined, this can result in flatter or steeper slopes. This is why in some calculated net sediment transport rates have the opposite direction than the measured transport rate. The run-up limit is the height (vertical) between the start of the swash until the end of the swash zone. The end of the swash zone is not that difficult to obtain from measured profiles. However, the start of the swash zone is more difficult to determine based on the profiles. Therefore, the start of the swash zone is determined by the measured velocity signal, profiles and wave height. Still, it is difficult to determine the beginning of the swash zone, which results in a higher or lower run-up limit and subsequently in a higher or lower net sediment transport rate. Which could cause the overestimations in the results. The last parameter is the calibration coefficient  $K_c$ . For this coefficient, the found value of Larson et al. (2004) is used. However, this is based on four field experiments with longer wave periods. As founded later with the improvement, this value is probably too high for Shaping the Beach and RESIST, which directly cause overestimations of the net sediment transport rate. Because if the  $K_c$ -value becomes five times higher, the transport rates also become five times higher. This results in that the formulation is sensitive for this calibration coefficient,  $K_c$ .

Another remark is that the chosen locations for the calculations are based on the locations of the instruments. During the calculation, it was founded that point  $x=2.28\text{m}$  from RESIST for the accretive condition and point  $x=3.08\text{m}$  of BARDEX II A6 are sometimes outside the swash zone (the points are too far on the beach). This causes strange results at these points. For RESIST this point is still used because for the erosive condition the location was within the swash zone. For BARDEX II, this point is still used because otherwise only one location could be used for wave condition A6.

### 7.3 Phase 3: Improvement of the formulation

Two improvements for the formulation are tested. The first one is the run-up limit. The run-up limit is determined with the initial proposed wave conditions, so the formulation can be used before an experiment. For this determination, two formulation are used. The formulations based on the velocity at the start of the swash zone gives for some wave conditions acceptable results. However, the calculated run-up limits are way too low. This means that the velocities at the beginning of the swash zone are underestimated or that this formulation is only valid for higher velocities. The second formulation based on the surf similarity parameter gives more realistic run-up limits. Also, the results of some individuals correspond with the measured run-up limit. As well, this formulation needs data which is easy to obtain, for example, the wave period and wave height.

The second improvement is the  $K_c$ -value. Different  $K_c$ -values are tested for the individual runs of Shaping the Beach and RESIST. The optimal  $K_c$ -values for the erosive wave condition were ten times smaller and for the accretive wave condition even 100-1000 times smaller. This means that the  $K_c$ -value is in general too high for these wave conditions. Which could be due to that the  $K_c$ -value of Larson et al. (2004) is calibrated for field data. Further, when also looked at the results of Larson et al. (2004), at first sight,

it seems like there is a tendency between the wave period and  $K_c$ -value. Larson et al. (2004) found the same tendency in combination with the swash period. However, one remark is essential, the  $K_c$ -values for Shaping the Beach and RESIST are only calibrated and not validated. This means that the results are a first indication, but more research is needed to conclude something.

Furthermore, the data that is used to analyse the improvement is minimal. Only eight wave conditions are used for the run-up limit and four for the  $K_c$ -value. To see if the improvements work or to see if there is a tendency, more data must be used to test the improvements. This can be, for example, the other wave conditions of Shaping the Beach, RESIST and BARDEX II.

## 8 Conclusions

The current research aims to assess and improve practical formulations for net cross-shore sand transport in the swash zone. As a final step, the research questions, as defined in paragraph 1.51, are examined in this chapter, and the objective will be reviewed.

### 8.1 Research questions

*What are the differences in net sediment transport between the different swash zone laboratory data sets (RESIST, BARDEX II and Shaping the Beach)?*

The net sediment transport rates are depended on the incoming wave condition, the hydrodynamics. From this analysis, it followed that Shaping the Beach (random waves) has the lowest wave height for the erosive and accretive wave condition, respectively 0.45 m and 0.25 m with a wave period of 3.6 s and 5.2 s. Followed by RESIST (bichromatic waves) with a wave height and period of 0.64 m and 3.7 s for the erosive and 0.32 m and 4.7 s for the accretive wave condition. BARDEX II used a wave height of 0.80 m with a period of 8 s (condition A1) and 0.60 m with a period of 12 s (condition A6).

Additionally, the velocities are analysed. This analysis shows that the velocities of RESIST are slightly higher than Shaping the Beach (see figure 4.5 and 4.10). For the BARDEX II data set the velocities are 1.5 times higher than Shaping the Beach and RESIST, which can be explained by the larger waves which are used. Further, all medium velocities are negative, which means that they are directed offshore.

The net sediment transport rates of Shaping the Beach are the lowest of the three data sets compared, in particular, the accretive wave condition. The lower transport rates can be explained by the lower bed shear stresses, which are dependent on the velocity. The transport rates of RESIST and wave condition A1 of BARDEX II are almost identical. However, the accretive wave conditions are in the opposite direction. The transport rates are the same despite that the BARDEX II experiment used higher waves and 1.5 times larger grain sizes, which reduces the net sediment transport. Wave condition A6 of BARDEX II has lower transport rates with accretion in the swash zone and erosion in the surf zone.

*To what extent do the net sediment transport formulations (of Larson et al. (2004) and the SANTOSS project) simulate the net sediment transport rate in the swash zone?*

Three formulations are used to simulate the net sediment transport rate. The first formulation is the SANTOSS formulation. The calculated net sediment transport rates are in general overestimated for both erosive and accretive wave conditions. The directions are mainly onshore directed, which is in the opposite direction as measured for the erosive wave condition. While for the accretive wave condition, it is the same direction as measured. This mainly onshore directed transport rate can be explained by the high velocity and acceleration skewness. Also, an essential offshore directed process is not included in the formulation, the bed slope effect.

The second formulation is the bed shear stress formulation by Larson et al. (2004). This second formulation calculates the net sediment transport rates better for the accretive wave conditions than for the erosive wave conditions. This is mainly due to the direction, which is determined by the difference in the time-average Shields parameter between the uprush and backwash period. During the erosive and accretive wave conditions of Shaping the Beach and RESIST, the time-averaged Shields parameters are higher during the uprush period than during the backwash period. The difference causes net onshore sediment transport, resulting in beach accretion. This onshore directed sediment is for the accretive wave conditions equal to the measured conditions. However, for the erosive wave conditions, the measured net sediment transport rates are offshore directed. The net sediment transport rates of the BARDEX II wave conditions are underestimated. This is caused by the absence of the velocity skewness, which results in almost the same amount of sediment transport during uprush and backwash resulting in a low net sediment transport rate.

Larson et al. (2004) also simplified the bed shear stress formulation resulting in a new formulation mainly based on the bed slope effects and the run-up limit of a swash event. For the direction, the formulations use the difference between the equilibrium slope and local slope. The amount of transported sediment is mainly determined by the calibration coefficient  $K_c$  and the run-up limit. For the erosive wave conditions and total wave conditions these parameters result in a net sediment transport direction that corresponds to the measured transport direction for respectively 77% and 100% of the data points, respectively. For the accretive wave conditions only 47% are in the same direction as measured. The amounts of net

transported sediment during the erosive and accretive wave conditions are far overestimated, resulting in a vertical line with data points. This may be due to the absence of velocity data (which is lost during the simplification) and/or an overestimation of the  $K_c$ -value or/and run-up limit. It is also noticeable that the formulation is better for a longer period (total wave conditions) than for shorter periods of time (individual runs).

Based on the results and the correlation coefficients of Spearman and Pearson, the formulation of Larson et al. (2004) based on the run-up limit was chosen to improve. This is because the results for the total wave condition are quite correct and for the individual runs most of the time the direction is the same as measured. In addition, a calibration coefficient is included in the formulation, which has the potential to be improved.

*How can the formulation with the best correlation be improved to increase the agreement between the simulated and the measured net sediment transport in the swash zone?*

There are two processes which have the most significant influence on the net sediment transport rate for Larson et al. (2004) based on the run-up limit. The first is the run-up limit itself. The run-up limit is initially determined with the final profiles. However, if the formulation would be used to predict the net sediment transport rate, it is not possible to use the final profile. Therefore, two formulations for the run-up limit are tested. The first uses the velocity at the start of the swash zone, and the second is based on the surf similarity parameter. Based on the RMSE and the correlation coefficients, the formulation which uses the surf similarity parameter, is the best. However, the measured run-up limit is still the best but cannot be used to predict the net sediment transport rate. Therefore, if the formulation is used when the final profiles are available, these profiles can be used for the run-up limit; otherwise the formulation based on the surf similarity parameter is the best.

The second parameter, which has a significant influence is the  $K_c$ -value. This calibration coefficient is directly proportional to the net sediment transport rate. For Shaping the Beach and RESIST wave conditions, the  $K_c$ -values have been calibrated. The calibrated  $K_c$ -values for the erosive wave conditions are ten times smaller. While for the accretive wave conditions, the  $K_c$ -values are 100-1000 times smaller. Furthermore, the calibrated  $K_c$ -values in combination with the four  $K_c$ -values of Larson et al. (2004) show a tendency of decreasing  $K_c$ -value with decreasing wave period, which means that the  $K_c$ -value should be lower and is depended on the wave period. Larson et al. (2004) also found this tendency. However, the  $K_c$ -values have not been validated, and four wave conditions (and four of Larson et al. (2004)) are not significant enough to conclude whether the  $K_c$ -value should indeed be lower.

## 8.2 Goal of the research

The goal, as established at the beginning of this research is:

*"The goal of this research is to assess and improve practical formulations for net cross-shore sand transport in the swash zone."*

Reflecting on the purpose of this study, three formulations have been analyzed and assessed. The formula of Larson et al. (2004) based on the run-up limit had the best results/assessment. Therefore, this formulation has been chosen to be improved. Furthermore, two improvements have been proposed with some promising results. However, validation and more research is needed before the improvements can be implemented.

## 9 Recommendations

Further research can improve the results of this research and take the next step to improve a net sediment transport formulation to predict the transport rates in the swash zone. As mentioned before the velocity which is used as an input for the formulation is a representative velocity signal for one swash cycle. For an improved result and a better understanding of the swash zone, it will be recommended to check if the velocity signal can be used instead of the representative velocity signal. Because the real velocity signal and the corresponding bed shear stress should improve the quality of the model predictions for all the tested formulations. Also, it will be useful to check if there is a better formulation for the equilibrium bed slope. This could improve the direction for the formulation of Larson et al. (2004) based on the run-up limit.

Secondly, more research is needed to continue the proposed improvements. For the run-up limit, it will be useful to look if there is a better formulation to determine the run-up limit and research which run-up limit is required (for example the maximum, highest 2% or mean). For the  $K_c$ -value it would be interesting to calibrate this value for more data sets and see if there is a correlation between the wave period and/or swash period and to see the difference between field and lab data. Further, it is needed to validate the obtained  $K_c$ -values to control if they are better in general or just for this wave condition. So, in general, it would be useful for the improvement to test more wave conditions and check for correlations.

Finally, it will be recommended to see if the missing processes can be added to the formulation, maybe instead of the  $K_c$ -value or to calculate the  $K_c$ -value. Especially, the swash-swash interaction could result in an improvement. Because there is already a small tendency between the wave period (and/or swash period) and this is a crucial aspect of swash-swash interaction. Other interesting processes which influences the sediment transport in the swash zone, are groundwater effect (general), bore turbulence (onshore) and sediment response time (offshore). For the sediment response time, maybe the friction factor and specific weight of the sediment can help because these are not included in the formulation.

## References

- Abreu, T., Silva, P. A., Sancho, F., & Temperville, A. (2010). Analytical approximate wave form for asymmetric waves. *Coastal Engineering*, *57*(7), 656–667. doi: <https://doi.org/10.1016/j.coastaleng.2010.02.005>
- Artusi, R., Verderio, P., & Marubini, E. (2002). Bravais-pearson and spearman correlation coefficients: meaning, test of hypothesis and confidence interval. *The International journal of biological markers*, *17*(2), 148–151.
- Austin, M., Masselink, G., O'Hare, T., & Russell, P. (2009). Onshore sediment transport on a sandy beach under varied wave conditions: Flow velocity skewness, wave asymmetry or bed ventilation? *Marine Geology*, *259*(1-4), 86–101. doi: <https://doi.org/10.1016/j.margeo.2009.01.001>
- Bakhtyar, R., Barry, D. A., Li, L., Jeng, D.-S., & Yeganeh-Bakhtiary, A. (2009). Modeling sediment transport in the swash zone: A review. *Ocean Engineering*, *36*(9-10), 767–783. doi: <https://doi.org/10.1016/j.oceaneng.2009.03.003>
- Bakhtyar, R., Ghaheri, A., Yeganeh-Bakhtiary, A., & Barry, D. A. (2009). Process-based model for nearshore hydrodynamics, sediment transport and morphological evolution in the surf and swash zones. *Applied Ocean Research*, *31*(1), 44–56. doi: <https://doi.org/10.1016/j.apor.2009.05.002>
- Benesty, J., Chen, J., Huang, Y., & Cohen, I. (2009). Pearson correlation coefficient. In *Noise reduction in speech processing* (pp. 1–4). Springer.
- Cáceres, I., & Alsina, J. M. (2012). A detailed, event-by-event analysis of suspended sediment concentration in the swash zone. *Continental Shelf Research*, *41*, 61–76. doi: <https://doi.org/10.1016/j.csr.2012.04.004>
- Chai, T., & Draxler, R. R. (2014). Root mean square error (rmse) or mean absolute error (mae)?—arguments against avoiding rmse in the literature. *Geoscientific model development*, *7*(3), 1247–1250. doi: <https://doi.org/10.5194/gmd-7-1247-2014>
- Chardón-Maldonado, P., Pintado-Patiño, J. C., & Puleo, J. A. (2015). Advances in swash-zone research: Small-scale hydrodynamic and sediment transport processes. *Coastal Engineering*, *115*, 8–25. Retrieved from <http://dx.doi.org/10.1016/j.coastaleng.2015.10.008> doi: <https://doi.org/10.1016/j.coastaleng.2015.10.008>
- Dean, R. G., et al. (1973). Heuristic models of sand transport in the surf zone. In *First australian conference on coastal engineering, 1973: Engineering dynamics of the coastal zone* (p. 215).
- de Winter, J. C., Gosling, S. D., & Potter, J. (2016). Comparing the pearson and spearman correlation coefficients across distributions and sample sizes: A tutorial using simulations and empirical data. *Psychological methods*, *21*(3), 273. doi: <https://doi.org/10.1037/met0000079>
- Dionísio António, S., van der Werf, J., Vermeulen, B., Cáceres, I., Alsina, J. M., Larner, M., ... Hulscher, S. (2020). Cross-shore sediment transport in the swash zone: large-scale laboratory experiments.
- Eichentopf, S., Baldock, T. E., Cáceres, I., Hurther, D., Karunarathna, H., Postacchini, M., ... Alsina, J. M. (2019). Influence of storm sequencing and beach recovery on sediment transport and beach resilience (resist). In *Proceedings of the hydralab+ joint user meeting, bucharest, romania* (pp. 21–25).
- Eichentopf, S., Van der Zanden, J., Cáceres, I., Baldock, T. E., & Alsina, J. M. (2020). Influence of storm sequencing on breaker bar and shoreline evolution in large-scale experiments. *Coastal engineering*, *157*, 103659. doi: <https://doi.org/10.1016/j.coastaleng.2020.103659>
- Elfrink, B., & Baldock, T. (2002). Hydrodynamics and sediment transport in the swash zone: a review and perspectives. *Coastal Engineering*, *45*(3-4), 149–167. doi: [https://doi.org/10.1016/S0378-3839\(02\)00032-7](https://doi.org/10.1016/S0378-3839(02)00032-7)
- Grasso, F., Michallet, H., & Barthélemy, E. (2011). Sediment transport associated with morphological beach changes forced by irregular asymmetric, skewed waves. *Journal of Geophysical Research: Oceans*, *116*(C3). doi: <https://doi.org/10.1029/2010JC006550>
- Hegge, B. J., & Masselink, G. (1996). Spectral analysis of geomorphic time series: auto-spectrum. *Earth Surface Processes and Landforms*, *21*(11), 1021–1040. doi: [https://doi.org/10.1002/\(SICI\)1096-9837\(199611\)21:11<1021::AID-ESP703>3.0.CO;2-D](https://doi.org/10.1002/(SICI)1096-9837(199611)21:11<1021::AID-ESP703>3.0.CO;2-D)
- Horn, D. (2006). Measurements and modelling of beach groundwater flow in the swash-zone: a review. *Continental Shelf Research*, *26*, 622–652. doi: <https://doi.org/10.1016/j.csr.2006.02.001>
- Horstman, E. M., Dohmen-Janssen, C. M., Narra, P., Van den Berg, N., Siemerink, M., & Hulscher, S. J. (2014). Wave attenuation in mangroves: A quantitative approach to field observations. *Coastal engineering*, *94*, 47–62. doi: <https://doi.org/10.1016/j.coastaleng.2014.08.005>
- Hughes, M. G. (1992). Application of a non-linear shallow water theory to swash following bore collapse on

- a sandy beach. *Journal of Coastal Research*, 562–578. doi: <https://www.jstor.org/stable/4298006>
- Jackson, N., & Masselink, K., G. and Nordstrom. (2004). The role of bore collapse and local shear stresses on the spatial distribution of sediment load in the up-rush of an intermediate-state beach. *Marine Geology*, 203, 109–118. doi: [https://doi.org/10.1016/S0025-3227\(03\)00328-1](https://doi.org/10.1016/S0025-3227(03)00328-1)
- Jongedijk, C. (2017). *Improving xbeach non-hydrostatic model predictions of the swash morphodynamics of intermediate-reflective beaches* (Tech. Rep.). Delft university of technology.
- Kobayashi, N. (1999). Numerical modeling of wave run-up on coastal structures and beaches. *Marine Technology Society journal*, 33(3), 33–37. doi: <https://doi.org/10.4031/MTSJ.33.3.5>
- Lanckriet, T. (2016). *Near-bed hydrodynamics and sediment transport in the swash zone*. University of Delaware.
- Larson, M., Kubota, S., & Erikson, L. (2004). Swash-zone sediment transport and foreshore evolution: Field experiments and mathematical modeling. *Marine Geology*, 212(1-4), 61–79. doi: <https://doi.org/10.1016/j.margeo.2004.08.004>
- Madsen, O. S. (1991). Mechanics of cohesionless sediment transport in coastal waters. In *Coastal sediments* (pp. 15–27).
- Madsen, O. S. (1993). Sediment transport on the shelf. *Proceedings of the Sediment Transport Workshop DRP, TA1*.
- Mase, H., & Iwagaki, Y. (1985). Run-up of random waves on gentle slopes. In *Coastal engineering 1984* (pp. 593–609).
- Masselink, G. (1993). Simulating the effects of tides on beach morphodynamics. *Journal of Coastal Research*, 180–197. doi: <https://www.jstor.org/stable/25735729>
- Masselink, G., Conley, D., & Ruju, A. (2012). *Data Storage Report* (Tech. Rep.). Plymouth University.
- Masselink, G., & Puleo, J. A. (2006). Swash-zone morphodynamics. *Continental Shelf Research*, 26(5), 661–680. doi: <https://doi.org/10.1016/j.csr.2006.01.015>
- Masselink, G., Ruju, A., Conley, D., Turner, I., Ruessink, G., Matias, A., ... others (2016). Large-scale barrier dynamics experiment ii (bardex ii): Experimental design, instrumentation, test program, and data set. *Coastal Engineering*, 113, 3–18. doi: <https://doi.org/10.1016/j.coastaleng.2015.07.009>
- Masselink, G., Turner, I., Conley, D., Ruessink, G., Matias, A., Thompson, C., ... Wolters, G. (2013). Bardex ii: Bringing the beach to the laboratory—again! *Journal of Coastal Research*, 65(sp2), 1545–1551. doi: <https://doi.org/10.2112/SI65-261.1>
- Milivojević, N., Simić, Z., Orlić, A., Milivojević, V., & Stojanović, B. (2009). Parameter estimation and validation of the proposed swat based rainfall-runoff model: Methods and outcomes. *Journal of Serbian Society for Computational Mechanics*, 3(1), 86–110.
- Moreno, M., Ferrero, T., Granelli, V., Marin, V., Albertelli, G., & Fabiano, M. (2006). Across shore variability and trophodynamic features of meiofauna, in a microtidal beach of the nw mediterranean estuarine. *Coastal and Shelf Science*, 66, 357–367. doi: <https://doi.org/10.1016/j.ecss.2005.08.016>
- Nam, P. T., Larson, M., Hanson, H., et al. (2009). A numerical model of nearshore waves, currents, and sediment transport. *Coastal Engineering*, 56(11-12), 1084–1096. doi: <https://doi.org/10.1016/j.coastaleng.2009.06.007>
- Nomden, H. G. (2011). *Santoss sand transport model: Implementing and testing within the morphological model unibest-tc* (Unpublished master's thesis). University of Twente.
- Pontius, R. G., Thontteh, O., & Chen, H. (2008). Components of information for multiple resolution comparison between maps that share a real variable. *Environmental and Ecological Statistics*, 15(2), 111–142. doi: <https://doi.org/10.1007/s10651-007-0043-y>
- Posanski, D. (2018). STENCIL GWK experiments May - June 2018 Net transport rates analysis - Preliminary version. (June).
- Puleo, J., Beach, R., Holman, R. A., & Allen, J. (2000). Swash zone sediment suspension and transport and the importance of bore-generated turbulence. *Journal of Geophysical Research: Oceans*, 105(C7), 17021–17044. doi: <https://doi.org/10.1029/2000JC900024>
- Puleo, J. A., Lanckriet, T., Conley, D., & Foster, D. (2016). Sediment transport partitioning in the swash zone of a large-scale laboratory beach. *Coastal Engineering*, 113, 73–87. doi: <http://dx.doi.org/10.1016/j.coastaleng.2015.11.001>
- Ribberink, J. S. (2011). *River Dynamics II : Transport Processes and Morphology* (Tech. Rep. No. March). University of Twente.
- Rocha, M. (2014). *Nonlinearities of waves propagating over a mild-slope beach: laboratory and numerical results*. Available at <http://www.legi.grenoble-inp.fr/web/spip.php?article885&lang=en> (2019/12/13).

- Rooijen, A. A. V. (2011). *Modelling sediment transport in the swash zone* (Tech. Rep. No. August). Delft University of Technology.
- Ruessink, B., Ramaekers, G., & Van Rijn, L. (2012). On the parameterization of the free-stream non-linear wave orbital motion in nearshore morphodynamic models. *Coastal Engineering*, 65, 56–63. doi: <https://doi.org/10.1016/j.coastaleng.2012.03.006>
- Spearman, C. (1961). "general intelligence" objectively determined and measured. doi: <https://doi.org/10.1037/11491-006>
- Turner, I. L., Rau, G. C., Andersen, M. S., Austin, M. J., Puleo, J. A., & Masselink, G. (2013). Coastal sand barrier hydrology—observations from the bardex ii prototype-scale laboratory experiment. *Journal of Coastal Research*, 65(sp2), 1886–1891. doi: <https://doi.org/10.2112/SI65-319.1>
- Van der A, D. A., Ribberink, J. S., Van der Werf, J. J., O'Donoghue, T., Buijsrogge, R. H., & Kranenburg, W. M. (2013). Practical sand transport formula for non-breaking waves and currents. *Coastal Engineering*, 76, 26–42. doi: <http://dx.doi.org/10.1016/j.coastaleng.2013.01.007>
- van der Werf, J., Dionísio António, S., Kranenburg, J., Vermeulen, B., Campmans, G., van der Zanden, J., ... Hulscher, S. (2019). Shaping the beach: Cross-shore sand transport in the swash zone. *Coastal Structures 2019*, 803–811. doi: [https://doi.org/10.18451/978-3-939230-64-9\\_080](https://doi.org/10.18451/978-3-939230-64-9_080)
- van der Zanden, J., Cáceres, I., Eichtopf, S., Ribberink, J. S., van der Werf, J. J., & Alsina, J. M. (2019). Sand transport processes and bed level changes induced by two alternating laboratory swash events. *Coastal Engineering*, 152(June), 103519. Retrieved from <https://doi.org/10.1016/j.coastaleng.2019.103519> doi: <https://doi.org/10.1016/j.coastaleng.2019.103519>
- Van Rijn, L. (2013). Simple general formulae for sand transport in rivers, estuaries and coastal waters. Retrieved from [www.leovanrijn-sediment.com](http://www.leovanrijn-sediment.com), 1–16.
- Veen, R. (2014). *The implementation and testing of the santoss sand transport model in delft3d* (Unpublished master's thesis). University of Twente.
- Walstra, D., Van Rijn, L., Van Ormondt, M., Brière, C., & Talmon, A. (2007). The effects of bed slope and wave skewness on sediment transport and morphology. In *Coastal sediments' 07* (pp. 137–150).
- Waters, R. (2008). *Energy from ocean waves: full scale experimental verification of a wave energy converter* (Unpublished doctoral dissertation). Universitetsbiblioteket.
- Wenneker, I., Hoffmann, R., & Hofland, B. (2016). Wave generation and wave measurements in the new delta flume. In *6th international conference on the application of physical modelling in coastal and port engineering and science*.
- Wright, L. D., & Short, A. D. (1984). Morphodynamic variability of surf zones and beaches: a synthesis. *Marine geology*, 56(1-4), 93–118. doi: [https://doi.org/10.1016/0025-3227\(84\)90008-2](https://doi.org/10.1016/0025-3227(84)90008-2)

## A Representative velocity and acceleration signal

The analytical expression of Abreu et al. (2010) can be used to obtain a representation of the velocity (equation 22) and acceleration (equation 23).

$$U(t) = U_{rms} \sqrt{2} f \frac{\left[ \sin(\omega t) + \frac{r \sin(\phi)}{1 + \sqrt{1 - r^2}} \right]}{[1 - r \cos(\omega t + \phi)]} \quad (22)$$

$$a(t) = U_{rms} \sqrt{2} f \frac{\left[ \cos(\omega t) - r \cos(\phi) - \frac{r^2}{1 + \sqrt{1 - r^2}} \sin(\phi) \sin(\omega t + \phi) \right]}{[1 - r \cos(\omega t + \phi)]^2} \quad (23)$$

Where (Veen, 2014):

- $U_{rms}$  = Root mean square velocity
- $\omega$  = angular frequency ( $\omega = 2\pi/T$ )
- $\phi$  = waveform parameter
- $r$  = parameter of skewness or nonlinearity
- $f$  = dimensionless factor ( $f = \sqrt{1 - r^2}$ )

The nonlinear parameters  $r$  and  $\phi$  which are used in the equations of Abreu et al. (2010) can be estimated by a parameterization presented by Ruessink et al. (2012). This estimation is based on the wave skewness ( $S_u$ ) and wave asymmetry ( $A_u$ ) which are described by:

$$S_u = \frac{\overline{U_w^3(t)}}{\sigma_{U_w}^3} \quad (24)$$

$$A_u = \frac{\overline{H(U_w^3)}}{\sigma_{U_w}^3} \quad (25)$$

Where (Ruessink et al., 2012):

- $\sigma_{u_w}$  = the standard deviation of  $U_w(t)$
- $U_w$  = Wave orbital velocity amplitude

The wave skewness and wave asymmetry were combined into a total non-linearity ( $B$ ) and phase ( $\psi$ ).

$$B = \sqrt{S_u^2 + A_u^2} \quad (26)$$

$$\phi = \tan^{-1}(A_u/S_u) - \frac{1}{2}\pi \quad (27)$$

To find  $r$  Ruessink et al. (2012) fitted a third order polygon to the relation between  $B$  and  $r$ . This third order polygon is as follows:

$$r = 0.0517B^3 - 0.4095B^2 + 1.085B - 0.0099 \quad (28)$$

## B Hydrodynamic and morphological processes

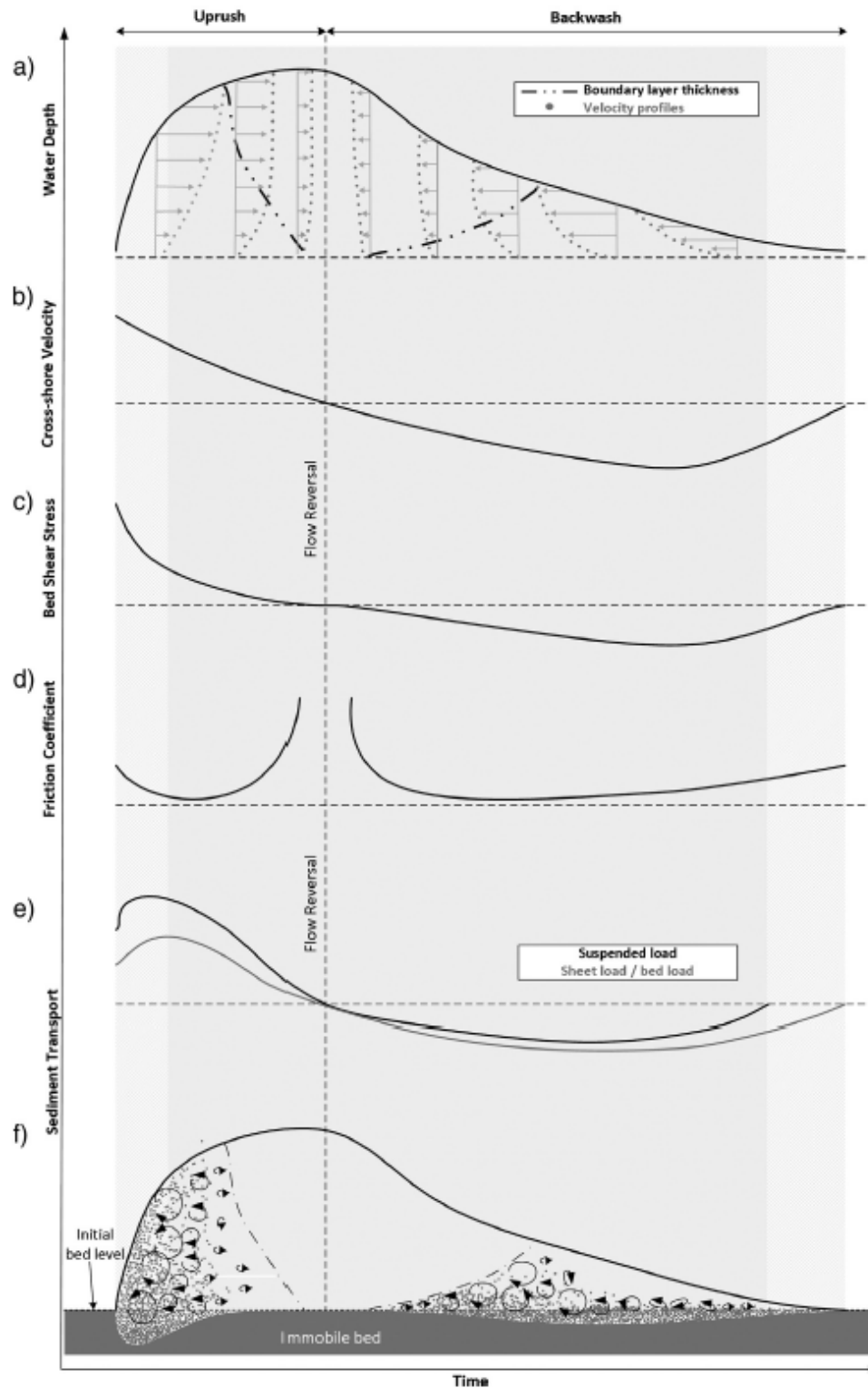


**Figure B.1:** Schematic of hydrodynamic and sediment transport processes occurring within a single swash event (Chardón-Maldonado et al., 2015).

## C Hypotheses

### C.1 Hypotheses SANTOSS

**Table C.1:** *Hypotheses SANTOSS for each run off the different wave condition*

| Data set | Run   | Wave skewness and asymmetry | Mean velocity | Bed shear stress | Hypothesis                      |
|----------|-------|-----------------------------|---------------|------------------|---------------------------------|
| StB-E    | 3     | Velocity skewed             | Offshore      | Onshore          | Onshore sediment transport      |
| StB-E    | 4     | Velocity skewed             | Almost zero   | Onshore          | Onshore sediment transport      |
| StB-E    | 6     | Velocity skewed             | Almost zero   | Onshore          | Onshore sediment transport      |
| StB-E    | 7     | Velocity skewed             | Almost zero   | Onshore          | Onshore sediment transport      |
| StB-E    | 8     | Velocity skewed             | Offshore      | Onshore          | Onshore sediment transport      |
| StB-E    | 9     | Velocity skewed             | Offshore      | Onshore          | Onshore sediment transport      |
| StB-A    | 11    | Velocity skewed             | Offshore      | Onshore          | Onshore sediment transport      |
| StB-A    | 12    | Velocity skewed             | Low offshore  | Onshore          | Onshore sediment transport      |
| StB-A    | 13    | Velocity skewed             | Low offshore  | Onshore          | Onshore sediment transport      |
| StB-A    | 14    | Velocity skewed             | Low offshore  | Onshore          | Onshore sediment transport      |
| StB-A    | 15    | Velocity skewed             | Low offshore  | Onshore          | Onshore sediment transport      |
| StB-A    | 16    | Velocity skewed             | Low offshore  | Onshore          | Onshore sediment transport      |
| StB-A    | 17    | Velocity skewed             | Low offshore  | Onshore          | Onshore sediment transport      |
| StB-A    | 18    | Velocity skewed             | Offshore      | Onshore          | Onshore sediment transport      |
| StB-A    | 19    | Velocity skewed             | Offshore      | Onshore          | Onshore sediment transport      |
| RES-E    | 88    | Velocity skewed             | High offshore | Strong onshore   | Onshore sediment transport      |
| RES-E    | 89    | Velocity skewed             | High offshore | Strong onshore   | Onshore sediment transport      |
| RES-E    | 90    | Velocity skewed             | High offshore | Strong onshore   | Onshore sediment transport      |
| RES-E    | 91    | Velocity skewed             | High offshore | Strong onshore   | Onshore sediment transport      |
| RES-A    | 24/25 | Velocity skewed             | Offshore      | Strong onshore   | Onshore sediment transport      |
| RES-A    | 26/27 | Velocity skewed             | High offshore | Onshore          | Low offshore sediment transport |
| RES-A    | 28    | Velocity skewed             | Offshore      | Onshore          | Low onshore sediment transport  |
| RES-A    | 29    | Velocity skewed             | High offshore | Onshore          | Low offshore sediment transport |
| RES-A    | 30    | Velocity skewed             | High offshore | Onshore          | Low onshore sediment transport  |

| Data set | Run   | Wave skewness and asymmetry | Mean velocity | Bed shear stress | Hypothesis                      |
|----------|-------|-----------------------------|---------------|------------------|---------------------------------|
| RES-A    | 31    | Velocity skewed             | High offshore | Onshore          | Low onshore sediment transport  |
| RES-A    | 32    | Velocity skewed             | Offshore      | Onshore          | Low onshore sediment transport  |
| RES-A    | 33    | Velocity skewed             | Offshore      | Onshore          | Low onshore sediment transport  |
| RES-A    | 34    | Velocity skewed             | High offshore | Onshore          | Low offshore sediment transport |
| RES-A    | 35    | Velocity skewed             | Offshore      | Onshore          | Low onshore sediment transport  |
| BAR-A1   | 1-5   | Sinus                       | Almost zero   | Weak onshore     | Almost no sediment transport    |
| BAR-A1   | 6/7   | Sinus                       | Almost zero   | Weak onshore     | Almost no sediment transport    |
| BAR-A1   | 8/9   | Sinus                       | Low offshore  | Weak onshore     | Almost no sediment transport    |
| BAR-A1   | 10/11 | Sinus                       | Low offshore  | Weak onshore     | Almost no sediment transport    |
| BAR-A1   | 12/13 | Sinus                       | Low offshore  | Weak onshore     | Almost no sediment transport    |
| BAR-A6   | 34-38 | Acceleration skewed         | Almost zero   | Weak onshore     | Onshore sediment transport      |
| BAR-A6   | 39    | Acceleration skewed         | Almost zero   | Weak onshore     | Onshore sediment transport      |
| BAR-A6   | 40/41 | Acceleration skewed         | Low offshore  | Weak onshore     | Weak onshore sediment transport |
| BAR-A6   | 42/43 | Acceleration skewed         | Low offshore  | Weak onshore     | Weak onshore sediment transport |
| BAR-A6   | 44/45 | Acceleration skewed         | Low offshore  | Weak onshore     | Weak onshore sediment transport |

## C.2 Hypotheses formulation of Larson: Bed shear stress

**Table C.2:** Hypotheses Larson et al. (2004) based on bed shear stress for each run off the different wave condition

| Wave event | Run   | Shields parameters difference  | Hypothesis                       |
|------------|-------|--------------------------------|----------------------------------|
| StB-E      | 3     | 2-5 times higher during uprush | Onshore sediment transport       |
| StB-E      | 4     | 2-5 times higher during uprush | Onshore sediment transport       |
| StB-E      | 6     | 2-4 times higher during uprush | Onshore sediment transport       |
| StB-E      | 7     | 2-4 times higher during uprush | Onshore sediment transport       |
| StB-E      | 8     | 4 times higher during uprush   | Onshore sediment transport       |
| StB-E      | 9     | 3-5 times higher during uprush | Onshore sediment transport       |
| StB-A      | 11    | 3-9 times higher during uprush | High onshore sediment transport  |
| StB-A      | 12    | 3-9 times higher during uprush | High onshore sediment transport  |
| StB-A      | 13    | 3-7 times higher during uprush | High onshore sediment transport  |
| StB-A      | 14    | 3-8 times higher during uprush | High onshore sediment transport  |
| StB-A      | 15    | 2-7 times higher during uprush | High onshore sediment transport  |
| StB-A      | 16    | 2-6 times higher during uprush | Onshore sediment transport       |
| StB-A      | 17    | 2-6 times higher during uprush | Onshore sediment transport       |
| StB-A      | 18    | 2-6 times higher during uprush | Onshore sediment transport       |
| StB-A      | 19    | 2-6 times higher during uprush | Onshore sediment transport       |
| RES-E      | 88    | 2-3 times higher during uprush | Onshore sediment transport       |
| RES-E      | 89    | 2-3 times higher during uprush | Onshore sediment transport       |
| RES-E      | 90    | 3 times higher during uprush   | Onshore sediment transport       |
| RES-E      | 91    | 3-5 times higher during uprush | Onshore sediment transport       |
| RES-A      | 24/25 | 3-8 times higher during uprush | High onshore sediment transport  |
| RES-A      | 26/27 | 3-5 times higher during uprush | Onshore sediment transport       |
| RES-A      | 28    | 3-4 times higher during uprush | Onshore sediment transport       |
| RES-A      | 29    | 3-5 times higher during uprush | Onshore sediment transport       |
| RES-A      | 30    | 2-5 times higher during uprush | Onshore sediment transport       |
| RES-A      | 31    | 3-4 times higher during uprush | Onshore sediment transport       |
| RES-A      | 32    | 2-4 times higher during uprush | Onshore sediment transport       |
| RES-A      | 33    | 1-3 times higher during uprush | Onshore sediment transport       |
| RES-A      | 34    | 2-3 times higher during uprush | Onshore sediment transport       |
| RES-A      | 35    | 2 times higher during uprush   | Onshore sediment transport       |
| BAR-A1     | 1-5   | 1.2 times higher during uprush | Weak offshore sediment transport |
| BAR-A1     | 6/7   | 1.2 times higher during uprush | Weak offshore sediment transport |
| BAR-A1     | 8/9   | 1.3 times higher during uprush | Weak offshore sediment transport |
| BAR-A1     | 10/11 | 1.2 times higher during uprush | Weak offshore sediment transport |
| BAR-A1     | 12/13 | 1.1 times higher during uprush | Weak offshore sediment transport |
| BAR-A6     | 34-38 | 1.2 times higher during uprush | Weak offshore sediment transport |
| BAR-A6     | 39    | +/- the same                   | No sediment transport            |
| BAR-A6     | 40/41 | 1.3 times higher during uprush | Weak offshore sediment transport |
| BAR-A6     | 42/43 | 1.3 times higher during uprush | Weak offshore sediment transport |
| BAR-A6     | 44/45 | 1.3 times higher during uprush | Weak offshore sediment transport |

### C.3 Hypotheses formulation of Larson: Run-up limit

**Table C.3:** *Hypotheses Larson et al. (2004) based on the run-up limit for each run off the different wave condition*

| Wave event | Run   | Run-up limit | Elevation                        | Local slope vs Equilibrium slope         | Hypothesis                       |
|------------|-------|--------------|----------------------------------|--|----------------------------------|
| StB-E      | 3     | 0.52m        | 0.013m, 0.076m, 0.149m           | Local slope steeper as equilibrium slope | Offshore sediment transport      |
| StB-E      | 4     | 0.53m        | 0.022m, 0.080m, 0.141m           | Local slope steeper as equilibrium slope | Offshore sediment transport      |
| StB-E      | 6     | 0.54m        | 0.023m, 0.078m, 0.139m           | Local slope steeper as equilibrium slope | Offshore sediment transport      |
| StB-E      | 7     | 0.54m        | 0.018m, 0.068m, 0.131m           | Local slope steeper as equilibrium slope | Offshore sediment transport      |
| StB-E      | 8     | 0.55m        | 0.016m, 0.068m, 0.134m           | Local slope steeper as equilibrium slope | Offshore sediment transport      |
| StB-E      | 9     | 0.56m        | 0.016m, 0.066m, 0.133m           | Local slope steeper as equilibrium slope | Offshore sediment transport      |
| StB-A      | 11    | 0.51m        | 0.012m, 0.061m, 0.147m           | Equilibrium slope steeper as local slope | Onshore sediment transport       |
| StB-A      | 12    | 0.54m        | 0.006m, 0.074m, 0.181m           | Equilibrium slope steeper as local slope | Onshore sediment transport       |
| StB-A      | 13    | 0.54m        | 0.012m, 0.071m, 0.182m           | Equilibrium slope steeper as local slope | Onshore sediment transport       |
| StB-A      | 14    | 0.55m        | 0.009m, 0.079m, 0.195m           | Equilibrium slope steeper as local slope | Onshore sediment transport       |
| StB-A      | 15    | 0.56m        | 0.024m, 0.089m, 0.211m           | Equilibrium slope steeper as local slope | Onshore sediment transport       |
| StB-A      | 16    | 0.57m        | 0.030m, 0.092m, 0.224m           | Equilibrium slope steeper as local slope | Onshore sediment transport       |
| StB-A      | 17    | 0.57m        | 0.028m, 0.100m, 0.234m           | Equilibrium slope steeper as local slope | Low onshore sediment transport   |
| StB-A      | 18    | 0.58m        | -0.035m, 0.088m, 0.241m          | Equilibrium slope steeper as local slope | Low onshore sediment transport   |
| StB-A      | 19    | 0.60m        | -0.028m, 0.118m, 0.265m          | Equilibrium slope steeper as local slope | Low onshore sediment transport   |
| RES-E      | 88    | 0.78m        | 0.035m, 0.093m, 0.164m, 0.229m   | Local slope steeper as equilibrium slope | Offshore sediment transport      |
| RES-E      | 89    | 0.85m        | 0.037m, 0.078m, 0.174m, 0.244m   | Local slope steeper as equilibrium slope | Offshore sediment transport      |
| RES-E      | 90    | 0.85m        | 0.028m, 0.067m, 0.123m, 0.216m   | Equilibrium slope steeper as local slope | Onshore sediment transport       |
| RES-E      | 91    | 0.84m        | 0.030m, 0.062m, 0.106m, 0.191m   | Local slope steeper as equilibrium slope | High offshore sediment transport |
| RES-A      | 24/25 | 0.44m        | 0.023m, 0.079m, 0.138m, 0.206m   | Equilibrium slope steeper as local slope | Onshore sediment transport       |
| RES-A      | 26/27 | 0.43m        | -0.001m, 0.037m, 0.090m, 0.227m  | Local slope steeper as equilibrium slope | Offshore sediment transport      |
| RES-A      | 28    | 0.44m        | -0.004m, 0.023m, 0.068m, 0.207m  | Equilibrium slope steeper as local slope | Onshore sediment transport       |
| RES-A      | 29    | 0.42m        | -0.018m, -0.013m, 0.037m, 0.170m | Equilibrium slope steeper as local slope | Onshore sediment transport       |
| RES-A      | 30    | 0.40m        | -0.004m, -0.007m, 0.027m, 0.129m | Local slope steeper as equilibrium slope | Offshore sediment transport      |

| Wave event | Run   | Run-up limit | Elevation                      | Local slope vs Equilibrium slope         | Hypothesis                      |
|------------|-------|--------------|--------------------------------|--|---------------------------------|
| RES-A      | 31    | 0.39m        | 0.014m, 0.034m, 0.055m, 0.165m | Equilibrium slope steeper as local slope | Onshore sediment transport      |
| RES-A      | 32    | 0.39m        | 0.018m, 0.033m, 0.049m, 0.185m | Equilibrium slope steeper as local slope | Onshore sediment transport      |
| RES-A      | 33    | 0.39m        | 0.012m, 0.033m, 0.052m, 0.186m | Equilibrium slope steeper as local slope | Onshore sediment transport      |
| RES-A      | 34    | 0.38m        | 0.019m, 0.041m, 0.075m, 0.208m | Equilibrium slope steeper as local slope | Onshore sediment transport      |
| RES-A      | 35    | 0.38m        | 0.005m, 0.035m, 0.075m, 0.230m | Equilibrium slope steeper as local slope | Onshore sediment transport      |
| BAR-A1     | 1-5   | 1.12m        | 0.149m, 0.256m                 | Equilibrium slope steeper as local slope | Onshore sediment transport      |
| BAR-A1     | 6/7   | 1.20m        | 0.196m, 0.340m                 | Equilibrium slope steeper as local slope | Onshore sediment transport      |
| BAR-A1     | 8/9   | 0.1.24m      | 0.227m, 0.352m                 | Local slope steeper as equilibrium slope | Offshore sediment transport     |
| BAR-A1     | 10/11 | 1.29m        | 0.220m, 0.406m                 | Local slope steeper as equilibrium slope | Low offshore sediment transport |
| BAR-A1     | 12/13 | 1.24m        | 0.132m, 0.271m                 | Equilibrium slope steeper as local slope | Onshore sediment transport      |
| BAR-A6     | 34-38 | 1.65m        | 0.430m, 0.645m                 | Local slope steeper as equilibrium slope | Offshore sediment transport     |
| BAR-A6     | 39    | 1.55m        | 0.342m, 0.519m                 | Local slope steeper as equilibrium slope | Offshore sediment transport     |
| BAR-A6     | 40/41 | 1.57m        | 0.364m, 0.554m                 | Local slope steeper as equilibrium slope | Low offshore sediment transport |
| BAR-A6     | 42/43 | 1.52m        | 0.356m, 0.550m                 | Local slope steeper as equilibrium slope | Offshore sediment transport     |
| BAR-A6     | 44/45 | 1.52m        | 0.355m, 0.551m                 | Local slope steeper as equilibrium slope | Offshore sediment transport     |

## D The run-up limits for the different methods

**Table D.1:** Run-up limits.  $R$  = based on the beach profiles,  $U$  = based on the velocity (Hughes, 1992) and  $W$  = based on the deep water wave conditions (Mase & Iwagaki, 1985)

| Data set          | Run      | Run-up limits |       |       |
|-------------------|----------|---------------|-------|-------|
|                   |          | R             | U     | W     |
| Shaping the Beach | E3       | 0.52m         | 0.05m | 0.24m |
| Shaping the Beach | E4       | 0.53m         | 0.05m | 0.25m |
| Shaping the Beach | E6       | 0.54m         | 0.04m | 0.25m |
| Shaping the Beach | E7       | 0.54m         | 0.04m | 0.23m |
| Shaping the Beach | E8       | 0.55m         | 0.04m | 0.22m |
| Shaping the Beach | E9       | 0.56m         | 0.04m | 0.21m |
| Shaping the Beach | A11      | 0.51m         | 0.03m | 0.20m |
| Shaping the Beach | A12      | 0.54m         | 0.02m | 0.25m |
| Shaping the Beach | A13      | 0.54m         | 0.02m | 0.26m |
| Shaping the Beach | A14      | 0.55m         | 0.01m | 0.19m |
| Shaping the Beach | A15      | 0.56m         | 0.01m | 0.27m |
| Shaping the Beach | A16      | 0.57m         | 0.02m | 0.34m |
| Shaping the Beach | A17      | 0.57m         | 0.02m | 0.37m |
| Shaping the Beach | A18      | 0.58m         | 0.02m | 0.46m |
| Shaping the Beach | A19      | 0.60m         | 0.02m | 0.44m |
| RESIST            | E88      | 0.78m         | 0.07m | 0.28m |
| RESIST            | E89      | 0.85m         | 0.11m | 0.27m |
| RESIST            | E90      | 0.85m         | 0.09m | 0.27m |
| RESIST            | E90      | 0.84m         | 0.10m | 0.25m |
| RESIST            | A24/25   | 0.44m         | 0.01m | 0.17m |
| RESIST            | A26/27   | 0.43m         | 0.01m | 0.31m |
| RESIST            | A28      | 0.44m         | 0.01m | 0.10m |
| RESIST            | A29      | 0.42m         | 0.01m | 0.13m |
| RESIST            | A30      | 0.40m         | 0.01m | 0.44m |
| RESIST            | A30      | 0.39m         | 0.01m | 0.17m |
| RESIST            | A32      | 0.39m         | 0.01m | 0.12m |
| RESIST            | A33      | 0.39m         | 0.01m | 0.17m |
| RESIST            | A34      | 0.38m         | 0.01m | 0.02m |
| RESIST            | A35      | 0.38m         | 0.01m | 0.12m |
| BARDEX II         | A1 1-5   | 1.12m         | 0.02m | 0.54m |
| BARDEX II         | A1 6-7   | 1.20m         | 0.03m | 0.55m |
| BARDEX II         | A1 8-9   | 1.24m         | 0.04m | 0.67m |
| BARDEX II         | A1 10-11 | 1.29m         | 0.05m | 0.69m |
| BARDEX II         | A1 12-13 | 1.24m         | 0.05m | 0.59m |
| BARDEX II         | A6 1-5   | 1.65m         | 0.05m | 0.99m |
| BARDEX II         | A6 6-7   | 1.55m         | 0.06m | 0.97m |
| BARDEX II         | A6 8-9   | 1.57m         | 0.06m | 0.82m |
| BARDEX II         | A6 10-11 | 1.52m         | 0.06m | 1.08m |
| BARDEX II         | A6 12-13 | 1.52m         | 0.06m | 1.07m |
| Total             | StB_E    | 0.52m         | 0.05m | 0.25m |
| Total             | StB_A    | 0.49m         | 0.02m | 0.20m |
| Total             | RES_E    | 0.78m         | 0.09m | 0.28m |
| Total             | RES_A    | 0.44m         | 0.01m | 0.16m |
| Total             | BAR_A1   | 1.12m         | 0.03m | 0.54m |
| Total             | BAR_A6   | 1.65m         | 0.05m | 0.99m |

## E Figures: improvement run-up limit each run

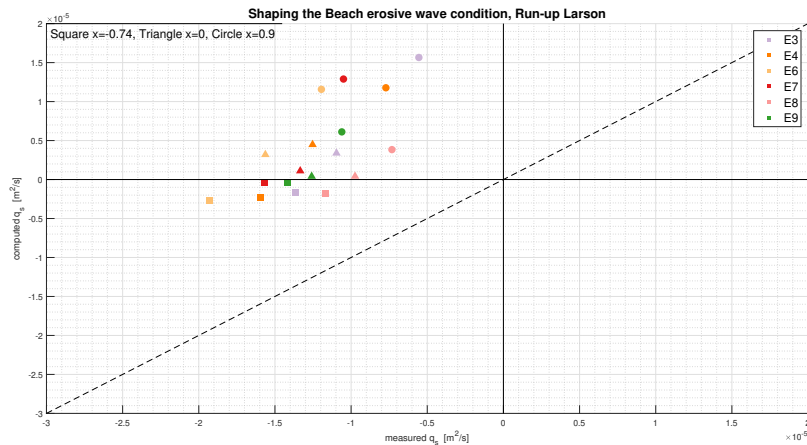


**Figure E.1:** *Shaping the Beach erosive wave condition net sediment transport calculated using the run-up limit based on the velocity (Hughes, 1992)*

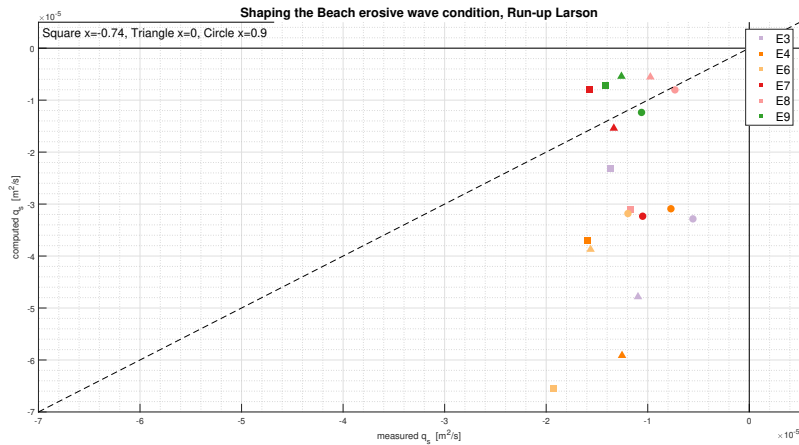


**Figure E.2:** *Shaping the Beach erosive wave condition net sediment transport calculated using the run-up limit based on the deep water wave conditions (Mase & Iwagaki, 1985)*

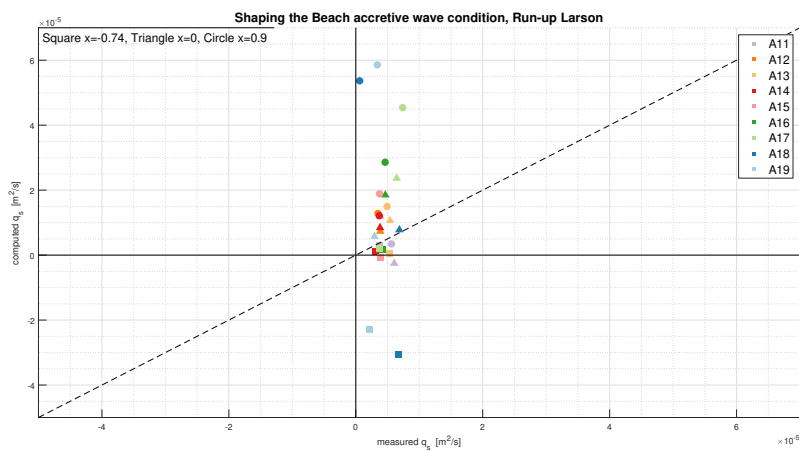


**Figure E.3:** *Shaping the Beach accretive wave condition net sediment transport calculated using the run-up limit based on the velocity (Hughes, 1992)*

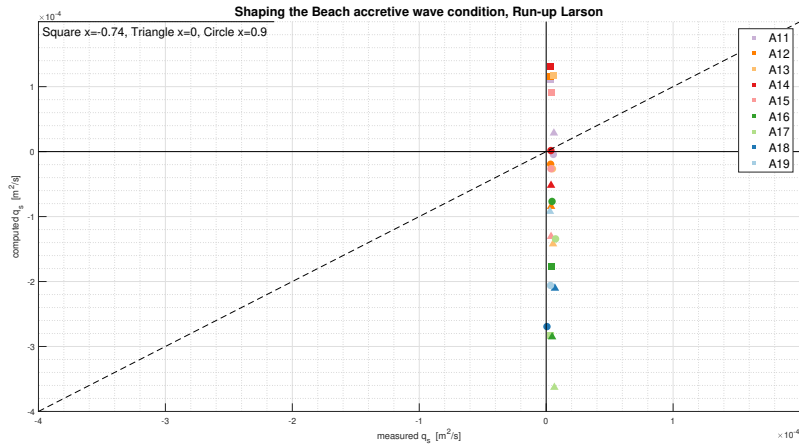


**Figure E.4:** *Shaping the Beach accretive wave condition net sediment transport calculated using the run-up limit based on the deep water wave conditions (Mase & Iwagaki, 1985)*

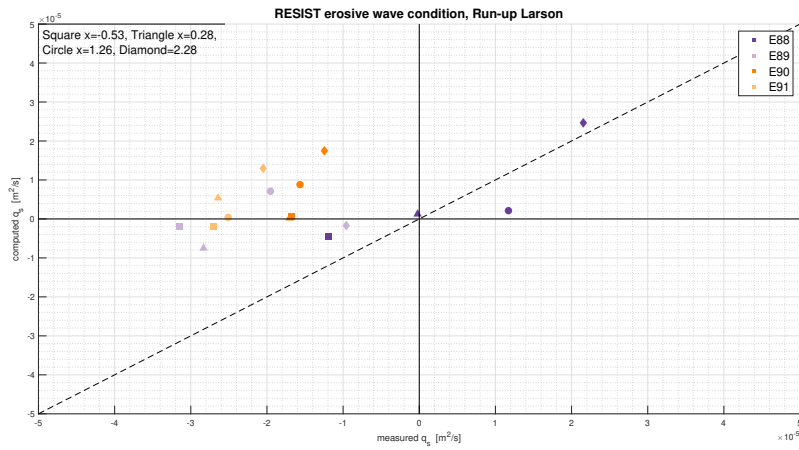


**Figure E.5:** *RESIST erosive wave condition net sediment transport calculated using the run-up limit based on the velocity (Hughes, 1992)*

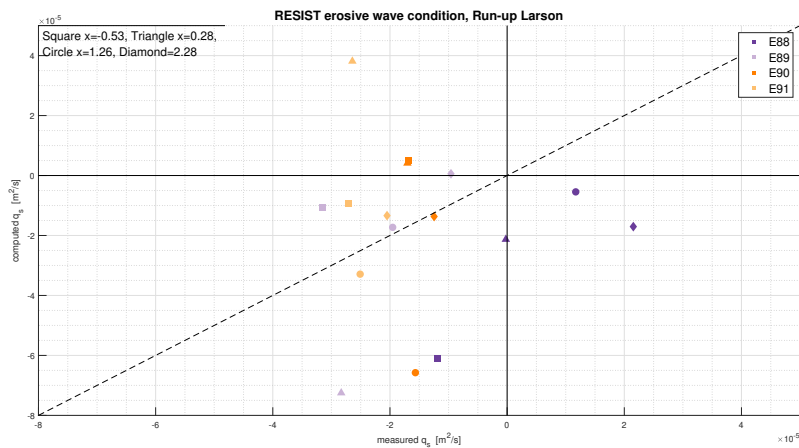


**Figure E.6:** *RESIST erosive wave condition net sediment transport calculated using the run-up limit based on the deep water wave conditions (Mase & Iwagaki, 1985)*

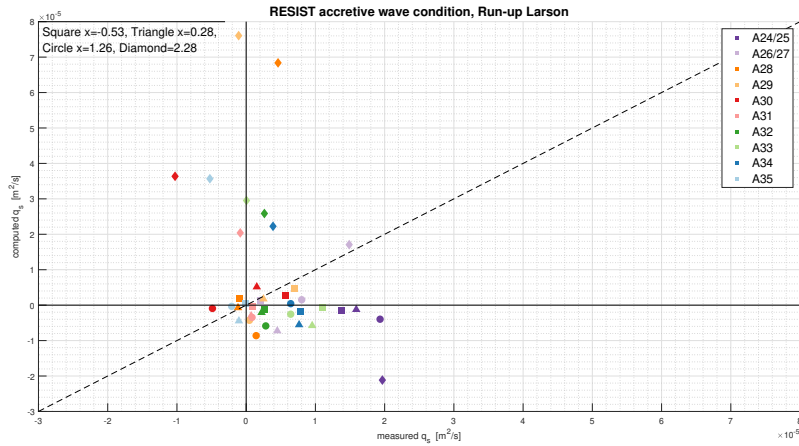


Figure E.7: RESIST accretive wave condition net sediment transport calculated using the run-up limit based on the velocity (Hughes, 1992)

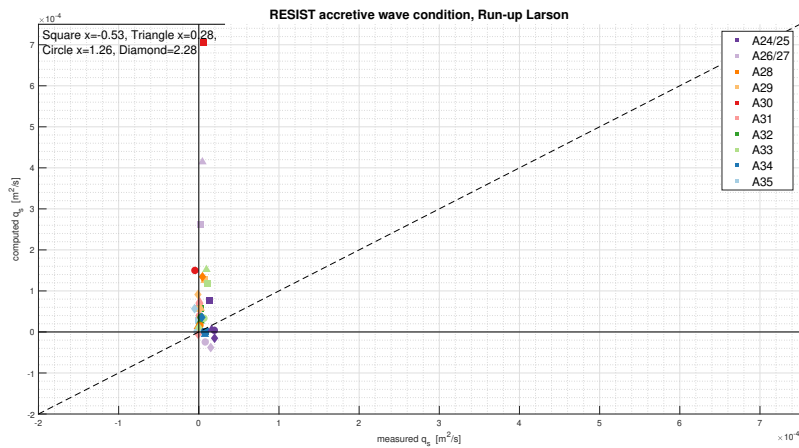


Figure E.8: RESIST accretive wave condition net sediment transport calculated using the run-up limit based on the deep water wave conditions (Mase & Iwagaki, 1985)

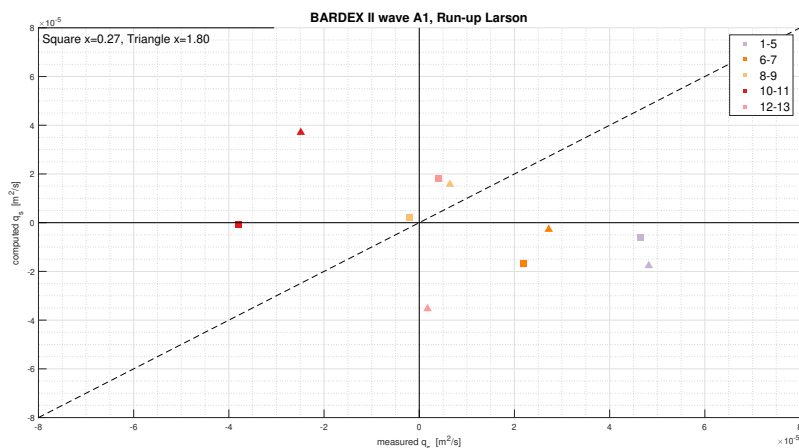
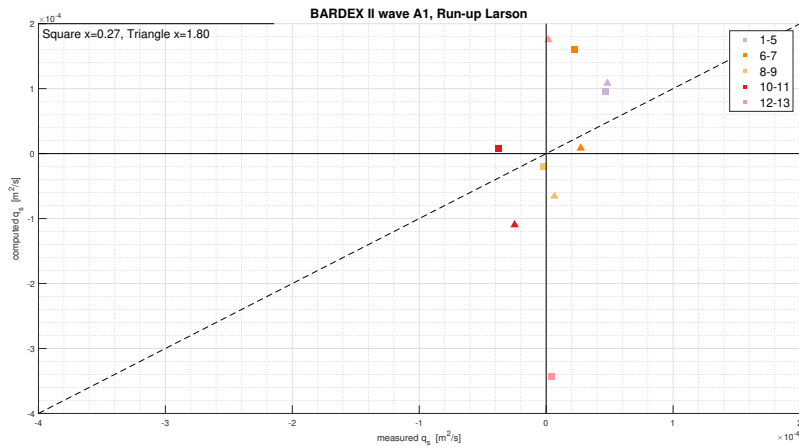
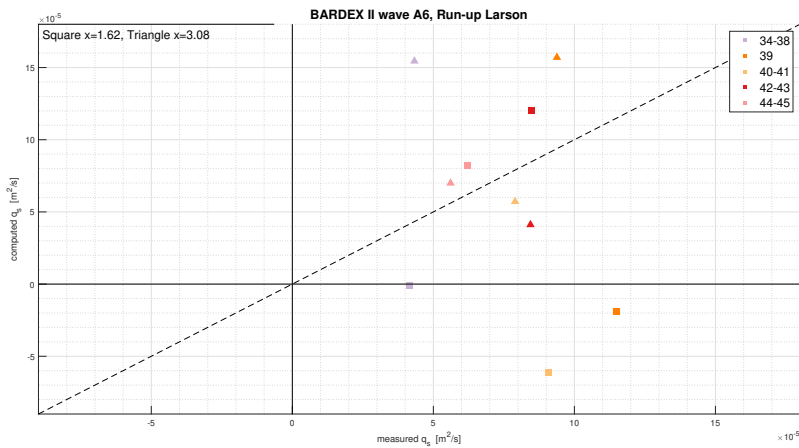


Figure E.9: BARDEX II erosive wave condition net sediment transport calculated using the run-up limit based on the velocity (Hughes, 1992)



**Figure E.10:** BARDEX II erosive wave condition net sediment transport calculated using the run-up limit based on the deep water wave conditions (Mase & Iwagaki, 1985)



**Figure E.11:** BARDEX II accretive wave condition net sediment transport calculated using the run-up limit based on the velocity (Hughes, 1992)

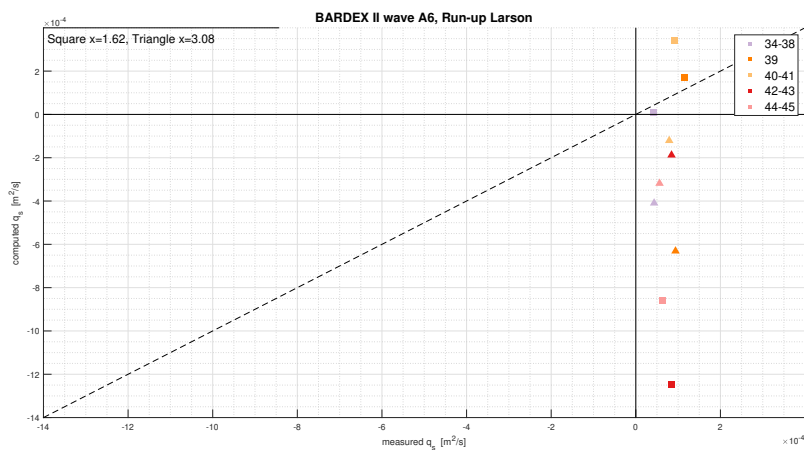


**Figure E.12:** BARDEX II accretive wave condition net sediment transport calculated using the run-up limit based on the deep water wave conditions (Mase & Iwagaki, 1985)